

The Performance and Behavior of Lightweight Wood
Exposed to Fire Conditions

By

Brian Twomey

A Thesis

Submitted to the Faculty

of the

WORCESTER POLYTECHNIC INSTITUTE

in partial fulfillment of the requirements for the

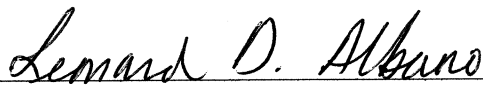
Degree of Master of Science

in

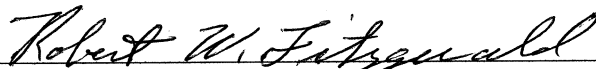
Civil Engineering

May 2007

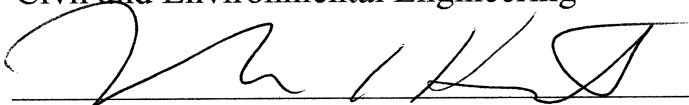
APPROVED:



Professor Leonard D. Albano, Major Advisor
Civil and Environmental Engineering



Professor Robert W. Fitzgerald, Co-Advisor
Civil and Environmental Engineering



Professor Fredrick L. Hart, Head of Department
Civil and Environmental Engineering

Abstract

Lightweight wood construction is one of the most common forms of residential construction in the United States. Unprotected lightweight wood structural members are extremely sensitive to elevated temperatures often experienced in fire conditions. Residential fires are a commonly occurring incident across the globe and consequently make up a large percentage of residential property loss and damage.

In the United States, building code provisions limit lightweight construction to particular building types. These building codes prescribe protected lightweight wood assemblies in building types for which they are allowed.

Although many components of lightweight wood buildings are required to be protected in some form, there are still many parts of the building that are not necessarily required to be protected, especially in private residential structures. A fire may start in an area of a building that is protected, but may propagate into areas that are not. This leaves portions of the unprotected structure vulnerable to rapid fire damage. Lightweight wood members can quickly lose load resistance due to a loss of cross-section as a result of charring.

Analytical models currently exist and are generally accepted for heavy timber elements, but the applications of these models do not extend to lightweight wood members. As a result, this thesis investigated the application of an analytical model to lightweight wood elements. In developing this model, the finite element method and finite difference models were used to investigate the phenomenon of wood char in fire conditions. Finite difference models were explored as an alternative to finite element models because finite difference formulations did not require specialty programs. Following the development of analytical char models, mechanics-based analyses were conducted to evaluate the performance of lightweight beams and columns exposed to fire conditions.

Table of Contents

Abstract.....	i
Table of Contents.....	ii
Table of Figures.....	iv
List of Tables.....	vi
1 Introduction.....	1
1.1 Objective.....	3
1.2 Scope of Work.....	4
2 Background and Literature Review.....	6
2.1 Fire in the United States.....	6
2.2 Building Codes.....	8
2.3 Standard and Natural Fires.....	12
2.4 Design of Structural Wood Elements.....	15
2.5 Thermal Degradation of Wood.....	17
2.6 Heat Transfer.....	25
2.6.1 Finite Difference Method.....	27
2.6.2 Finite Element Method.....	29
2.6.3 Thermal Properties of Wood.....	30
3 Methodology.....	34
3.1 Material Property Parameters.....	36
3.2 Finite Element Method Model in ANSYS.....	38
3.3 Finite Difference Method in Excel.....	44
3.4 Natural Fire Char Depth Analysis.....	46
3.5 Mechanics-Based Analysis Tool in Excel.....	47
4 Excel Spreadsheet Analysis Tools.....	49
4.1 Finite Difference Method Char Depth Analysis.....	49
4.2 Mechanics-Based Time to Failure Analysis.....	54
4.2.1 Beams.....	55
4.2.2 Columns.....	60
5 Results.....	65
5.1 Char Depth Models.....	65
5.1.1 ASTM E-119 Fire.....	66
5.1.2 Models of Natural Fires.....	82
5.2 Mechanics-Based Analysis to Predict Time to Failure.....	86
5.2.1 ASTM E-119 Fire.....	87
5.2.2 Models of Natural Fires.....	92
6 Conclusions.....	95
6.1 Modeling the Performance of Wood.....	96
6.2 Analysis in Practice.....	97
6.3 Recommendations for Future Work.....	99
7 Bibliography.....	101
Appendix.....	103
Appendix A – Specific Heat Variations.....	104
Appendix B – ASTM E-119 Char Depth Results.....	107

Appendix C – Natural Fire Char Depth Results	125
Appendix D – TR-10 Beam and Column Time to Failure Comparisons	129
Appendix E – 2x10 Beam Time to Failure	133
Appendix F – 2x6 Column Time to Failure.....	138

Table of Figures

Figure 1 - Fire Fatalities in Residential and Non-Residential Structures, 1996 – 2005	7
Figure 2 - Example of One-Hour Rated Wall Assembly (taken from DCA-3, 2002)	10
Figure 3 - ASTM E-119 Time-Temperature Curve	13
Figure 4 - Natural Fire Grown and Decay Periods	14
Figure 5 - Degradation zones of wood section exposed to fire (taken from White, 2002).....	18
Figure 6 - Beam with three sided exposure (taken from TR-10, 2003)	21
Figure 7 - Illustration of Temperature Gradient	28
Figure 8 - Wood Density – T.T. Lie	31
Figure 9 - Specific Heat – Buchanan	32
Figure 10 - Thermal Conductivity - Knudson and Schneiwind.....	33
Figure 11 - Methodology Flowchart.....	36
Figure 12 - ANSYS Model Element Mesh.....	40
Figure 13 - Additive Method to Account for Char Consumption.....	42
Figure 14 - Revised Thermal Conductivity	43
Figure 15 - LD-MI and SD-HI Natural Fires vs. ASTM E-119 Standard Fire.....	47
Figure 16 - Finite Difference Char Depth Analysis Spreadsheet Input/Output.....	51
Figure 17 - Finite Difference Char Depth Analysis Spreadsheet Nodal Calculations.....	53
Figure 18 - Mechanics-Based Beam Analysis Input/Output	56
Figure 19 - Mechanics-Based Beam Analysis Calculations Spreadsheet.....	58
Figure 20 - Mechanics-Based Column Analysis Input/Output Spreadsheet	61
Figure 21 - Mechanics-Based Column Analysis Calculations Spreadsheet	63
Figure 22 - TR-10 Char Depth vs. Time.....	66
Figure 23 - Case 4 FEM vs. TR-10 Char Depth	67
Figure 24 - FEM Case 4 Variations vs. TR-10 Char Depths	69
Figure 25 - FEM Case 1 vs. TR-10 Char Depth	71
Figure 26 - FEM Case 2 vs. TR-10 Char Depth	71
Figure 27 - FEM Case 3 vs. TR-10 Char Depth	72
Figure 28 - FEM Case 4 vs. TR-10 Char Depth	72
Figure 29 - FEM Case 5 vs. TR-10 Char Depth	73
Figure 30 - FEM Case 6 vs. TR-10 Char Depth	73
Figure 31 - FEM Case 7 vs. TR-10 Char Depth	74
Figure 32 - FEM Case 8 vs. TR-10 Char Depth	74
Figure 33 - Case 4 FEM vs. Case 4 FDM with Model Instabilities.....	76
Figure 34 - Case 1 FEM vs. Case 1 FDM Char Depth	77
Figure 35 - Case 1 FEM vs. FDM Adaptive Time Step Method.....	78
Figure 36 - Case 2 FEM vs. FDM Adaptive Time Step Method.....	79
Figure 37 - FDM Adaptive Time Step Selection Comparison - Case 6	80
Figure 38 - FDM Adaptive Time Step Selection Comparison - Case 4	81
Figure 39 - Best Fit FEM and FDM Char Depth Models	82
Figure 40 - FDM and FEM Char Depth - LDMI Fire - Case 2	83
Figure 41 - FDM and FEM Char Depth - SD-HI Fire - Case 2	84
Figure 42 - FDM vs. FEM Case 2 - LD-MI.....	85

Figure 43 - FDM vs. FEM Case 2 - SD-HI.....	86
Figure 44 - TRADA Beam TR-10 vs. FEM and FDM.....	88
Figure 45 - FCNSW-BB Beam TR-10 vs. FEM and FDM	88
Figure 46 - R15A Column TR-10 vs. FEM and FDM.....	89
Figure 47 - R20C Column TR-10 vs. FEM and FDM.....	90
Figure 48 - Lightweight Beam TR-10 vs. FEM and FDM	91
Figure 49 - Lightweight Beam FDM Case 2 - % to Design Capacity Variation.....	92
Figure 50 - 2x10 Beam Loaded to 75% of Design Capacity - LD-MI	93
Figure 51 - 2x10 Beam Loaded 75% - Exposure Comparison	94

List of Tables

Table 1 - T.T. Lie Equations for Calculating Time to Failure of Beams and Columns ...	23
Table 2 - Material Property Variation Matrix.....	38
Table 3 - Finite Difference Char Depth Analysis Input/Output Details	52
Table 4 - Finite Difference Char Depth Analysis Nodal Calculation Details.....	54
Table 5 - Mechanics-Based Beam Analysis Input/Output Details	57
Table 6 - Mechanics-Based Beam Analysis Calculations Spreadsheet Details.....	59
Table 7 - Mechanics-Based Column Analysis Input/Output Spreadsheet Details	62
Table 8 - Mechanics-Based Column Analysis Calculations Spreadsheet Details	64

1 Introduction

Lightweight wood and engineered wood products are some of the most commonly used materials in residential construction. Many single and multi-family homes are built using what is commonly known as “stick construction.” As the name implies, the structural members are primarily small dimensional lumber. Lightweight wood construction’s popularity stems from high availability of material and ease of use during construction. Dimensional lumber is typically available in all parts of the country, and most construction companies can build with lightweight wood without any specialized laborers or equipment. The combination of these factors ultimately leads to relatively low cost and rapid erection time when compared to other conventional forms of construction.

As with most buildings, fire poses one of the biggest threats to property damage and occupant hazard. Every year in the United States, billions of dollars and thousands of lives are lost due to damage caused by fires in residential structures. A large percentage of residential structures are made up of lightweight wood elements that are extremely sensitive to fire. Unprotected lightweight wood members are combustible and highly sensitive to loss of cross-section when exposed to the elevated temperatures experienced during fire conditions. If substantial, this loss of cross-section can lead to structural failure of the element and possibly collapse of the structure. For this reason, building codes routinely limit the application of lightweight wood construction methods to residential structures and small-scale commercial buildings.

When lightweight wood materials are permitted, fire protective finishes are typically required. To determine the amount of fire protection needed, building codes prescribe a fire resistance rating. In the United States, these ratings are based on the ASTM E-119 standard fire test procedure. The fire resistance rating designates the amount of time for which the structure must sufficiently carry load. Depending on the structural system used, catalogued assemblies have approved fire resistance ratings. In many cases, gypsum wallboard is generally acceptable and provides satisfactory fire resistance levels in accordance with building codes for lightweight wood construction.

Although building codes require protective coverings in most living spaces, some areas of the structures are not required to have protection. These areas include unoccupied spaces such as basements and attics. Fires can begin in protected spaces but can quickly propagate to other portions of the structure by way of openings or lack of effective fire stops. Once fire has made its way into unprotected spaces, it can often be a matter of minutes before lightweight wood elements lose their ability to carry load and undergo extreme deflections. The loss of load carrying capacity and/or extreme deflection is what commonly defines structural failure, and likely collapse. It is this failure and collapse that causes property loss and endangers occupants and fire rescue personnel.

Currently, building codes allow prescribed protective coverings to provide fire resistance for lightweight wood structures without any analytical assessment by an engineer. The structural engineer is rarely involved in the process concerning fire protection (except in specialized areas of fire protection engineering), even though he/she

has the most comprehensive understanding of the materials and mechanics of the building.

Although the practice of assessing fire performance of lightweight wood structures is seldom done in the typical structural engineering office, provisions for doing so are provided by the American Wood Council. In section 16 of the National Design Specification for Wood Construction, an expression for char depth is given. This expression of char depth is developed in more detail in another American Wood Council document (TR-10), which is intended to provide direction for performance-based design of wood members exposed to fire conditions. With this char expression, the engineer can determine the effective remaining cross-section of wood elements when exposed to the ASTM E-119 design fire. Following this, the engineer can establish the load-carrying capacity of the element based on analytical mechanics methods that he or she would use to design wood elements at ambient temperatures.

One major limitation to this analytical method is that its application is limited to members of large cross sections. This means that the governing body over structural wood design in the United States does not yet have a suggested analytical method for assessing fire performance of lightweight wood members.

1.1 Objective

The objective of this thesis is to develop an analytical method that could be used by a structural engineer to assess the time to failure and analyze performance of lightweight wood structural elements during fire conditions. To develop this method, analytical approaches to determining the fire endurance of heavy timber members will be investigated as a base for the analysis of lightweight wood members. The primary

component of heavy timber and lightweight wood analytical methods will be the assessment of loss of cross section due to wood charring. As a result, a large portion of the development of this analytical method will be comprised of modeling the char depth of wood members when exposed to fire conditions. Once these models for char depth are determined, they will be used in an analytical tool to analyze performance determine time to failure for lightweight wood members during fire conditions.

1.2 Scope of Work

The following lists the major steps that were taken to complete the objectives of this thesis:

- Model wood char depth using analytical methods presented in American Wood Council's Technical Report 10 (TR-10)
- Investigate basic principles of heat transfer and their application to wood
- Develop a model for one-dimensional prediction of wood char using Finite Element Method (FEM) analysis
- Benchmark FEM char depth results with accepted published data (TR-10)
- Develop a model for one-dimensional prediction of wood char using Finite Difference Method (FDM) analysis. This model will be developed in a spreadsheet and be transparent to the user so that the heat transfer process and the temperature changes within the cross-section are visible.
- Benchmark Finite Difference Methods of assessing char depth with the FEM results and accepted published data (TR-10)
- Investigate the sensitivities of the two char depth evaluation methods to input data such as thermal properties and design fires
- Develop a spreadsheet analysis tool for evaluating time to failure of lightweight wood members exposed to fire conditions. This tool will utilize expressions of char depth from the FEM and FDM analyses for analytical mechanics evaluations. This tool will be transparent to the user such that the mechanics of the problem are visible. Additionally, this tool will have flexibility of cross-sectional geometry, member type, loading,

strength properties, and char expression so the user may utilize the tool for a variety of conditions.

The Background and Literature Review chapter of this thesis provides a review of literature and introduces information pertinent to the performance of lightweight wood construction exposed to fire conditions. The Methodology chapter then discusses the development of the analytical char depth models and mechanics-based time to failure calculations used to evaluate the performance of wood members. Analysis tools were developed in Excel spreadsheets to evaluate char depth models and conduct time to failure calculations. These spreadsheets are detailed in the Excel Spreadsheet Analysis Tools chapter. The Results chapter compares and summarizes the results of the char depth models and time to failure analysis for beams and columns exposed to standard and natural fires. The Conclusions chapter discusses the outcome of the analytical modeling of fire performance of lightweight wood members and the impact it may have on structural engineering practice. Furthermore, the Conclusions chapter provides recommendations for future work in the area of performance of lightweight wood members exposed to fire conditions. Located in the Appendix are more complete sets of graphical results of char depth models and time to failure calculations.

2 Background and Literature Review

This chapter provides a review of literature and information pertinent to the performance of lightweight wood construction exposed to fire conditions. The intent of this chapter is to present material as a foundation for the development of analytical char depth models and mechanics based time to failure analysis of wood beams and columns.

2.1 *Fire in the United States*

Structural fires have been a problem that has threatened the safety of individuals and property since buildings first started being erected. Historically there have been fires that have devastated substantial portions of large cities. In 1871, for example, Chicago suffered one of the worst fires in modern history.¹ In the case of major urban fires of the 19th century, buildings were located extremely close together and were made of combustible materials that had little protection against the propagation of fire. This often led to extensive structural failures, resulting in severe loss of property and life. Although the idea of fire protection was evident in latter part of the 19th century², it was not until the advent of the modern building codes that structures were required to have such protection.

Even with advancing technology and developed building codes, structural fires still claim thousands of lives and cause billions of dollars in damage every year in the United States. Although fires occur in all types of structures across the country, the most devastating are those that claim human lives. According to the U.S. Fire Administration,

¹ “The Great Conflagration,” Chicago Historical Society and the Trustees of Northwestern University.

² Freitag, J.K.

the greatest loss of life from fire occurs in residential structures. Figure 1 shows the comparison of lives lost in residential fires compared with non-residential fires between 1996 and 2005. Of all fatal structure fires in 2002, 94 percent occurred in residential structures and most of these fatal fires (78 percent) occurred in one- and two-family homes.^{3,4}

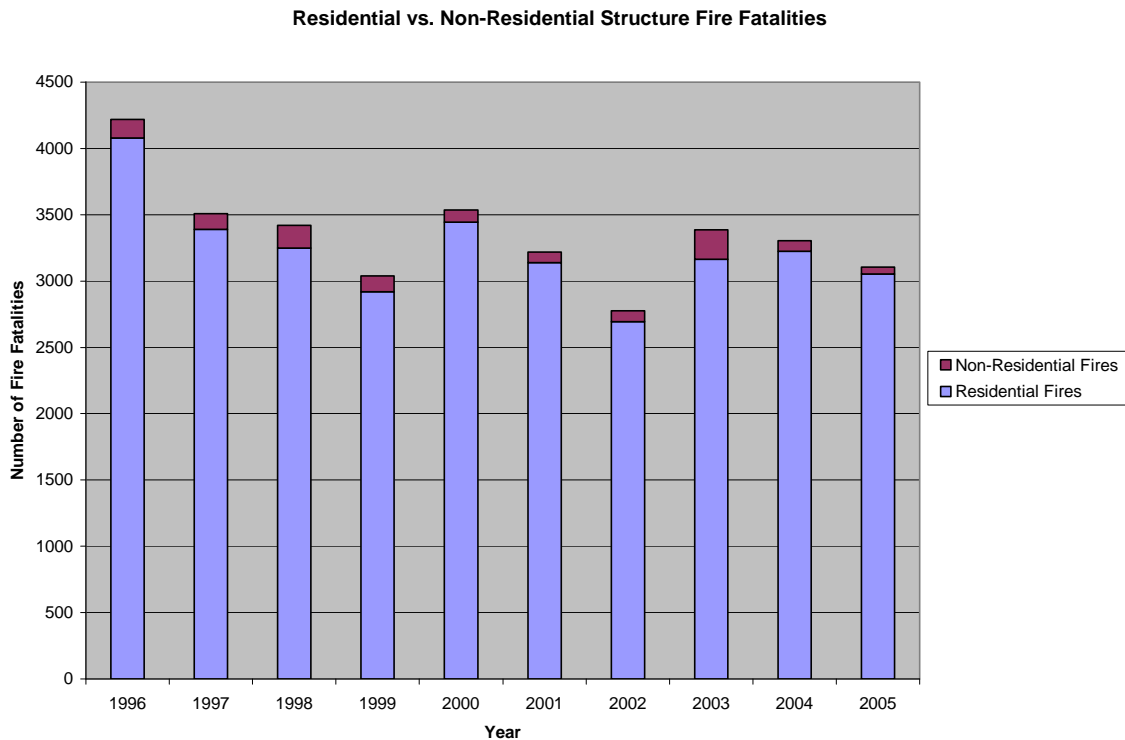


Figure 1 - Fire Fatalities in Residential and Non-Residential Structures, 1996 – 2005⁵

Over the ten year period in which the U.S Fire administration reported statistics on residential and non-residential structure fires, on average, 5.5 of the 8.25 billion dollars directly lost per year were due to residential fires (these statistics do not reflect the events of September 11, 2001).⁶ Clearly, there is an overwhelming amount of loss due to

³ “Fatal Fires,” U.S. Fire Administration/ National Fire Data Center.

⁴ “Fire in the United States 1992 – 2002,” U.S. Fire Administration/ National Fire Data Center. p.49

⁵ “National,” U.S. Fire Administration, Department of Homeland Security.

⁶ “Fatal Fires” U.S. Fire Administration/ National Fire Data Center.

residential structure fires in the United States. Many residential structures in the United States are constructed with lightweight wood or engineered wood products.

2.2 Building Codes

Building codes provide a standard by which engineers and architects can design buildings to an accepted level of safety. Building codes also establish guidelines for construction and building approval processes. Criteria generally taken into consideration when designing buildings include size, intended use, desired materials, and location. In theory, building codes provide a consistent, acceptable guide for professionals to reference when designing buildings. In practice, in the United States, different building codes are allowed depending on the state and, in some cases, local municipalities.

One of the most widely accepted building codes is the International Building Code published by the International Code Council. The International Building Code is a model building code that is intended to provide a base for local building codes. It is published every few years, the most recent of which is the International Building Code 2006 (IBC 2006). An alternative model building code is the NFPA 5000: Building Construction and Safety Code. Because of its wide acceptance (47 US states and the District of Columbia), the IBC 2006 building code will be the code of reference in this thesis.⁷

The IBC 2006 requires a performance-based design for structural systems at ambient temperatures, meaning structural engineers must analyze loadings on structural elements and design accordingly. In the case of design of structural systems for fire conditions, the IBC 2006 designates a prescriptive approach for establishing structural

⁷ “International Code Adoption,” International Code Council

fire protection. This means that the code assumes responsibility for the selection of fire protection materials without the need for a fire performance analysis. This prescriptive approach has a long history, and it has been adopted because of the specialized nature of work required to conduct a performance-based fire analysis. Most structural engineers do not have sufficient knowledge or experience to conduct a structural fire performance analysis. In fact, the process of selecting fire protection, based on tested assemblies, is generally done by an architect.

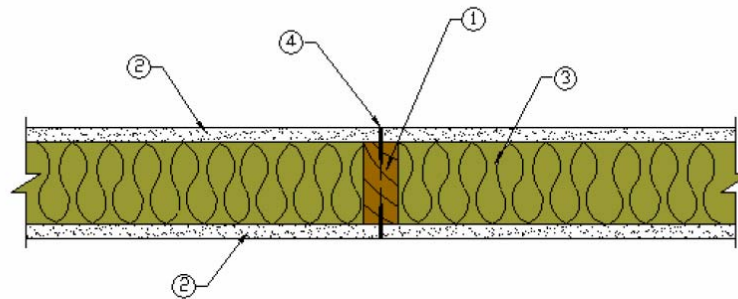
The IBC 2006 bases the allowable construction materials on construction types. The construction type is designated by the occupancy use group and size of the building. The occupancy use group is determined by the intended use of the building. In the case of lightweight wood construction, only non-critical occupancies are allowed, and are limited in sizes no larger than two to three stories and 7000 to unlimited square feet (depending on occupancy).⁸ Lightweight wood construction falls under the category of construction Type V. The most common types of structures that fall under Type V construction are one- and two- family homes, and small commercial buildings.

For buildings that allow Type V construction, certain fire resistance criteria must be met. The critical variable in fire resistive design is the fire resistance rating. The fire resistance rating designates the amount of time that a particular assembly resists failure during standard furnace tests. Failure may be defined by loss of load-carrying capacity, flame penetration through the assembly, and/or excessive heat transfer to the unexposed surface. Assemblies prescribed by the IBC 2006 are tested by independent laboratories to determine the amount of time an assembly sufficiently supports loads when exposed to the ASTM E-119 standard furnace fire. In the case of lightweight wood construction,

⁸ International Building Code 2006, Table 503, p.76

gypsum board is commonly used to provide a fire resistive layer. Figure 2 is an example of a tested wall assembly with a fire resistance rating of one hour.

WS4-1.1 One-Hour Fire-Resistive Wood Wall Assembly
2x4 Wood Stud Wall - 100% Design Load - ASTM E 119 / NFPA 251



1. Framing - Nominal 2x4 wood studs, spaced 16 in. o.c., double top plates, single bottom plate
2. Sheathing - 5/8 in. Type X gypsum wallboard, 4 ft. wide, applied horizontally, unblocked. Horizontal application of wallboard represents the direction of least fire resistance as opposed to vertical application.
3. Insulation - 3-1/2 in. thick mineral wool insulation (2.5 pcf, nominal)
4. Fasteners - 2-1/4 in. Type S drywall screws, spaced 12 in. o.c.
5. Joints and Fastener Heads - Wallboard joints covered with paper tape and joint compound, fastener heads covered with joint compound

Figure 2 - Example of One-Hour Rated Wall Assembly (taken from DCA-3, 2002)⁹

This prescriptive approach to resistive design is essentially one of “one size fits all.” This is accepted by the majority authorities having jurisdiction because of the recognized complexity of fire and the limited knowledge of performance-based fire resistive design. This perspective is slowly beginning to change, and building codes in other countries are shifting toward a performance-based approach because of progress in fire safety technology and development of engineering tools.¹⁰ It is this change to performance-based design that will give engineers reliability and consistency in fire resistive design.

⁹ “Design for Code Acceptance 3 – Fire Rated Wood Floor and Wall Assemblies” American Wood Council., p.4

¹⁰ Benichou, Nouredine and George Hadjisophocleous., p.3

The IBC 2006 allows performance-based analysis for fire resistive design. Additionally, the International Code Council published the 2006 ICC Performance Code for Buildings and Facilities. Although the title sounds promising for guidance for performance-based analysis, the ICC Performance Code has little information to aid in performance-based analysis and design. The ICC Performance Code provides discussion on the management of fire impact and prevention of fire events. The IBC 2006 actually provides the clearer commentary of allowing performance-based fire resistive design, stating:

The application of any of the alternative methods [for determining fire resistance] listed in this section shall be based on the fire exposure and acceptance criteria specified in ASTM E-119. The required fire resistance of a building element shall be permitted to be established by any of the following methods or procedures:

1. Fire-resistance designs documented in approved sources.
2. Prescriptive designs of fire-resistance-rated building elements as prescribed in Section 720.
3. Calculations in accordance with Section 721.
4. Engineering analysis based on a comparison of building element designs having fire-resistance ratings as determined by the test procedures set forth in ASTM E-119.
5. Alternative protection methods as allowed by Section 104.11.¹¹

Although the IBC 2006 allows for analytical procedures for fire resistive analysis and design, it shows little direction on how to do so. Also, this is not truly a performance-

¹¹ International Building Code 2006, Section 703.3, p.90

based design approach, since it must still be in compliance with required fire resistance ratings, and consequently is not an application of the limit states of design.

2.3 Standard and Natural Fires

One of the most important factors when assessing fire performance of any structural element is the description of the fire event itself. The size, duration, and intensity of a fire are dependent upon the fuel loads and ventilation available within a structure. The fuel load is defined by any material present that is available for combustion; it is ultimately a function of the occupancy of the structure. For example, a home may contain fuel in the form of furniture or other objects, while an office may provide a larger fuel load in the form of paper and furniture.

The ASTM E-119 is a standard furnace fire that is used to evaluate structural members. “The controlled ASTM E119 standard fire is fast starting,” rising to a temperature of 538°C in only five minutes.¹² After a period of rapid temperature growth, the temperature steadily rises to nearly 1300°C after eight hours. The ASTM E119 time-temperature curve is represented graphically in Figure 3. This eight hour fire test time greatly exceeds the highest fire resistance requirements set forth in the IBC 2006. Moreover, the continual rise in temperature after a period of rapid growth is not representative of a natural fire.¹³

¹² Gewain, Richard G., p.3

¹³ Ibid, p.3

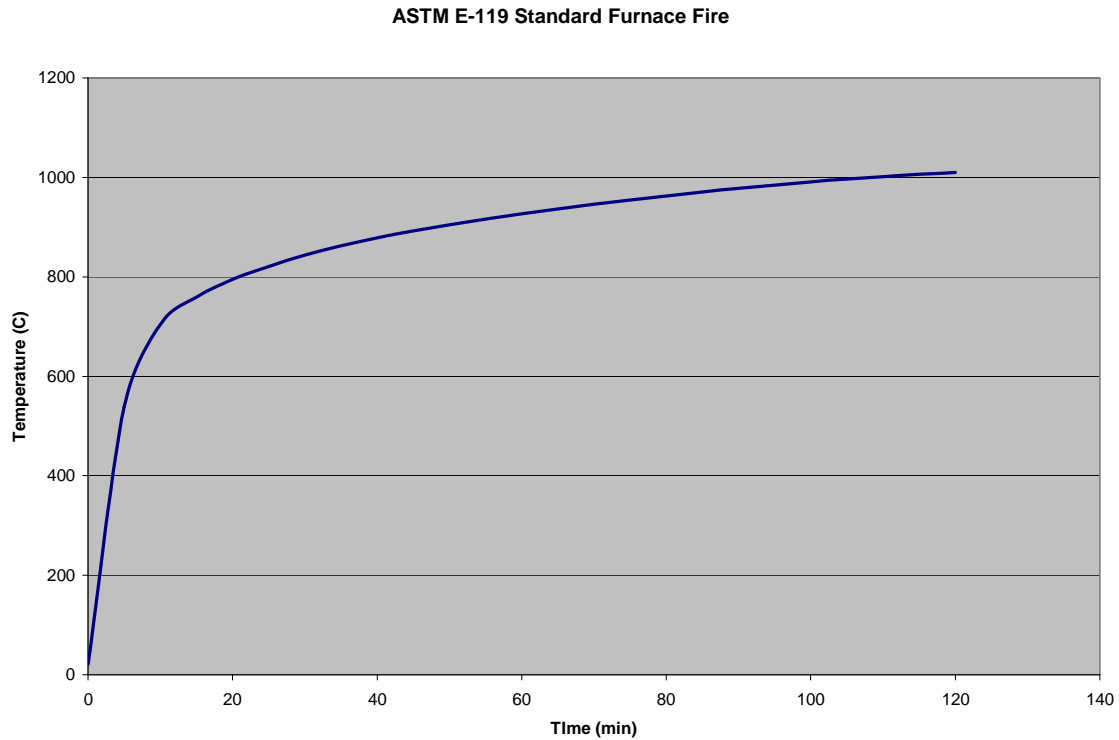


Figure 3 - ASTM E-119 Time-Temperature Curve

Natural fires are fires that occur during real fire events. Figure 4 illustrates the growth and decay period of a natural fire. These fires are extremely variable and difficult to predict. There are particular methods and software programs that can predict the temperature characteristics of a natural fire based on compartment size, construction materials, fuel load, ventilation, etc. Some of these methods include computational fluid dynamics models, and consequently, the determination of the time-temperature expressions of natural fires becomes an involved process. For this reason, the investigation of numerical models for the prediction of natural fires was not part of the scope for this thesis.

The ASTM E-119 standard fire “represents the most intense burning stage of a real fire, but with inexhaustible and increasing fuel supply.”¹⁴ In the event of a naturally occurring fire, eventually the fuel supply will be consumed and the temperature will start to diminish. The rate at which the temperature of the fire decreases is similarly variable to the temperature growth. For natural fires more representative of real fire growth and decay, section four of the SFPE Handbook of Fire Protection Engineering characterizes time-temperature relationships by an equation that is a function of time, fuel load, and opening factor.

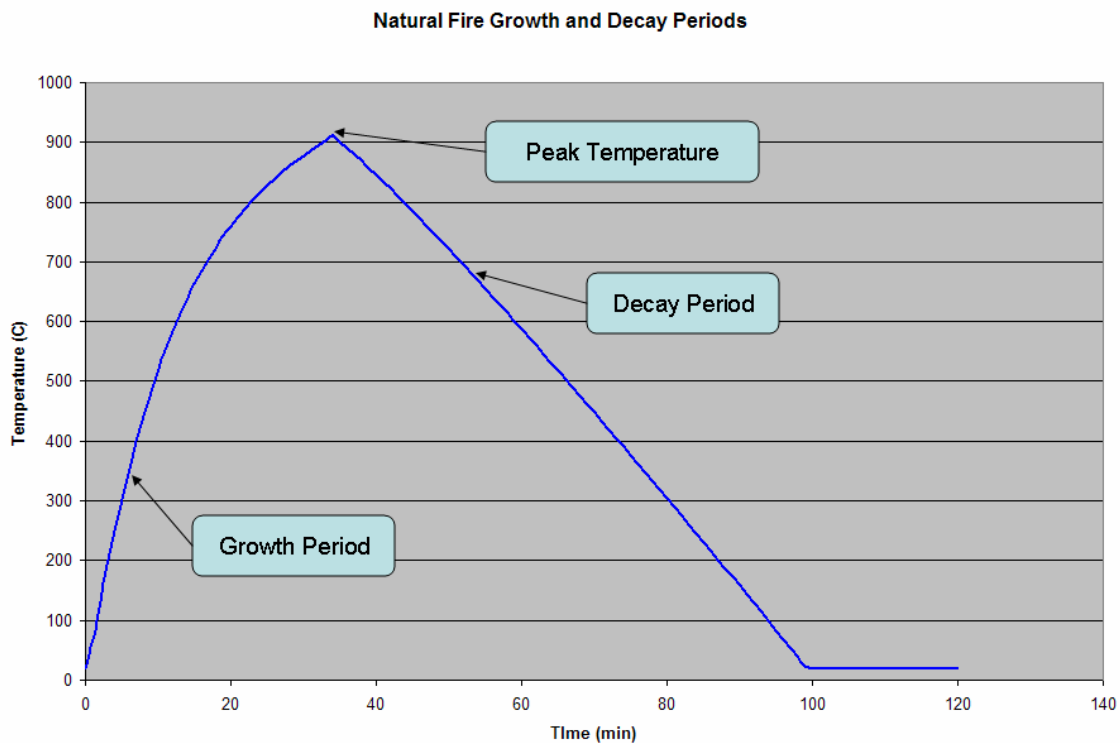


Figure 4 - Natural Fire Growth and Decay Periods

There are many different models of standard and natural fires beyond those mentioned previously that are used in fire performance evaluation throughout the international community. The ISO 834 is an example of another standard fire that is

¹⁴ Ibid, p.3

similar to the ASTM E-119 fire, which is used in other countries.¹⁵ The Eurocode also provides parametric equations to establish time-temperature curves more representative of natural fire behavior.¹⁶ Only the ASTM E-119 standard fire and two natural fires (using SFPE methods) will be investigated in the Methodology and Results chapters.

2.4 Design of Structural Wood Elements

In the United States, structural wood elements are designed in accordance with the provisions developed by the American Wood Council. The National Design Specification for the design of wood structures provides a guide by which engineers can confidently design wood structures. The design guidelines are based on fundamentals of analytical mechanics to evaluate loads, stresses, and element capacities. There are two analytical methods that are allowed in the NDS: Load Resistance Factor Design (LRFD) and Allowable Stress Design (ASD). ASD is the method most commonly used in the design of structural wood elements.

For the purposes of this thesis, only beam and column elements were investigated. The following equations present relevant equations from the National Design Specification for Allowable Stress Design of beam and column elements at normal temperatures.

Beam elements:

$$f_b = \frac{M}{S} \quad \text{Equation 1}$$

$$F_b' = F_b \times [C_d \cdot C_M \cdot C_t \cdot C_L \cdot C_F \cdot C_{fu} \cdot C_i \cdot C_r \cdot C_f] \quad \text{Equation 2}$$

$$f_b \leq F_b' \quad \text{Equation 3}$$

¹⁵ Buchanan, Andrew H., p.96

¹⁶ Ibid, p.75

Column elements:

$$f_c = \frac{P}{A} \quad \text{Equation 4}$$

$$F_c' = F_c \times [C_d \cdot C_M \cdot C_t \cdot C_F \cdot C_i \cdot C_p] \quad \text{Equation 5}$$

$$f_c \leq F_c' \quad \text{Equation 6}$$

Maximum allowable bending moments (for beams) and axial forces (for column) can be calculated based on the allowable stress equations shown. Please refer to Table 4.3.1 of the NDS for definitions of stress adjustment factors.¹⁷

The National Design Specification also has a chapter that provides a method for evaluating the capacity of elements exposed to fire conditions. This method uses an expression for char to calculate a reduced effective cross-section of an element exposed to fire. The expression for char is a function of time based on ASTM E-119 exposure; therefore char depth can be calculated at any desired time. After the reduced effective cross-section is determined, the element's structural capacity can be found using the analytical methods discussed previously. This is essentially the technique that is suggested by Konig and Walleigj.¹⁸ In this process, the only step that differentiates calculating element capacity at normal ambient temperatures and elevated temperatures is calculating char depth. The importance of an accurate representation of char depth becomes immediately clear.

The expression for char depth is developed further in another American Wood Council document, Technical Report 10 (TR-10). The TR-10 is discussed in more detail in the following section.

¹⁷ American Wood Council, National Design Specification For Wood Construction, p.27

¹⁸ Buchanan, p.350

2.5 Thermal Degradation of Wood

When calculating the capacity of wood members exposed to fire conditions, thermal degradation of the material and the formation of char is the most important factor. Wood undergoes material degradation in the form of pyrolysis when exposed to fire, which reduces the density of the wood, changing the wood to char.¹⁹ The char layer that develops has no effective strength, leaving the wood member with a reduced effective cross-section.²⁰ There is a transition layer in the cross-section known as the pyrolysis zone where the material is neither char, nor normal wood. This can be seen in Figure 5. The material in the pyrolysis zone has material properties that lie somewhere between those of char and wood at normal temperatures. Wood is assumed to begin to char at 288°C.²¹

¹⁹ White, Robert H. and Erik V. Nordheim, "Charring Rate of Wood for ASTM E119 Exposure," p.6

²⁰ Lau, Peter W.C., Robert White, and Ineke Van Zeeland, "Modeling the Charring Behaviour of Structural Lumber," p.209

²¹ Buchanan, p.277

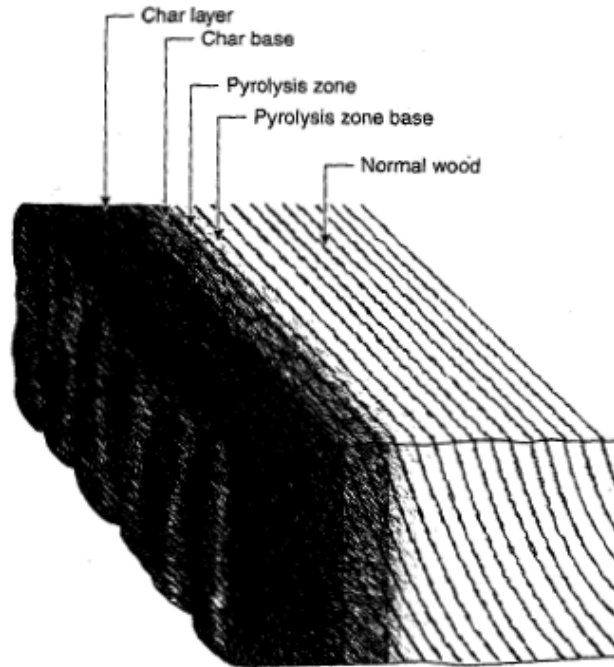


Figure 5 - Degradation zones of wood section exposed to fire (taken from White, 2002)²²

The cross-section is reduced by an amount equal to the char depth for each side of the section that is exposed to fire. Since the char depth depends on exposure conditions and time, the reduced cross-sectional area and section modulus are functions of time. These geometric properties of the cross-section contribute to determining the member capacity at a particular time.

There have been more than 50 mathematical models developed to represent the pyrolysis of wood since the middle of the 20th century.²³ Some of these models are so detailed as to include the chemical breakdown of the lignocellulosic material of the wood into char and gases.²⁴ Complex chemical models generally require a level of understanding of wood chemistry and pyrolysis that is beyond the background of the

²² White, Robert H., “Analytical Methods for Determining Fire Resistance of Timber Members”, Section Four, Chapter 11

²³ Janssens, Marc L., p.201

²⁴ Moghtaderi, Behdad

typical structural engineer. In fact, only 10 of the 50 models were developed with the intended use of structural applications.²⁵

One of the reasons why there are so many models developed to express charring of wood is that there are many discrepancies in the parameters of the models. Although it is generally agreed that wood begins to char at 288°C, thermal properties of wood greatly vary from source to source, even for similar species of wood. According to Janssens, material properties vary by as much as two orders of magnitude from source to source.²⁶

One of the most commonly used models for structural applications is one developed by Robert H. White (1992). This model was based on non-linear charring model developed by White and Nordheim (1992).²⁷ White and Nordheim developed their model as an alternative to physical testing because of the intrinsic high costs associated with testing. The predicted char rates were based on data obtained from furnace testing for a number of different wood species. They assumed char rate was a function of density, moisture content, transport properties, and chemical properties.²⁸ The general form of the time-location model of char from White and Nordheim is:

$$t = mx_c^a$$

Equation 7

where t is time, m is the reciprocal char rate, x_c is the char depth, and a is an empirical non-dimensional parameter. The determination of these parameters is further described in White and Nordheim (1992).²⁹

²⁵ Janssens, p.201

²⁶ Ibid, p.202

²⁷ White, Robert H., "Fire Resistance of Exposed Wood Members," p.338

²⁸ White, Robert H. and Erik V. Nordheim, p.11

²⁹ White, Robert H. and Erik V. Nordheim, p.16

Equation 7 establishes a relationship that allows for the calculation of fire exposure time based on the depth of char. This expression can be manipulated such that the char depth is calculated as a function of exposure time, which is shown in Equation 8

$$x_c = \beta_n t^{0.813}$$

Equation 8³⁰

where x_c is the char depth, β_n is the nominal char rate, and t is time. β_n is determined based physical test data for specific wood species. For use with NDS provisions, β_n of 1.5 in/hr is “commonly assumed for solid sawn and glued laminated softwood members” and the exponent on the time variable is empirically chosen to equal 0.813.³¹ Both the nominal char rate and the time exponent are related to the fire conditions and material properties of the wood. Equation 8 is empirically defined from ASTM E-119 furnace test data, and therefore is not applicable for fire conditions other than the ASTM E-119.³²

Equation 8 only represents the depth of the char layer. As previously discussed, there is a transitional pyrolysis zone where the material properties are neither those of char, nor wood. Also, wood cross sections undergo rounding of the corners during charring. Figure 6 illustrates the corner rounding and heated zone of the wood for a beam with three sided exposure to fire.

³⁰ “Calculating the Fire Resistance of Exposed Wood Members: Technical Report 10,” p.6

³¹ American Wood Council, National Design Specification For Wood Construction, p.140

³² Janssens, p.200

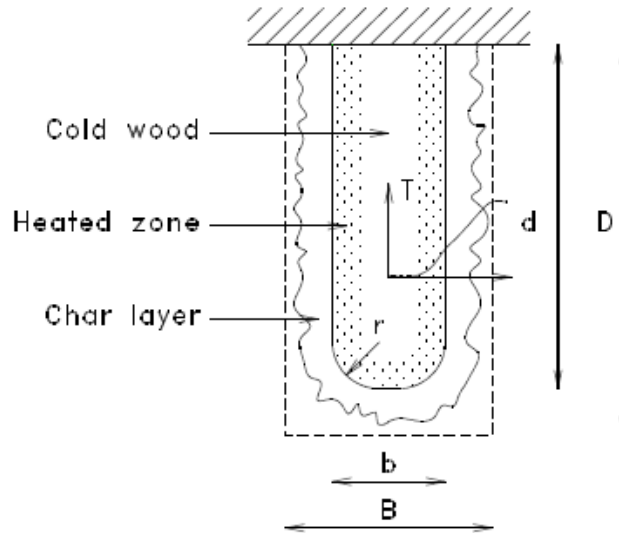


Figure 6 - Beam with three sided exposure (taken from TR-10, 2003)³³

To account for the transitional material properties of the pyrolysis zone and corner rounding, the TR-10 suggests a twenty percent increase in nominal char rate.³⁴ The final form of the equation is empirically shown in the American Wood Council’s National Design Specification for Wood Design and Technical Report 10 to represent an effective char rate as:

$$\beta_{eff} = \frac{1.2\beta_n}{t^{0.187}}$$

Equation 9³⁵

With this expression for effective char rate, char depth can be calculated and member design capacity can be evaluated as a function of time. Application of this equation will be illustrated in the Methodology chapter of this thesis. As Equation 9 shows, this model can be utilized with a basic understanding of evaluating mathematical functions and without the need to understand the complex chemical reaction of pyrolysis.

³³ “Calculating the Fire Resistance of Exposed Wood Members: Technical Report 10,” p.1

³⁴ Ibid, p.6

³⁵ Ibid, p.6

One limitation to the application of Equation 9 is member size. According to the TR-10, White's approach was developed for applications to "large wood members."³⁶

Oddly, the NDS document contains no mention of this limitation.

One other method discussed in the American Wood Council's TR-10 was developed by T.T. Lie (1977). Lie's method directly calculates the fire resistance time of beams or columns. Differently from White's method, Lie's method calculates the time to failure based solely on time of exposure to the ASTM E-119 standard fire and the loading of the element. This method does not calculate the reduced cross-section and thus eliminates the analytical mechanics step that is required in White's method. Lie assumed a constant char rate of 1.42 in/hr and ignored corner rounding of the section.³⁷ Although this model is mathematically simple, it is less accurate than White's model for many cases.³⁸ Equations used for T.T. Lie's method for calculating time to failure of beams and columns are shown in Table 1.

³⁶ Ibid, p.5

³⁷ Ibid, p.2

³⁸ "Calculating the Fire Resistance of Exposed Wood Members: Technical Report 10," p.11, 17

Table 1 - T.T. Lie Equations for Calculating Time to Failure of Beams and Columns³⁹

Beams	Columns
$t_f = 2.54 \cdot Z \cdot B \cdot \left(4 - \frac{2 \cdot B}{D}\right)$ (4-sided exposure)	$t_f = 2.54 \cdot Z \cdot D \cdot \left(3 - \frac{D}{B}\right)$ (4-sided exposure)
$t_f = 2.54 \cdot Z \cdot B \cdot \left(4 - \frac{B}{D}\right)$ (3-sided exposure)	$t_f = 2.54 \cdot Z \cdot D \cdot \left(3 - \frac{D}{2 \cdot B}\right)$ (3-sided exposure)
$Z = 1.3$ $R < 0.5$	Short Columns: $\frac{K_e \cdot l}{D} \leq 11$
$Z = 0.7 + \frac{0.3}{R}$ $R \geq 0.5$	$Z = 1.5$ $R < 0.5$
	$Z = 0.9 + \frac{0.3}{R}$ $R \geq 0.5$
	Long Columns: $\frac{K_e \cdot l}{D} > 11$
	$Z = 1.3$ $R < 0.5$
	$Z = 0.7 + \frac{0.3}{R}$ $R \geq 0.5$
t_f is time to failure in minutes R is ratio of applied load to allowable load Dimensions are in inches	

A more recent approach to model wood charring uses principles of conservation of energy to model heat transfer through wood sections. This model is called Charring Rate of Wood (CROW).⁴⁰ Janssens (2004) presented this model in order to “include all important features that need to be addressed” analytically.⁴¹ These features include wood properties (density, specific heat, thermal conductivity, moisture content, etc.), char

³⁹ Ibid, p.3-4

⁴⁰ Janssens, p.199

⁴¹ Ibid, p.202

properties, water evaporation, and char contraction. Janssens suggests that prior to CROW there were no models that analytically included these key components.⁴² Since Janssens recognized that there are discrepancies in published thermal properties of wood, he proposed his own method of establishing these parameters.⁴³ In contrast, models such as White's and Lie's addressed these issues empirically rather than analytically.

Buchanan (2002) suggests that thermal analysis calculations are not all that important for timber and lightweight construction.⁴⁴ He also implies little confidence in accurately calculating the performance of lightweight construction and says that such calculations should be used for research and development purposes only. Buchanan recommends the use of a finite element program if such thermal calculations are to be done.⁴⁵ He provides graphical representations of key thermal properties of wood such as specific heat and thermal conductivity as a function of temperature of the material, which could be used in finite element method models.

Although these methods of modeling thermal degradation of wood are trying to accomplish the same thing, the approaches are somewhat different. White and Lie both developed their model empirically from physical test data. Janssens' CROW model incorporates heat transfer fundamentals and uses the finite difference method for evaluation. As previously mentioned, Buchanan suggests a heat transfer model, solving by finite element method.

⁴² Ibid, p.202

⁴³ Ibid, p.202

⁴⁴ Buchanan, p.371

⁴⁵ Ibid, p.371

2.6 Heat Transfer

Based on the CROW model and the approach suggested by Buchanan, some development of heat transfer fundamentals is necessary to calculate char. In general, heat transfer principles are based on the principle of conservation of energy. Simply put, the principle of conservation of energy states that the amount of energy going into a system must equal the sum of the energy exiting the system and the energy stored in the system. Applying the principle of conservation of energy to heat transfer yields the first law of thermodynamics:

$$dU = dQ - dW$$

Equation 10

where dU is the change of internal energy in the system, dQ is the amount of heat added to the system, and dW is the amount of work done by the system.⁴⁶ This means that if no work is done by the system, the change in internal energy must equal the change in heat in the system.

The process of heat transfer generally involves three components: conduction, convection, and radiation. “Convection is the mechanism for heat transfer through solid materials.”⁴⁷ “Conduction is heat transfer by the movement of fluids, either gases or liquids.”⁴⁸ “Radiation is the transfer of energy by electromagnetic waves.”⁴⁹ For the purposes of this thesis, conduction is the only heat transfer mode investigated. Since conduction is the only heat transfer mode investigated, the surface temperature of the

⁴⁶ “First Law of Thermodynamics”

⁴⁷ Buchanan, p.48

⁴⁸ Ibid, p.51

⁴⁹ Ibid, p.52

wood was assumed to be equal to the fire temperature at any time. The steady-state equation for one-dimensional conduction is given by:

$$Q_x = -kA \frac{\partial T}{\partial x}$$

Equation 11

where Q_x is the rate of heat flow, A is the area normal to the direction of the heat flow,

$\frac{\partial T}{\partial x}$ is the temperature gradient in the direction of the heat flow, and k is the thermal conductivity of the material.⁵⁰

There are two limitations to this conduction expression that are critical to this thesis. The conduction expression is only valid if: thermal conductivity must remain constant except for small ∂x , and a “steady-state condition does not exist.”⁵¹ This means that thermal conductivity can be non-constant when ∂x is small and steady-state conditions must exist. These two limitations are important because the thermal conductivity of wood changes at different temperatures, and the analyses conducted are considered transient, meaning temperatures at the boundary conditions change with respect to time.

To address the transient (unsteady state) issue, problems can be solved using finite difference equations or finite element method.⁵² The formulations used in transient analyses are discussed below in the corresponding finite difference method and finite element method sections.

⁵⁰ Croft, David R., p.15

⁵¹ Ibid, p.15

⁵² Ibid, p.61

2.6.1 Finite Difference Method

The finite difference method is one of two common approximate numerical methods used for discrete solutions of differential equations. With the finite difference method, derivatives are replaced by difference equations that can be solved at a particular location, at a particular time.⁵³ By replacing derivatives with difference equations, problems can be solved without the need for calculus functions.

Finite difference equations can be applied to the study of transient heat transfer through the wood cross-section to find the extent of char depth as a function of time. The wood cross-section is broken up incrementally by adding nodes in the direction of the heat transfer. Furthermore, the exposure time is broken up into incremental time steps. These two modeling strategies essentially formulate the transient problem as an assembly of steady-state heat transfer problems between each node. Based on the nodal spacing, incremental time step, the material's thermal properties, and the thermal load conditions; the temperature gradient between any two adjacent nodes can be determined, which leads to the calculation of temperature at each node. At any time at any node, one can identify the location of the char front when the temperature exceeds 280°C. Figure 7 illustrates the temperature gradient between two nodes. Equation 12 is the general heat transfer equation used to find the change in temperature between two nodes separated by a material thickness, t . In the case of transient heat transfer problems, finite difference equations may be developed by energy balance techniques or partial differential equation replacement.⁵⁴

⁵³ Moaveni, Saeed, p.5

⁵⁴ Croft, p.61

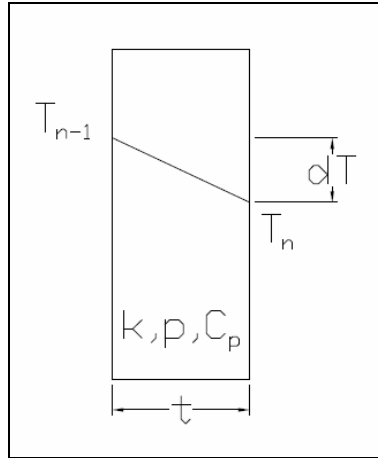


Figure 7 - Illustration of Temperature Gradient

$$\Delta T = \left(\frac{(T_{n-1} - T_n) \cdot \Delta t}{\frac{t}{k}} \right) \cdot \left(\frac{1}{\rho \cdot c_p \cdot t} \right)$$

Equation 12⁵⁵

By finding the difference in temperature between two selected nodes, the temperature at any one node can be found. Equation 13 calculates the temperature at a particular node (n) based on the temperature of two adjoining nodes at the previous time step.

$$T_n = \frac{1}{2}(T_{n-1} + T_{n+1})$$

Equation 13⁵⁶

Transient heat transfer models using finite difference method can be assembled in a spreadsheet, which is convenient for those who do not have access to advanced analytical software. Additionally, spreadsheet calculations are transparent, displaying to the user the thermal conditions at any node at any time step. One issue that must be

⁵⁵ Albano, Leonard D.

⁵⁶ Croft, p.141

considered in this analytical approach is that the model's stability is sensitive to nodal spacing and time step increment.⁵⁷ When developing this analysis, the user must be cognizant of these sensitivities.

2.6.2 Finite Element Method

Another method commonly used to approximate numerical solutions of differential equations is the finite element method. Unlike the finite difference method, the finite element method uses integral formulations to create a system of algebraic equations.⁵⁸ Since the finite element method organizes the analysis into a system of equations, it can be solved using matrix algebra. Because of this, finite element formulations are favorable for use in computer analysis. The finite element method can be used for a wide variety of analyses, including structural, fluid, and heat transfer.

Many commercial finite element programs are available to investigate a range of problems. One such program is ANSYS⁵⁹, which is used in this thesis. ANSYS solves the matrix algebra expression shown in Equation 14 to assess transient conduction heat transfer analyses.

$$\ddot{q} = \rho \cdot c \cdot \left[\frac{\partial T}{\partial t} + \{v\}^T \cdot \{L\}T \right] + \{L\}^T \cdot \{q\}$$

Equation 14⁶⁰

One of the benefits of evaluating heat transfer problems using finite element programs such as ANSYS is that they are extremely effective at solving complex problems because it assembles and solves the problems in matrix form. One of the major challenges of

⁵⁷ Ibid, p.146

⁵⁸ Moaveni, p.5

⁵⁹ ANSYS University Advanced, Version 9.0, ANSYS Inc.

⁶⁰ ANSYS User Manual, ANSYS University Advanced, Version 9.0, ANSYS Inc.

using finite element programs is that they are expensive and not readily available to the typical structural engineer. Furthermore, most structural engineers have little experience in using advanced programs such as ANSYS and would have a steep learning curve for the program.

2.6.3 Thermal Properties of Wood

Thermal properties of wood change as a function of material temperature. These varying thermal properties play an important role in the calculation of char depth as a function of time. Figure 8 through Figure 10 show the temperature-dependent thermal properties of wood that were considered in this thesis. Figure 8 approximately shows T.T. Lie's representation of wood density as a function of temperature. The density is expressed as a percentage of its original density. These values match closely with values presented by LeVan,⁶¹ and Beall and Eickner.⁶² Note that there is a sharp decline around 288°C, the temperature at which wood begins to char.

⁶¹ LeVan, S.L., p.272

⁶² Beall, F.C and H.W. Eickner, p.10

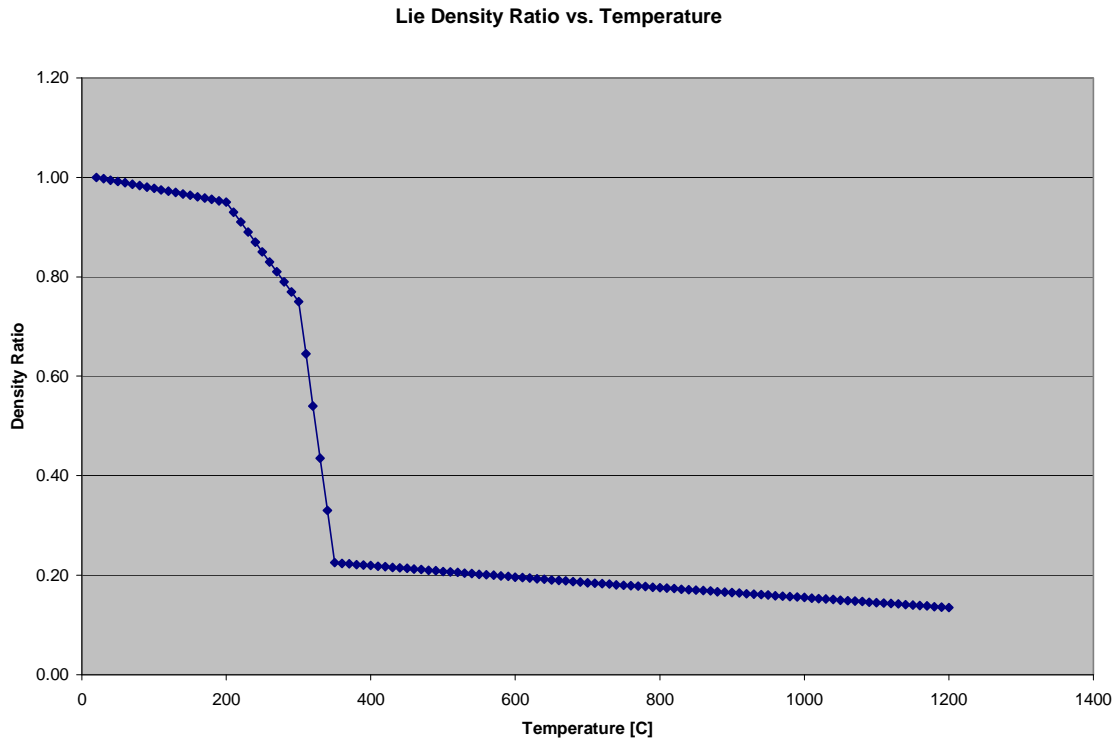


Figure 8 - Wood Density – T.T. Lie⁶³

Figure 9 shows König and Walleij’s expression for specific heat as a function of temperature. There is some variation of shape of this curve from source to source (i.e. Lie (1992),⁶⁴ but the magnitudes of the values are similar. Other graphical representations of specific heat are located in Appendix A – Specific Heat Variations. Note that there is a spike in specific heat at approximately 100°C. This spike is associated with the heat required to evaporate moisture in the wood.⁶⁵

⁶³ Lie, T.T., 1992, p.38

⁶⁴ Ibid, p.42

⁶⁵ Buchanan, p.278

Konig and Walleij Specific Heat vs. Temperature

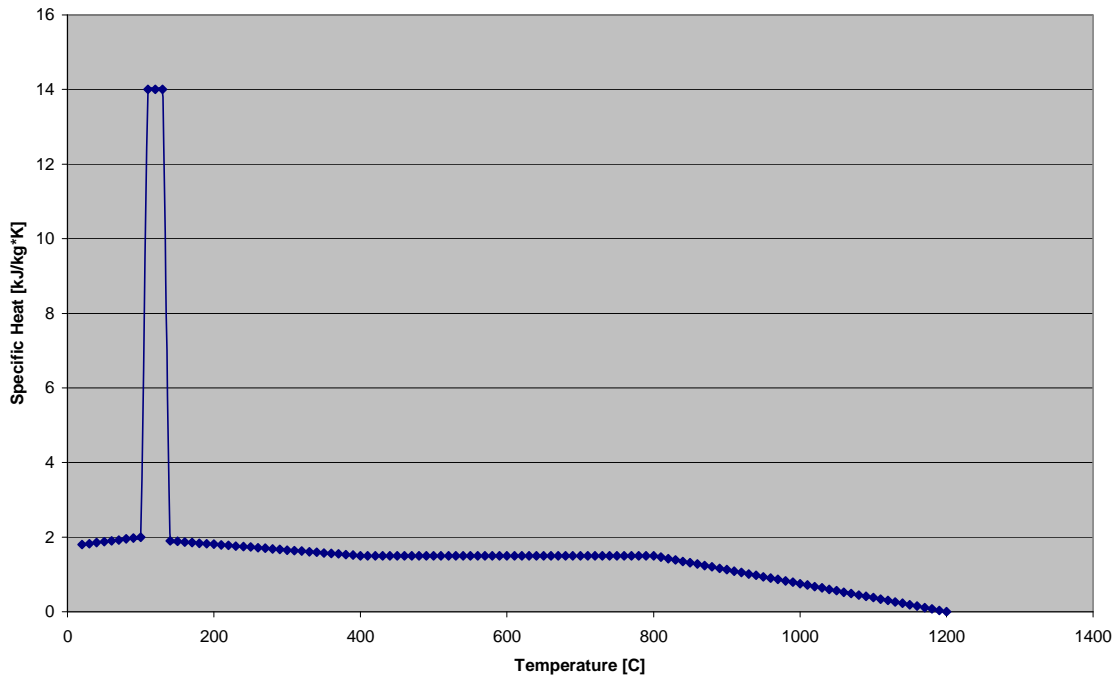


Figure 9 - Specific Heat – Buchanan⁶⁶

Figure 10 shows Knudson and Schneiwind's representation of thermal conductivity as a function of temperature. Figure 10 shows that the development of char at approximately 288°C should significantly impede heat transfer through the wood section because of the reduction of thermal conductivity. According to Buchanan, these values presented in Figure 10 are within average range among other published values.⁶⁷ For this reason, these values were used in this thesis.

⁶⁶ Ibid, p.279

⁶⁷ Ibid, p.278

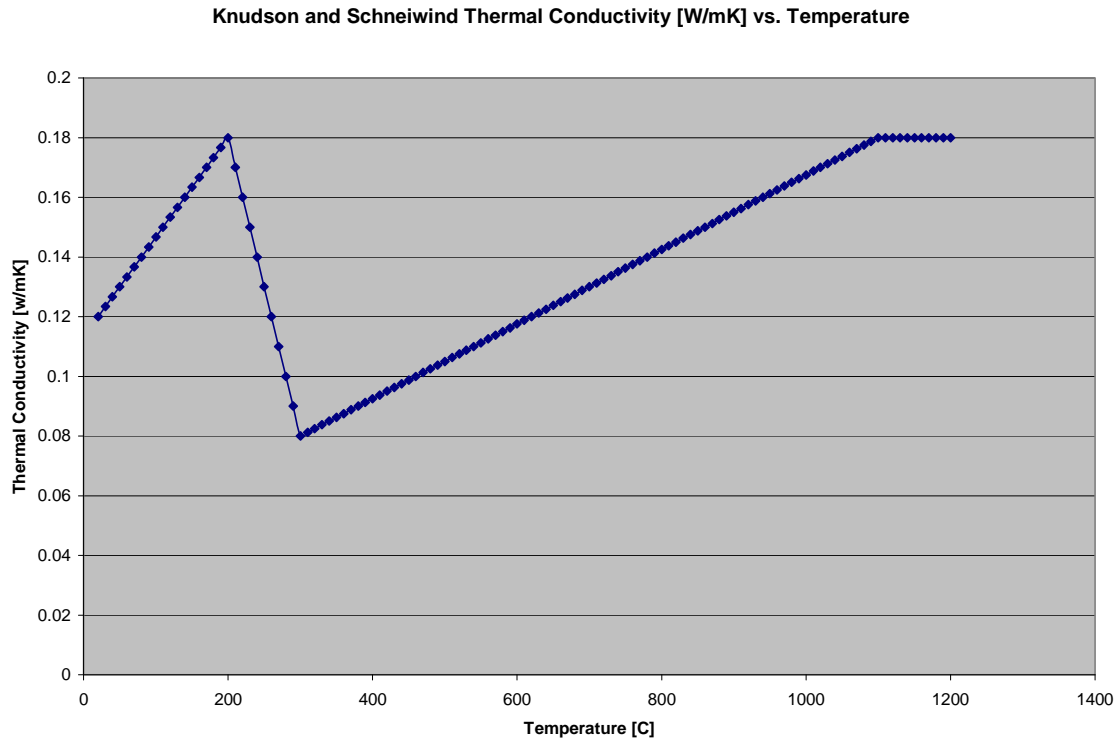


Figure 10 - Thermal Conductivity - Knudson and Schneiwind⁶⁸

Finite element and finite difference methods can be used to calculate transient heat transfer through wood cross-sections. Knowing the temperature at which charring occurs, char depth can be calculated at any particular time during the transient analysis. This char depth information can then be used to calculate reduced cross-sectional properties and the performance of wood members using NDS procedures to determine member capacity. The char depth and performance results can be compared to published data to validate the models to ASTM E-119 exposure. Furthermore, these numerical methods can be used to investigate natural fire exposure, to study the performance of members exposed to conditions other than a standard fire. The procedures for completing these steps for this thesis are discussed further in the Methodology chapter.

⁶⁸ Ibid, p.279

3 Methodology

The primary objective of this thesis was to develop a simple, yet reliable analysis tool that provides structural engineers insight into the behavior of wood exposed to fire, has limited computational complexity, and is consistent with wood design practice. In order to assemble this tool, expressions for char depth needed to be developed to determine the loss of cross section as a function of time. Although the TR-10 provides an empirical expression for char depth and an empirical calculation to define explicitly time to failure, there is a narrow range of conditions for which these techniques can accurately be applied.

Figure 11 graphically shows the primary steps of the Methodology. To develop expressions for char depth and a calculation tool for time to failure, three major areas were investigated. First, numerical char depth models were developed and benchmarked against empirical models. Finite element method (FEM) one-dimensional char depth models were developed to serve as a proxy for physical tests. These FEM models were compared to TR-10 expressions for char depth to validate their results, and identify model sensitivities. Consistent with the TR-10 formulation, the ASTM E-119 standard fire curve was used as input to the FEM benchmarking. Various FEM material models were developed to determine model sensitivities to material property variation. Next, finite difference method (FDM) one-dimensional char depth models were developed. The FDM models were developed to show that relatively simple spreadsheet applications could predict char depth results similar to the more sophisticated FEM models. FDM

model results were compared to FEM results to show correspondences between the results of the two numerical methods.

Application of these models to the study of natural fire exposure comprised the second area of interest. Char depth results for two natural fires using the most representative FEM and FDM models were compared to ASTM E-119 results. A long duration – medium intensity fire (LD-MI) and short duration – high intensity fire (SD-HI) were investigated. The LD-MI reached a maximum temperature lower than that of the SD-HI fire, but lasted for a longer duration. The comparison between fire exposures was made to demonstrate the impact that the natural fire exposure has on char depth, and consequently, time to failure.

Last, time to failure studies of beams and columns was the third major area of investigation. The three fire exposure char depths for FEM and FDM models were used in calculating time to failure of beams and columns. Calculations for time to failure of beams and columns were formulated from mechanics-based relationships as discussed in the TR-10 and NDS. Trends and observations of the time to failure behavior and performance of beams and columns were compared.

The following sections discuss FEM and FDM procedures for analytically developing char depth expressions, and the development of a mechanics-based analysis tool to calculate time to failure for beams and columns.

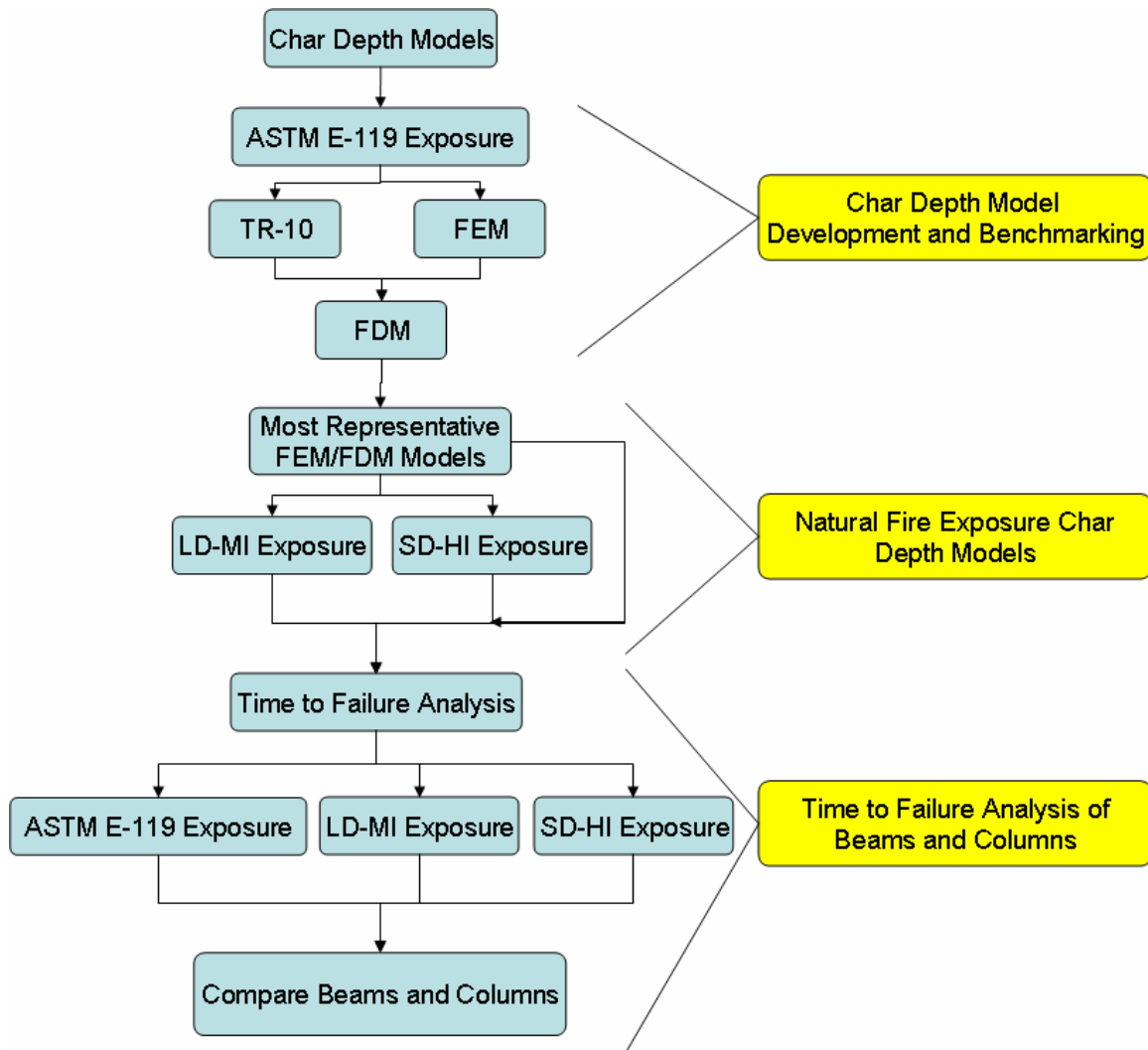


Figure 11 - Methodology Flowchart

3.1 Material Property Parameters

Strength properties of wood are considered to deteriorate with elevated temperatures (below 288°C) according to Buchanan (2002). Rather than calculating the properties of a composite cross-section with variable material strengths, the TR-10 suggests incorporating temperature-sensitive material strength by increasing the char depth by 20 percent. This 20 percent increase of char depth also includes considerations for corner rounding of the cross-section. To remain consistent with developing a

simplified model, the TR-10 suggestion of 20 percent increase of char depth was used to include considerations for strength degradation at elevated temperatures.

Moisture content plays an important role in the strength properties of wood, as well as thermal properties of wood. Moisture content of wood changes as the temperature of the material increases. As water in the wood cross-section starts to boil, moisture is released in the form of steam, and moisture migrates toward the cooler center of the wood. The impact of moisture content was neglected for strength properties of the numerical modeling for simplicity reasons previously mentions. Moisture content was also neglected for thermal properties and the heat transfer equations. The thermal material properties were discrete functions of temperature alone.

In the case of transient heat transfer analyses, thermal material properties define how a material behaves. The three material properties investigated in the development of char analysis were density, specific heat, and thermal conductivity. As shown in the Background and Literature Review, these properties can be expressed as a function of temperature. Table 2 shows the matrix of eight combinations of constant and nonlinear material properties investigated for this thesis. With three material properties changing as a function of temperature, transient thermal analytical models are mathematically complex. For this reason, constant material properties were also modeled and investigated to determine if the analysis could be simplified and still accurately predict char. The constant values used were equal to the material properties at normal temperatures (20°C).

Table 2 - Material Property Variation Matrix

Case	Density	Specific Heat	Thermal Conductivity
1	Constant	Constant	Constant
2	Constant	Constant	Nonlinear
3	Constant	Nonlinear	Nonlinear
4	Nonlinear	Nonlinear	Nonlinear
5	Nonlinear	Constant	Nonlinear
6	Nonlinear	Nonlinear	Constant
7	Constant	Nonlinear	Constant
8	Nonlinear	Constant	Constant

3.2 Finite Element Method Model in ANSYS

The finite element analyses for this thesis were conducted with the ANSYS⁶⁹ finite element program. ANSYS is capable of calculating transient thermal analyses based on material properties, geometric model, loading conditions, and boundary conditions. Inherently, other analysis parameters needed to be chosen, such as mesh size, time step, and duration of analysis.

Initially, the material properties were input based on the nonlinear values as a function of temperature (identified as Case 4 in Table 2). These properties are graphically represented in the Background and Literature Review chapter. Later, the seven remaining cases detailed in Table 2 were explored.

The geometry of the model only had one critical dimension since the thermal analysis was one-dimensional. The critical dimension was the in the direction of the applied load. The depth was chosen to be substantially larger than the deepest expected char depth so that the boundary condition at the far end of the geometry would not interfere with the heat transfer on the char front. The element essentially became semi-infinite by selecting the overall depth much larger than the expected char depth.

⁶⁹ ANSYS University Advanced, Version 9.0, ANSYS Inc.

The ASTM E-119 time-temperature curve was the only loading condition on the model. This load was applied on one face of the member, and the boundary condition was set at 20°C at the end of the model farthest from the applied load. There was only one boundary condition for this model since it was only a one dimensional analysis. The temperature of the entire member began at 20°C for the model's initial conditions. The convection mode of heat transfer from the fire gases to the wood surface was not investigated. As a result, the temperature at the exposed surface was set equal to the time-temperature curve for the fire exposure.

The mesh of the model was prepared based on the predicted behavior of the model. The element mesh used is shown in Figure 12. Initially, a coarse mesh was applied to the entire geometry. It was refined to a finer mesh closer to the applied temperature, and further refined closest to the applied temperature. The reason for having three stages of meshing was to reduce the number of calculations ANSYS needed to complete, especially for elements with little interaction with the heat transfer.

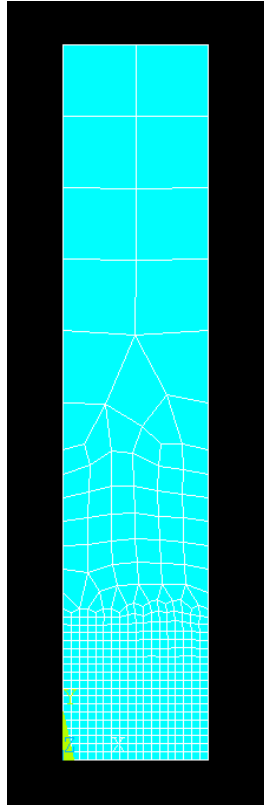


Figure 12 - ANSYS Model Element Mesh

When preparing the input data for analysis, one important parameter was the time step. As discussed in the Background and Literature Review, analysis stability is sensitive to nodal spacing and time step. ANSYS allows the user to select manually the time step, or the user may opt to have the program automatically select the time step based on solution convergence. Automatic time stepping was selected for these analyses because of the program's ability to actively update the most effective time step. In addition to specifying the time step, the user can select the total duration of the analysis to be modeled. For the purposes of this thesis, durations between 0 and 7200 seconds were investigated.

With all of these parameters prepared, the model was ready for analysis. After running the solution, temperatures at any node at the end of the model duration were

graphically displayed using a post-processing function. The location of the leading edge of the char front was determined by finding the node with a temperature of 288°C. This procedure was repeated for each of the eight material property cases previously shown in Table 2.

The data that resulted was then compared with char depth values calculated from TR-10 methods. As will be discussed further in the Results chapter, some discrepancies appeared between the published data and the finite element results. The finite element results began to diverge from published data at approximately 1000 seconds, which related to a fire gas temperature of approximately 800°C. It was proposed that this discrepancy was likely due to the loss of insulation due to char degradation and consumption of the char layer in physical testing. The initial finite element model did not account for this effect.

Two methods for incorporating loss of char insulation were investigated. The first method approximated that the char depth was incorrect by an amount equal to the depth where 800°C was reached. This method approximated the char depth by adding the 288°C depth and 800°C depth. For the purposes of this thesis, this method was called the “additive method.” The additive method is illustrated in Figure 13.

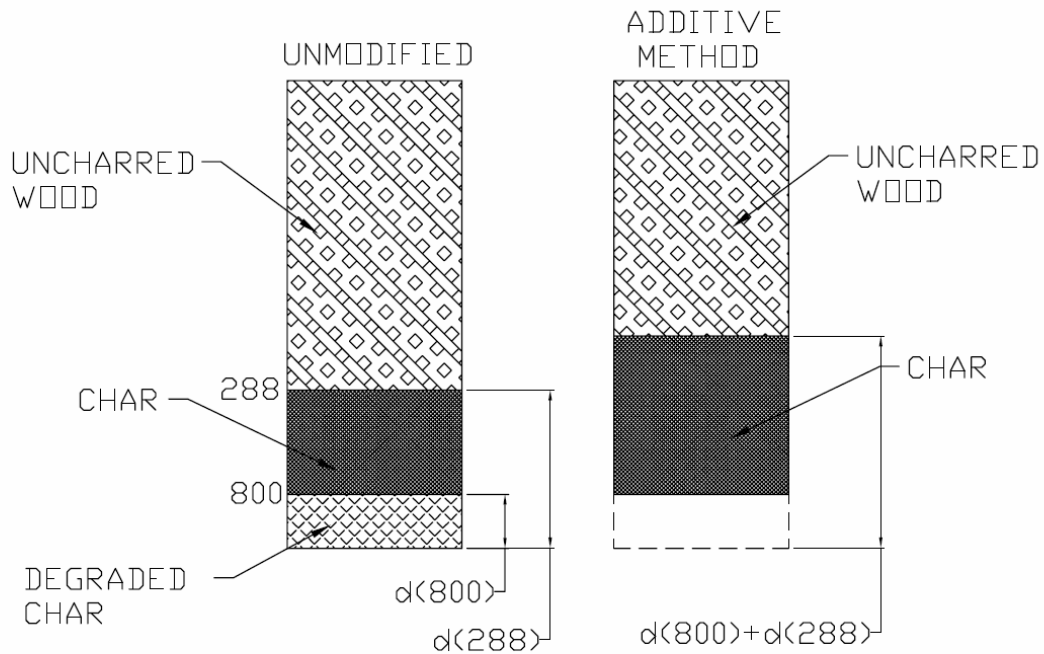


Figure 13 - Additive Method to Account for Char Consumption

The second approach to account for consumption of the char layer was based more on principles of heat transfer and simulating the properties of degraded char. ANSYS has a function that allows the user to “kill” an element based on its nodal results. ANSYS kills an element by making it infinitely flexible. In structural mechanics, this means that an element’s ability to resist mechanical loads would approach zero. In heat transfer, this means that the element’s ability to resist heat flow would approach zero. The kill command in ANSYS is problematic for transient thermal analyses because it is unable to restart a solution after its first time step. After investigating how ANSYS kills elements, it was determined that the same kill effect could be modeled by making the thermal conductivity substantially higher at the desired temperature. For this reason, the thermal conductivity was increased by approximately one order of magnitude for

temperatures greater than approximately 800°C. Figure 14 shows the revised thermal conductivity used in the char depth analyses.

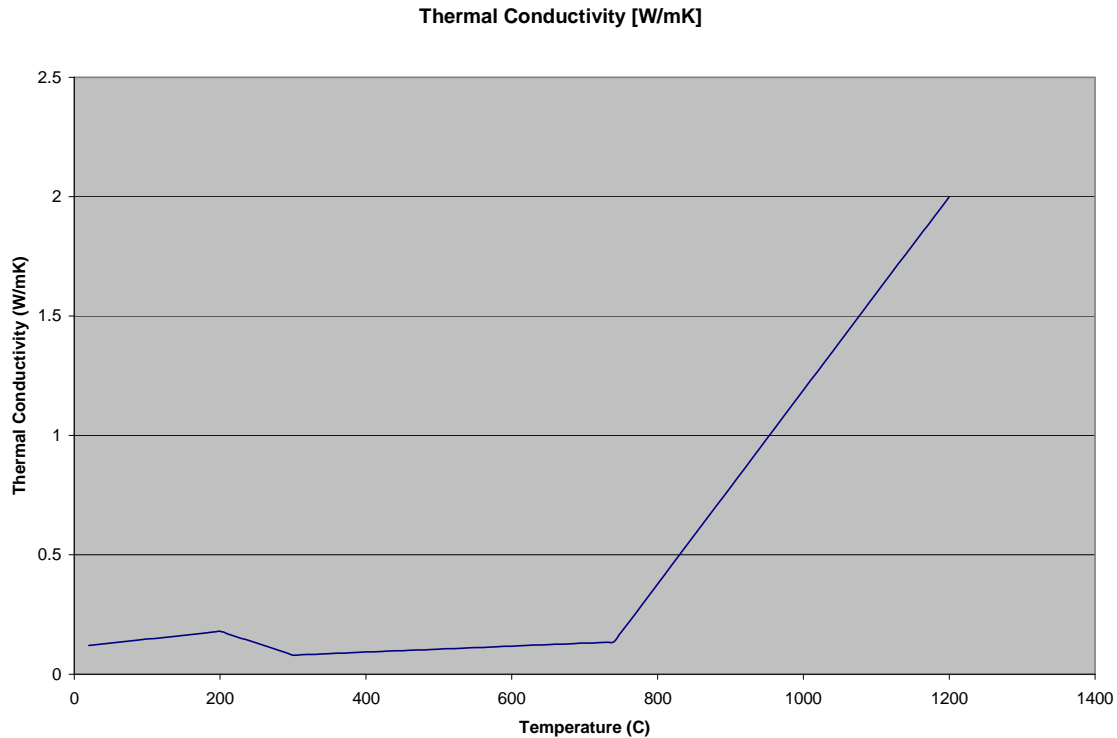


Figure 14 - Revised Thermal Conductivity

Although there is a divergence in solutions at 800°C, it was decided that the increase of thermal conductivity should change progressively over a range of temperatures because the material would not abruptly become infinitely flexible. For this reason, the thermal conductivity was increased by an order of magnitude between 740°C and 1200°C. The slope of the thermal conductivity increase was determined by trial and error to produce a char depth curve that had no abrupt changes in shape. For the purposes of this thesis, this method was called “progressive element death.” The char depth for this method was determined by the location of the node with a temperature of 288°C. Numerical expressions were then calculated for char depth as a function of time by fitting a third-order best fit curve to the data points.

3.3 Finite Difference Method in Excel

The finite difference method of heat transfer analysis was assembled in an Excel spreadsheet. Similar to the finite element method, finite difference analysis is dependent on material properties, loading conditions, nodal spacing, time step, and duration of analysis. The material properties used in the finite difference method were the same as the finite element method. Since the task of developing a finite difference model was completed after the finite element analysis, the modified thermal conductivity was also used to simulate degradation and consumption of the char layer. All eight cases of variation presented in Table 2 were also investigated with the finite difference method.

The spreadsheet development of the finite difference method was treated as a series of steady-state heat transfer analyses assembled piecewise. The temperature loading on the surface node was assumed to be equal to the ASTM E-119 temperatures, as a function of time. Using heat transfer equations discussed in the Background and Literature Review chapter, changes in temperature were calculated between nodes for each time step. The nodal spacing and time step were initially chosen arbitrarily and kept constant. The temperatures at each time step were calculated based on material properties and temperatures of the previous time step. The details of the calculations in the finite difference spreadsheet are developed in Chapter 4 Excel Spreadsheet Analysis Tools.

As will be discussed further in the Results chapter, some of the material cases for the finite difference model experienced instabilities that resulted in unreasonable data after particular times.

The model was refined such that the appropriate time step could be utilized to increase the stability of the model. The duration of each time step was calculated based on a relationship between the Fourier number (Fo) and material properties at that time step. According to one finite difference text, the Fourier number should be less than or equal to 0.5 for transient thermal analyses.⁷⁰ Equation 15 shows the relationship between the time step, nodal spacing, Fourier number, and material properties.

$$Fo = \frac{k}{\rho \cdot C_p} \cdot \frac{\Delta t}{(\Delta x)^2}$$

Equation 15⁷¹

By using the suggested Fourier number and selecting a nodal spacing, an appropriate time step duration for each node, at each time step was calculated. With the time step rationally determined, the efficiency and stability of the model was improved. This method is referred to as an adaptive time step, and its details are described in Chapter 4 Excel Spreadsheet Analysis Tools.

When the temperature of a node reached 288°C, char was considered to have reached that nodal depth. With successive nodal depths reaching 288°C at various times, the ordinates of char depth versus time were found. From these points, numerical expressions for char depth as a function of time were calculated based on a third-order best fit curve.

The char depth from the finite difference model was compared to the finite element and TR-10 char depths. These various expressions for char depth were then used in the development of a mechanics-based analytical tool.

⁷⁰ Croft, David R. "Heat Transfer Calculations Using Finite Difference Equations", Applied Science Publishers, Ltd., London, 1977. p.141

⁷¹ Ibid, p.140

3.4 Natural Fire Char Depth Analysis

Following the development and validation of the numerical char depth models for ASTM E-119 exposure, the performance of the char depth models was investigated for natural fire exposures. The size, duration, and intensity of natural fires are dependent upon fuel loads and ventilation available within a structure. Section four of the SFPE Handbook of Fire Protection Engineering characterizes natural fire time-temperature relationships by an equation that is a function of fuel load and opening factors. This equation was used to define two fire events.

The long duration – medium intensity (LD-MI) fire is intended to represent a fire that has a slowly burning fuel supply. This slowly burning fuel supply has a period of temperature growth similar to the ASTM E-119 design fire, but unlike the ASTM E-119, begins to decay. The short duration – high intensity (SD-HI) fire represents a fire in which the fuel supply is quickly consumed. The SD-HI fire reaches a higher maximum temperature than in the LD-MI fire, but temperature notably quicker than the LD-MI fire. The LD-MI and SD-HI natural fires were investigated for char depth modeling and time to failure analyses. These fires are compared graphically to the ASTM E-119 standard fire in Figure 15.

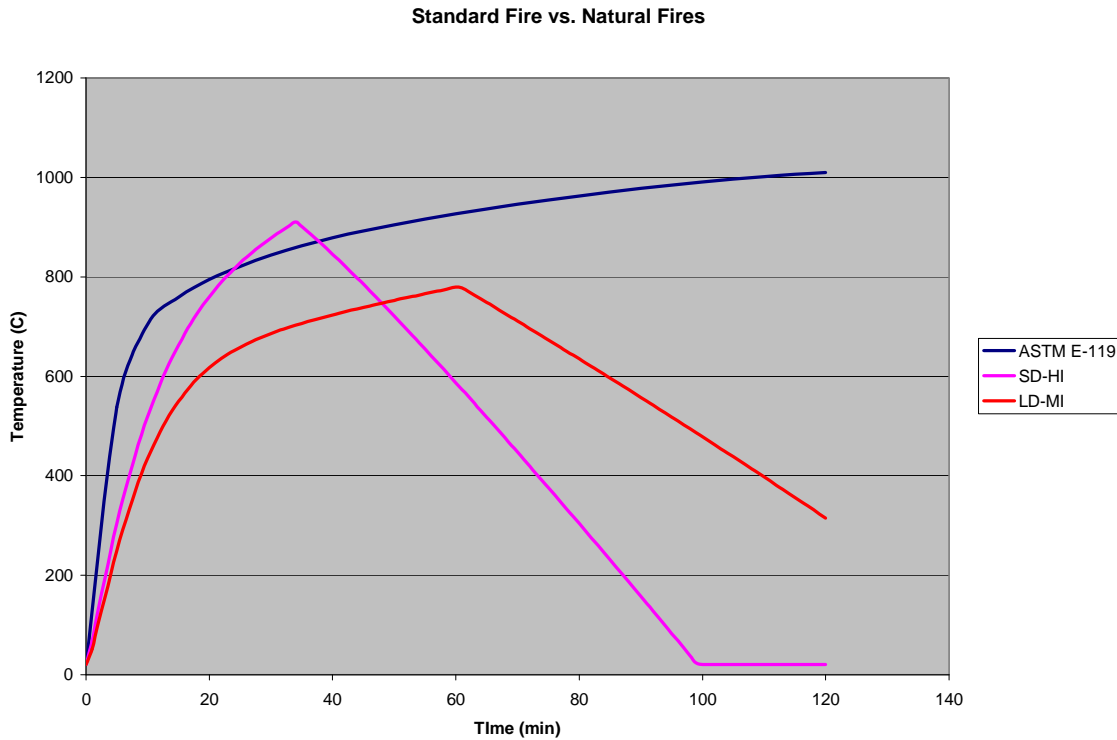


Figure 15 - LD-MI and SD-HI Natural Fires vs. ASTM E-119 Standard Fire

3.5 Mechanics-Based Analysis Tool in Excel

The primary objective of the mechanics-based analysis tool was to be able to predict analytically the performance of unprotected lightweight wood beams and columns. Because of the repetitive calculations required in this procedure, the proposed tool was assembled in an Excel spreadsheet. The details of the calculations used in the mechanics-based analysis tool, and the assembly of the spreadsheet are detailed in Chapter 4 Excel Spreadsheet Analysis Tools.

The most critical component of calculating fire resistance time was the expression of char. The char depth of the exposed member dictated how much effective cross-section remained. The analytical tool utilized the char depth expressions calculated from

the FEM and FDM models previously discussed. With a defined numerical expression for char depth, section properties such as cross-sectional area and section modulus were calculated as a function of time.

Using the same mechanics-based equations that would be used to analyze beams and columns at normal temperatures, capacity of beams and columns were calculated as a function of diminishing section properties. When the capacity of the member dropped below the required load, structural failure was concluded. For beams, failure was defined by exceeding allowable bending stresses. For long columns, failure was defined by exceeding allowable buckling stresses. For short columns, failure was defined by exceeding allowable compressive stresses. The time at which the element failed was considered the time to failure.

Time to failure from the mechanics-based analysis tool for members of large cross-section were compared for TR-10, finite element, and finite difference expressions of char depths. These fire resistance times were then compared to fire resistance time results of test fires documented in the TR-10. Following these benchmarking studies, the same three methods were investigated for members of lightweight cross-sections.

Furthermore, the finite element and finite difference procedures of char depth analysis and fire resistance time calculation were repeated for the LD-MI and SD-HI fires. This was done to determine whether any similarities between the two models extended to fire conditions other than the ASTM E-119.

4 Excel Spreadsheet Analysis Tools

As discussed in the Methodology chapter, FDM analysis calculations to determine char depth and mechanics-based analyses to calculate member time to failure were assembled in Excel spreadsheets. Because of the repetitive nature of the calculations, spreadsheets were critical in developing an efficient analytical approach. The spreadsheet formulation of analyses provided a transparent environment in which the user can see the calculations being performed. This chapter illustrates the details of the spreadsheets developed for this thesis.

4.1 *Finite Difference Method Char Depth Analysis*

There were two FDM char depth models investigated for this thesis. As will be discussed further in the Results chapter, an initial, sequentially assembled, steady-state heat transfer model led to unstable and unrepresentative results for char depth. The second FDM char depth analysis approach, using an adaptive time step, resulted in char depths that were more representative of the FEM char depths. For this reason, the FDM spreadsheets illustrating the adaptive time step model is the focus of this section. This spreadsheet is capable of calculating char depth curve data for ASTM E-119 exposure and a variety of natural fires for each of the eight material case variations discussed in the Methodology.

Figure 16 and Figure 17 represent two pieces of one integrated spreadsheet to evaluate char depth based on the three mentioned fire exposures. The two figures are shown separately for illustration purposes only. Figure 16 shows the input and output section of the FDM char depth analysis spreadsheet, and Figure 17 shows a sample of the

nodal calculations for temperature to establish the location of char. Input data from Figure 16 is utilized in the calculations shown in Figure 17. The results of these calculations are then shown in the output of Figure 16. Figure 17 only displays the surface and first interior node, which is only a small portion of the number of nodes used for analysis. A typical analysis involved 19 nodes. Table 3 and Table 4 annotate the specific cells identified in Figure 16 and Figure 17, respectively. These details include a brief description of the cell function, the equation used (if applicable), and the source of the equation used (if applicable).

Finite Difference element death by thermal conductivity			1
2	Fire	SD-HI	3
4	Opening Factor	0.08	8
5	Fire Load	15 kg/m ²	9
6	Fire Duration	34.1 minutes	10
7	Case?	Case 8	12
11	Density	Non Linear	480 [kg/m ³]
	C _p	Constant	1800 [kJ/kg*K]
	K	Constant	0.12 [W/mK]
	Fourier Number	0.5	13
	Nodal Spacing	0.005 [m]	14
			288
	Depth (mm)	Depth [m]	Time [sec]
	0	0	0
	5	0.0050	617.08824
	10	0.0100	909.65017
	15	0.0150	1210.3092
	20	0.0200	1589.6538
	25	0.0250	1949.2371
	30	0.0300	2416.6491
	35	0.0350	2943.7533
	40	0.0400	3764.9337
	45	0.0450	#N/A
	50	0.0500	#N/A
	55	0.0550	#N/A
	60	0.0600	#N/A
	65	0.0650	#N/A
	70	0.0700	#N/A
	75	0.0750	#N/A
	80	0.0800	#N/A
	85	0.0850	#N/A

Figure 16 - Finite Difference Char Depth Analysis Spreadsheet Input/Output

Table 3 - Finite Difference Char Depth Analysis Input/Output Details

Item	Description	Equation	Source
1	Fire exposure selection	Dropdown Selection	
2	Opening factor for natural fires only	Number	
3	Fuel load for natural fires only	Number	
4	Fire duration calculation	$[4] = \frac{60 \cdot [3]}{330 \cdot [2]}$	SFPE Handbook Ch. 4
5	Density condition	Based on Case Number	
6	Specific heat condition	Based on Case Number	
7	Thermal conductivity condition	Based on Case Number	
8	Ambient temperature density	Number	Background Chapter
9	Ambient temperature specific heat	Number	Background Chapter
10	Ambient temperature thermal conductivity	Number	Background Chapter
11	Fourier number	0.5 suggested	Croft
12	Nodal Spacing	Number	
13	Node depth	$[13] = [12] \cdot [node\# - 1]$	
14	Char time for corresponding node	Lookup where node=288°C	

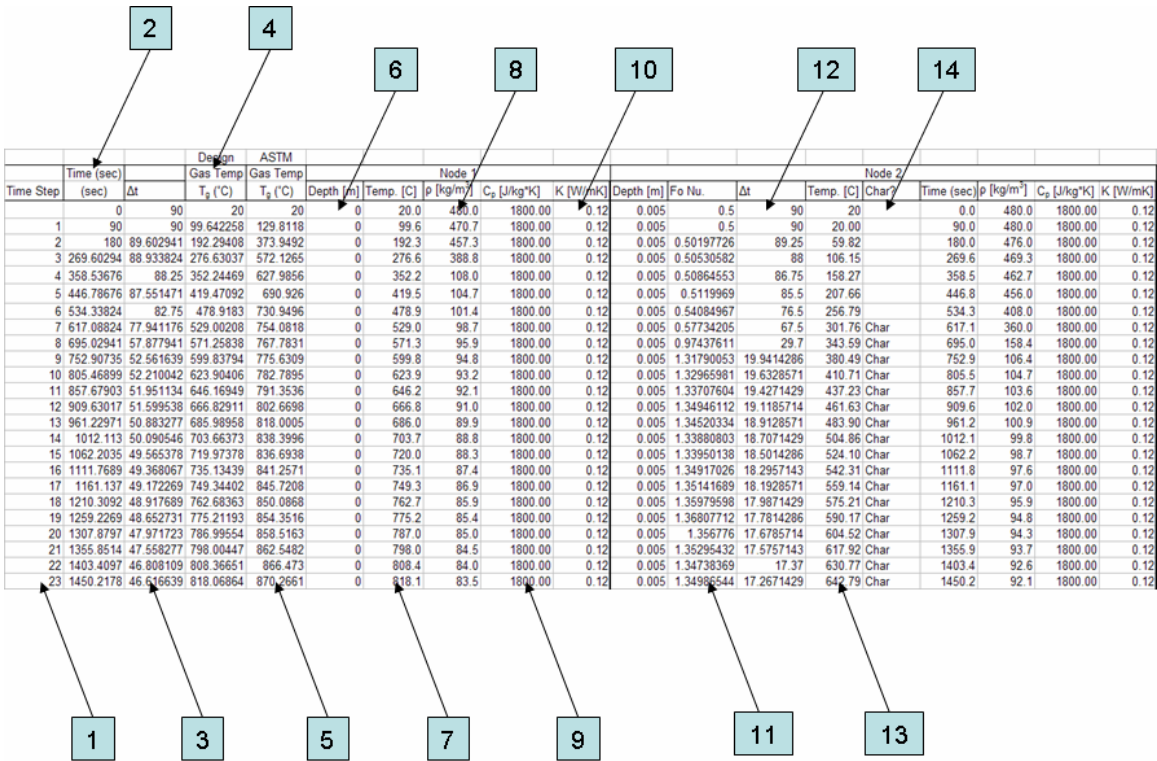


Figure 17 - Finite Difference Char Depth Analysis Spreadsheet Nodal Calculations

Table 4 - Finite Difference Char Depth Analysis Nodal Calculation Details

Item	Description	Equation	Source
1	Time step number	Number	
2	Time at particular time step	$[2]_n = [2]_{n-1} + [3]_{n-1}$	
3	Time step duration	$[3] = \text{mean}[\text{mean}[12]_{j=1 \rightarrow n}, \text{min}[12]_{j=1 \rightarrow n}]$	Original formulation
4	Fire exposure temperature	Calculated based on exposure, or equal to [5]	SFPE Handbook Ch.4
5	ASTM E-119 temperature	Lookup value from table	
6	Nodal Depth	$[6] = [\text{nodalspacing}] \cdot [\text{node\#} - 1]$	
7	Surface node temp	$[7] = [4]$	
8	Density at node-n	Lookup command finds tabulated values base on [7]	
9	Specific heat at node-n	Lookup command finds tabulated values base on [7]	
10	Thermal conductivity at node-n	Lookup command finds tabulated values base on [7]	
11	Calculated Fourier number at node-n, time-n	$[11]_n = \frac{[10]_n}{[9]_n \cdot [8]_n} \cdot [3]_n \cdot [\text{nodalspacing}]^2$	Croft
12	Calculated suggested time step duration at node-n, time-n	$[12]_n = \frac{Fo \cdot [\text{nodalspacing}]^2 \cdot [9]_n \cdot [10]_n}{[11]_n}$	Croft/original formulation for adaptive time step
13	Nodal temperature at node-n	$[13]_{n,n} = \frac{[13]_{n-1,n-1} + [13]_{n+1,n-1}}{2}$	Croft
14	Has the node charred at [2]?	$[14]_n = \text{"char"} \cdot \text{if}[13]_{n,n} \geq 288$	

4.2 Mechanics-Based Time to Failure Analysis

The primary objective of the mechanics-based analysis tool was to predict the performance of unprotected lightweight wood beams and columns. Because of the repetitive calculations required in this procedure, the proposed tool was assembled in an Excel spreadsheet. Three sets of analytical spreadsheets were developed for each of the three fire exposure cases investigated in this thesis. Each set of spreadsheets included separate analysis procedures for beams and columns.

4.2.1 Beams

Individual beam analysis spreadsheets were assembled for each of the three fire exposures investigated for this thesis because char depth expressions for each of the fire exposures were different. Incorporating all three exposures into one spreadsheet, with numerous analytical expressions for char depth, would significantly increase the complexity of the mechanics-based spreadsheet. Figure 18 and Figure 19 represent two pieces of one integrated beam analysis spreadsheet for ASTM E-119 exposure. The two figures are shown separately for illustration purposes only. Figure 18 shows the input and output data for the beam analysis. The input data includes member size, char evaluation method, material properties and design parameters, and the desired time step. This input data is used in calculations in the spreadsheet depicted in Figure 19. The output yields the time to failure of the beam from Figure 19 calculations, which are based on mechanics calculations from the NDS. Figure 19 demonstrates the calculation portion of the beam analysis spreadsheet. Table 5 and Table 6 detail the specific cells identified in Figure 18 and Figure 19, respectively. These details include a brief description of the cell function, the equation used (if applicable), and the source of the equation used (if applicable).

Mechanics-Based Design Method			
	Beams	ASTM	
1	β_n	1.5 in/hr	Assumed Char Rate
	Exposure	Sided Exposure	
3	Member size	2x10	
	Char Evaluation Method	Case 2 - FDM Progressive Death	
5	Valid Duration	7200 seconds	
	F_b	2400 psi	
7	C_D	1.00	
	C_M	1.00	
9	C_t	1.00	
	C_L	1.00	
	C_V	0.98	
12	F_c'	2352 psi	
	M'	4192.6 ft-lbs	
14	B	1.54 inches	
	D	9.25 inches	
16	R	0.5 Percent to Design Capacity	
	K	2.85 Adjustment Factor	
18	Timestep	200 seconds	
	t_f	13.3	
	t_f	13.3	
20	t_f	13.3 minutes	Time to Failure

Figure 18 - Mechanics-Based Beam Analysis Input/Output

Table 5 - Mechanics-Based Beam Analysis Input/Output Details

Item	Description	Equation	Source
1	# of sides of exposure	Dropdown menu selection	
2	Member size	Dropdown menu selection	
3	Char depth evaluation method	Dropdown menu selection	
4	Duration for which [3] is valid	Automatic Lookup command	Based on char depth evaluation method
5	Tabulated bending stress, F_b	Number – ambient conditions	NDS – Supplement
6	Size factor, C_F	Number – ambient conditions	NDS – 4.3.2
7	Wet service factor, C_M	Number – ambient conditions	NDS – 4.3.3
8	Temperature factor, C_t	Number – ambient conditions	NDS – 4.3.4
9	Beam stability factor, C_L	Number – ambient conditions	NDS – 4.3.5
10	Beam volume factor – for glulam, C_V	Number – ambient conditions	NDS
11	Allowable bending stress, F_b'	$[11] = [5] \cdot [6] \cdot [7] \cdot [8] \cdot [9] \cdot [10]$	NDS – 4.3
12	Moment capacity about major axis [ft-lbs]	$[12] = \frac{[13] \cdot [14]^2}{6} \cdot \frac{1}{12}$	
13	Member width	Automatic Lookup command, based on [2]	
14	Member depth	Automatic Lookup command, based on [2]	
15	Loading - % to design capacity	Number	
16	Ultimate stress adjustment factor	Number, [16]=2.85 for beam bending	NDS – 16.2.2
17	Time step duration	Number	
18	Time to failure	Lookup [Rs<1.0]	TR-10
19	Time to failure	Lookup [load ratio]>1.0	TR-10
20	Time to failure	$[20] = \min\{[18],[19]\}$	

time [sec]	Char Depth [in]	Unmodified [mm]	A(t) [in ²]	S _{xx} (t) [in ³]	S _{yy} (t) [in ³]	I _{xx} (t) [in ⁴]	I _{yy} (t) [in ⁴]	M' [ft-lbs]	R _s	1/R _s	Load Ratio
0	0	0	13.875	21.39063	3.46875	98.93164	2.601563	11948.8	2.85	0.350877	0.154386
200	0.1315816	2.79	11.278	17.13958	2.32484	78.14293	1.437724	9574.17	2.283608	0.437904	0.2189518
400	0.2580239	5.46	8.847674	13.25968	1.450948	59.61536	0.713832	7406.857	1.766666	0.566038	0.283019
600	0.3795084	8.03	6.572885	9.717453	0.811733	43.09929	0.30074	5428.17	1.294714	0.772371	0.3861857
800	0.4962165	10.50	4.443132	6.48237	0.375865	28.37263	0.095388	3621.052	0.863685	1.15783	0.578915
1000	0.6083295	12.88	2.448539	3.526578	0.115629	15.23776	0.016381	1969.947			
1200	0.716029	15.16	0.579816	0.824689	0.006566	3.518935	0.000223	460.6711			
1400	0.8194962	17.35	0	0	0	0	0	0			

Figure 19 - Mechanics-Based Beam Analysis Calculations Spreadsheet

Table 6 - Mechanics-Based Beam Analysis Calculations Spreadsheet Details

Item	Description	Equation	Source
1	Time	$[1]_n = [1]_{n-1} + \Delta t$	
2	Char depth	$[2]_n = \frac{1.2 \cdot [3]_n}{25.4}$	
3	Unmodified char depth from FDM/FEM analyses	Varies based on char depth analysis method	TR-10/FEM/FDM analyses
4	Cross-sectional area	$[4]_{n,3-sided} = [width - 2 \cdot [2]_n] \cdot [depth - [2]_n]$ $[4]_{n,4-sided} = [width - 2 \cdot [2]_n] \cdot [depth - 2 \cdot [2]_n]$	TR-10
5	Section modulus about major axis, S_{x-x}	$[5]_{n,3-sided} = \frac{[width - 2 \cdot [2]_n] \cdot [depth - [2]_n]^2}{6}$ $[5]_{n,4-sided} = \frac{[width - 2 \cdot [2]_n] \cdot [depth - 2 \cdot [2]_n]^2}{6}$	TR-10
6	Section modulus about minor axis, S_{y-y}	Same eqns. as [5], but switch width and depth	
7	Moment of inertia about major axis, I_{x-x}	$[7]_{n,3-sided} = \frac{[width - 2 \cdot [2]_n] \cdot [depth - [2]_n]^3}{12}$ $[7]_{n,4-sided} = \frac{[width - 2 \cdot [2]_n] \cdot [depth - 2 \cdot [2]_n]^3}{12}$	TR-10
8	Moment of inertia about minor axis, I_{y-y}	Same eqns. as [7], but switch width and depth	
9	Moment capacity about major axis	$[9]_n = F_b' \cdot K \cdot [5]_n$	NDS
10	Maximum design load ratio, R_s	$[10]_n = \frac{K \cdot [5]_n}{[5]_1 \cdot C_D \cdot C_M \cdot C_t}$	TR-10
11	Reciprocal maximum design load ratio	$[11]_n = \frac{1}{[10]_n}$	
12	Load ratio	$[12]_n = \frac{[5]_1 \cdot R}{[5]_n \cdot K}$	Original formulation

4.2.2 Columns

Individual column analysis spreadsheets were assembled for each of the three fire exposures investigated for this thesis because char depth expressions for each of the fire exposures were different. Incorporating all three exposures into one spreadsheet, with numerous analytical expressions for char depth for each exposure, would significantly increase the complexity of the mechanics based spreadsheet. Figure 20 and Figure 21 represent two pieces of one integrated column analysis spreadsheet for ASTM E-119 exposure. The two figures are shown separately for illustration purposes only. Figure 20 shows the input and output data for the column analysis spreadsheet. The input data includes member size, model geometry, initial loading, char evaluation method, material properties and design parameters, and the desired time step. This input data is used in calculations in the spreadsheet depicted in Figure 21. The output yields the time to failure of the column from Figure 21 calculations, which are based on mechanics calculations from the NDS. Figure 21 demonstrates the calculation portion of the column analysis spreadsheet. Table 7 and Table 8 detail the specific cells identified in Figure 20 and Figure 21, respectively. These details include a brief description of the cell function, the equation used (if applicable), and the source of the equation used (if applicable).

New Mechanics-Based Design Method			
2	Columns	ASTM	1
4	β_n	1.5	3
4	Exposure	4-Sided Exposure	5
6	Material Type	Sawn Lumber	7
6	E'	1700000 psi	7
8	F_c	2200 psi	9
8	c	0.8	9
8	C_D	1.25	9
8	C_M	1	10
8	C_t	1	10
11	P_{dead}	500 lbs	12
13	P_{live}	1000 lbs	14
13	P_{total}	1500 lbs	14
15	P'	5831.2 lbs	16
15	F_c'	2536 psi	16
17	F_{cE}	761.6 psi	18
17	α_c	0.304	18
19	C_p	0.279	20
19	F_c''	706.4 psi	20
21	r_s	0.26	22
21	Member size	2x6	22
23	Char Evaluation Method	Case 2 - FDM Progressive Death	24
23	Valid Duration	7200 seconds	24
25	B	1.5 inches	26
25	D	5.4 inches	26
27	K_e	1	28
27	L	16.0 in	28
27	D	1.5	28
29	Timestep	200 seconds	30
31	t_r	13 minutes	30
31	t_r	14 minutes	30
31	t_r	13 minutes	30
			Time to Failure

Figure 20 - Mechanics-Based Column Analysis Input/Output Spreadsheet

Table 7 - Mechanics-Based Column Analysis Input/Output Spreadsheet Details

Item	Description	Equation	Source
1	Nominal char rate	Number, 1.5	TR-10
2	Sides of exposure	Dropdown selection	
3	Material type	Dropdown selection	
4	Modulus of elasticity, E	Number	NDS
5	Tabulated compression stress, F_c	Number	NDS
6	Stability calculation parameter, c	[6]=0.8 for sawn lumber [6]=0.8 for glulam	NDS – 3.7.1
7	Load duration factor – ambient, C_D	Number	NDS – 4.3.1
8	Wet service factor – ambient, C_M	Number	NDS – 4.3.3
9	Temperature factor – ambient, C_t	Number	NDS – 4.3.4
10	Axial dead load, P_{dead}	Number	
11	Axial live load, P_{live}	Number	
12	Total axial load, P_{total}	[12]=[10]+[11]	
13	Allowable axial load, P'	[13]=[18]*Area	
14	Adjusted compressive stress, F_c^*	[14]=[5]*[7]*[8]*[9]	NDS – 4.3
15	Critical buckling compressive stress, F_{cE}	Number	NDS - 3.7.1
16	Compressive stress ratio, α_c	[16]=[15]/[14]	
17	Column stability factor, C_p	[17] = $\frac{1+[16]}{2-[6]} - \sqrt{\left[\frac{1+[16]}{2-[6]}\right]^2 - \frac{[16]}{[6]}}$	NDS – 3.7.1
18	Allowable compressive stress, F_c'	[18]=[17]*[14]	NDS – 4.3
19	Design capacity load ratio, r_g	[19]=[12]/[13]	
20	Member size	Dropdown selection	
21	Char evaluation method	Dropdown selection	
22	Duration for which [21] is valid	Automatic lookup function	
23	Member width	Automatic lookup function based on [20]	
24	Member depth	Automatic lookup function based on [20]	
25	Buckling length coefficient, K	Number, 1.0 for pin-ended members	
26	Column height	Number	
27	Member dimension in unbraced dimension	Number, [23] or [24]	
28	Time step duration	Number	
29	Time to failure	Lookup [Rs<1.0]	TR-10
30	Time to failure	Lookup [load ratio]>1.0	TR-10
31	Time to failure	[31]=min{[29],[30]}	

time [sec]	Char Depth [in]	Unmodified [mm]	A(t) [in ²]	d [in]	I _{xx} (t) [in ⁴]	F _{cE} (t) [psi]	α _c (t)	C _p (t)	F _c ' (t) [psi]	P' (t) [lbs]	R _s (t)	1/R _s (t)	Load Ratio
0	0	0	8.25	5.5	20.79688	1546.07	0.272387	0.25494	1447.0	11938.1	2.03	0.49	0.126
200	0.1315816	2.79	6.477112	5.236837	14.80261	1401.65	0.246944	0.232814	1321.5	8559.2	1.44	0.69	0.175
400	0.2580239	5.46	4.90397	4.983952	10.15113	1269.55	0.22367	0.212234	1204.6	5907.5	0.99	1.01	0.254
600	0.3795084	8.03	3.512989	4.740983	6.580098	1148.79	0.202394	0.193147	1096.3	3851.3	0.64	1.56	0.389
800	0.4962165	10.50	2.287893	4.507567	3.873814	1038.45	0.182955	0.175485	996.1	2278.9	0.38	2.64	0.658
1000	0.6083295	12.88	1.213646	4.283341	1.855565	937.71	0.165206	0.159179	903.5	1096.5			
1200	0.716029	15.16	0.276385	4.067942	0.381138	845.77	0.149008	0.144152	818.2	226.1			
1400	0.8194962	17.35	0	3.861008	0	761.91	0.134234	0.130328	739.7	0.0			

Figure 21 - Mechanics-Based Column Analysis Calculations Spreadsheet

Table 8 - Mechanics-Based Column Analysis Calculations Spreadsheet Details

Item	Description	Equation	Source
1	Time	$[1]_n = [1]_{n-1} + \Delta t$	
2	Char depth	$[2]_n = \frac{1.2 \cdot [3]_n}{25.4}$	
3	Unmodified char depth from FDM/FEM analyses	Varies based on char depth analysis method	TR-10/FEM/FDM analyses
4	Cross-sectional area	$[4]_{n,3-sided} = [width - 2 \cdot [2]_n] \cdot [depth - [2]_n]$ $[4]_{n,4-sided} = [width - 2 \cdot [2]_n] \cdot [depth - 2 \cdot [2]_n]$	TR-10
5	Member depth	$[5] = D - 2 \cdot [2]$	
6	Moment of inertia about major axis, I_{x-x}	$[6]_{n,3-sided} = \frac{[width - 2 \cdot [2]_n] \cdot [depth - [2]_n]^3}{12}$ $[6]_{n,4-sided} = \frac{[width - 2 \cdot [2]_n] \cdot [depth - 2 \cdot [2]_n]^3}{12}$	TR-10
7	Critical buckling compressive stress, $F_{cE}(t)$	$[7] = \frac{2.03 \cdot 0.418 \cdot E'}{\left(\frac{l}{[5]}\right)^2}$	NDS – 16.2.2
8	Compressive stress ratio, $\alpha_c(t)$	$[8] = \frac{[7]}{2.58 \cdot F_c}$	
9	Column stability factor, $C_p(t)$	$[9] = \frac{1 + [8]}{2 \cdot c} - \sqrt{\left[\frac{1 + [8]}{2 \cdot c}\right]^2 - \frac{[8]}{c}}$	
10	Allowable compressive stress, $F_c'(t)$	$[10] = 2.58 \cdot [9] \cdot F_c$	
11	Allowable axial load, $P'(t)$	$[11] = [10] \cdot [4]$	
12	Maximum design load ratio, R_s	$[12] = \frac{2.03 \cdot [6]}{C_m \cdot C_t \cdot r_s}$	
13	Reciprocal maximum design load ratio	$[13] = \frac{1}{[12]}$	
14	Load ratio	$[14] = \frac{1}{\left(\frac{[11]_e}{[11]_i}\right)}$	

5 Results

This chapter compares and summarizes results from Finite Element Method (FEM), Finite Difference Method (FDM), and TR-10 models of char depth for the ASTM E-119 standard fire. Additionally, Finite Element Method and Finite Difference Method char depth models for LD-MI, and SD-HI design fires are considered. By benchmarking the Finite Element Method models with published methods or data, the models can serve as a proxy for physical tests where wood sections are exposed to fires other than the ASTM E-119 temperature curve. Finite Difference Method models are then compared to corresponding FEM models to validate their use as an economical and transparent desktop alternative for Finite Element Method models.

The results of these char depth models are further compared by the impact that they have on the mechanics-based analysis for calculating beam and column time to failure. To benchmark the validity of the FEM and FDM models, they are compared to TR-10 analyses for various beam and column tests discussed in the TR-10. Because of the volume and graphical nature of the data that was generated, representative data will be presented. More complete sets of graphs are presented in a larger format in Appendix B through Appendix F.

5.1 Char Depth Models

The most critical component for calculating the performance of wood beams and columns exposed to fire is the loss of cross-section due to charring. The following sections provide results from FEM and FDM models for wood exposed to ASTM E-119,

LD-MI, and SD-HI time-temperature curves. The char depth predictions from some of these models are then utilized in the mechanics-based analysis to predict time to failure of beams and columns.

5.1.1 ASTM E-119 Fire

The TR-10 char depth expression is based on experimental test data obtained from wood sections exposed to the ASTM E-119 standard fire. The FEM char depth models are compared to the TR-10 char depth to establish their reliability for serving as a proxy for physical fire tests. Because both approaches were based on similar material properties and the same fire conditions, similar char depth results would validate the FEM model and justify its use to synthesize alternative fire conditions. Figure 22 shows the TR-10 expression of char depth as a function of time.

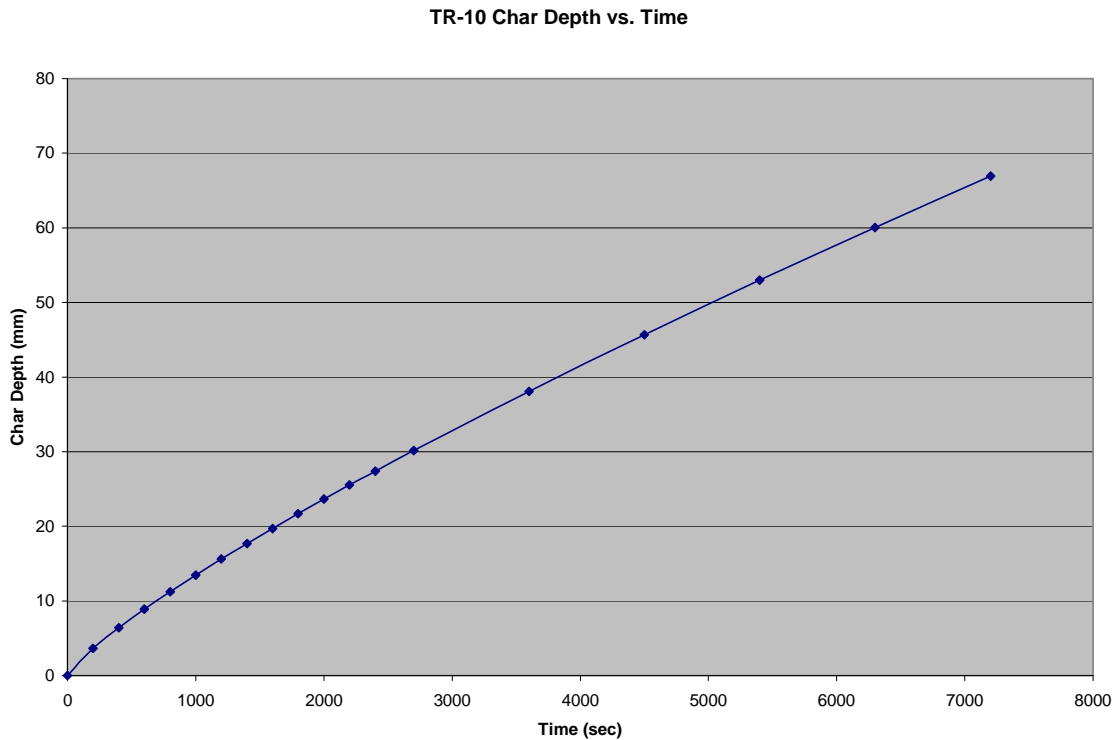


Figure 22 - TR-10 Char Depth vs. Time

Initially, it was believed that material property Case 4 from Table 2 would lead to the most accurate finite element model. Different from the other seven cases, Case 4 made no simplifying assumptions that any of the material properties were constant. Since all three material properties varied as a function of temperature, Case 4 was thought to best represent the behavior of the charring of wood. Figure 23 provides comparison of the finite element results from Case 4 with the char depth expression from the TR-10.

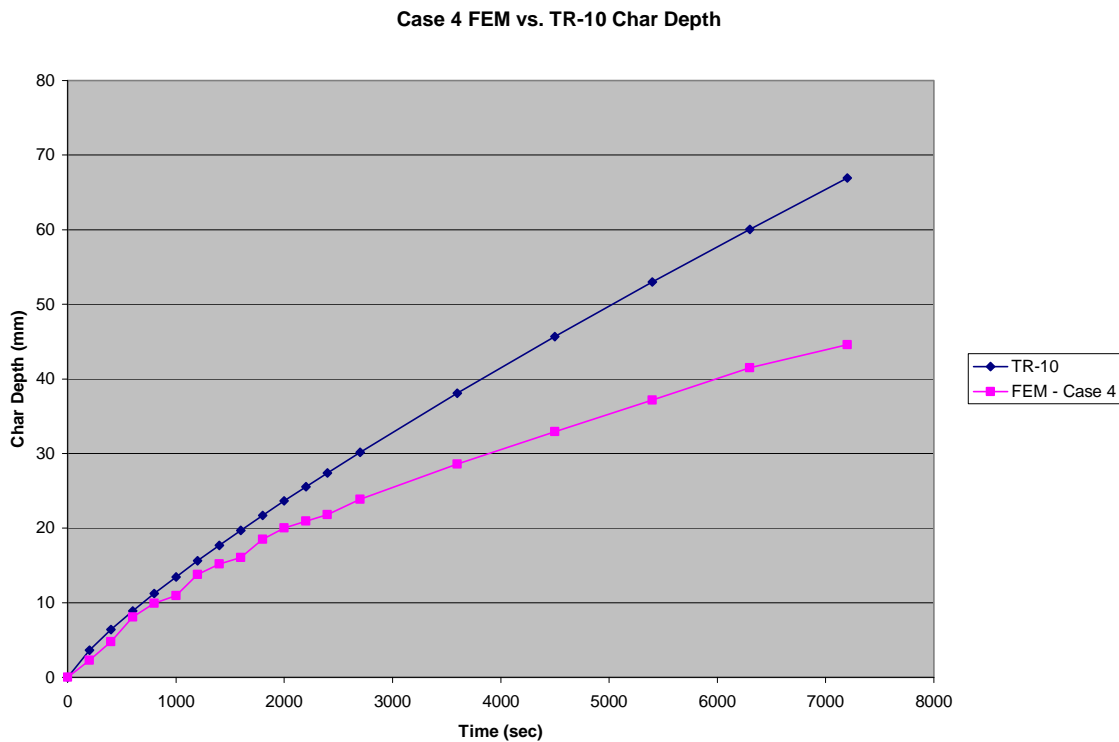


Figure 23 - Case 4 FEM vs. TR-10 Char Depth

Figure 23 demonstrates that there is a notable divergence of the FEM Case 4 from the TR-10 char depth. The FEM model increasingly underestimates the char depth as a function of time. As discussed in the Methodology, this discrepancy between the two sets of data was likely due to the loss of insulation in the actual test specimen as the char degraded and was consumed with increasing material temperatures. The divergence of

the two char depths occurs at approximately 1000 seconds. On the ASTM E-119 time-temperature curve, this time corresponds to approximately 800°C.

Two modeling techniques, the Additive Method and the Progressive Element Death Method, were investigated to simulate the loss of insulation due to char degradation. These methods are discussed in the Methodology. Figure 24 illustrates the results of modifying the FEM Case 4 model by using the Additive Method and the Progressive Element Death Method. By considering the loss of insulation due to the degradation and consumption of the char material at temperatures above 800°C, the FEM Case 4 model provided char depth data that was more similar to the TR-10 expression. For FEM Case 4, the Additive Method provided better correlation with the TR-10 data than the Progressive Element Death Method.

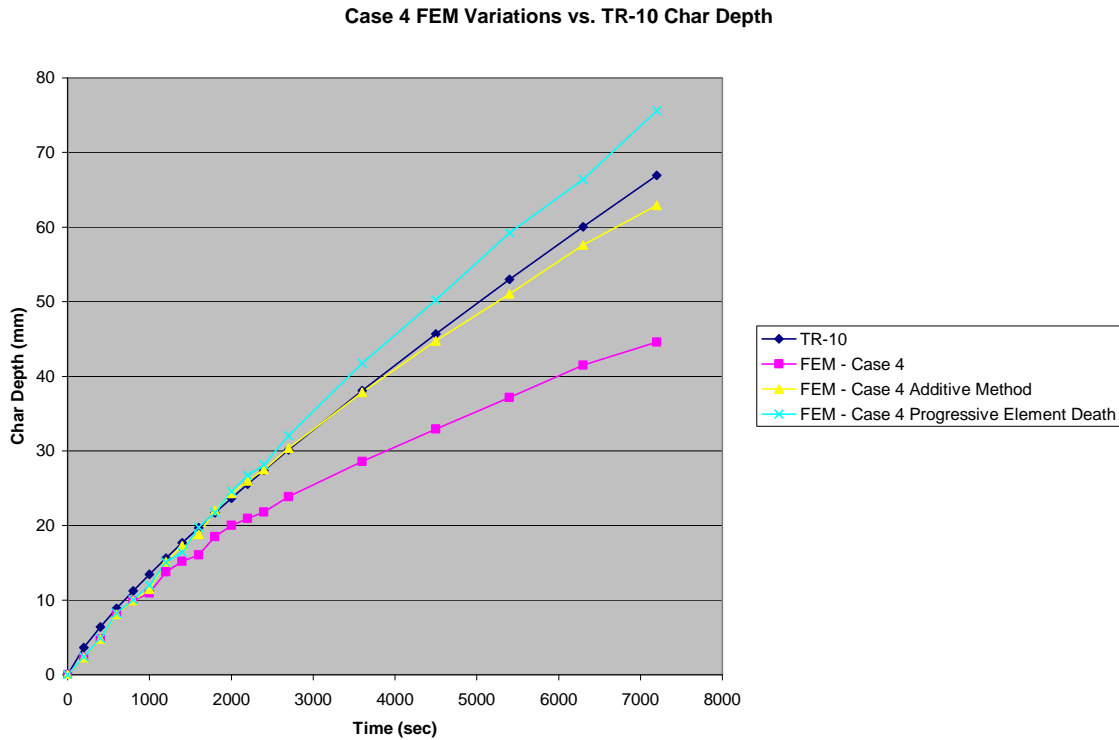


Figure 24 - FEM Case 4 Variations vs. TR-10 Char Depths

There were two practical limitations for these modifications to consider before developing the other seven cases defined in Table 2. The first limitation was that the Additive Method would increase the complexity of the finite difference evaluation of char depth by requiring depth vs. time curves for both 288°C and 800°C. The other limitation was that for studies involving constant thermal conductivity (i.e. Cases 1,6,7, and 8 in Table 2), the Progressive Element Death Method would neglect char degradation and consumption. Char degradation would be neglected because the material was “killed” by increasing the thermal conductivity by an order of magnitude at a desired temperature. With a constant thermal conductivity for all temperatures, the element death would not take place.

Although the Progressive Element Death Method would neglect char degradation for cases of constant thermal conductivity, it would not increase the complexity of the finite difference evaluations. Adaptation of the technique would not be complicated because only a slight change of the expression for thermal conductivity is necessary. As shown in Figure 24, Progressive Element Death and Additive methods appear to be similarly effective for modifying the numerical analysis to incorporate char degradation and consumption, where thermal conductivity is not constant. With this consideration, the Progressive Element Death Method was used for the remainder of the FEM and FDM analyses. The FEM and FDM models were not modified where thermal conductivity remained constant.

Figure 25 through Figure 32 enable comparison of the eight material property cases, modeled using the finite element method with the TR-10 char depths. Progressive Element Death was incorporated in Cases 2, 3, 4, and 5 (Figure 26 through Figure 29).

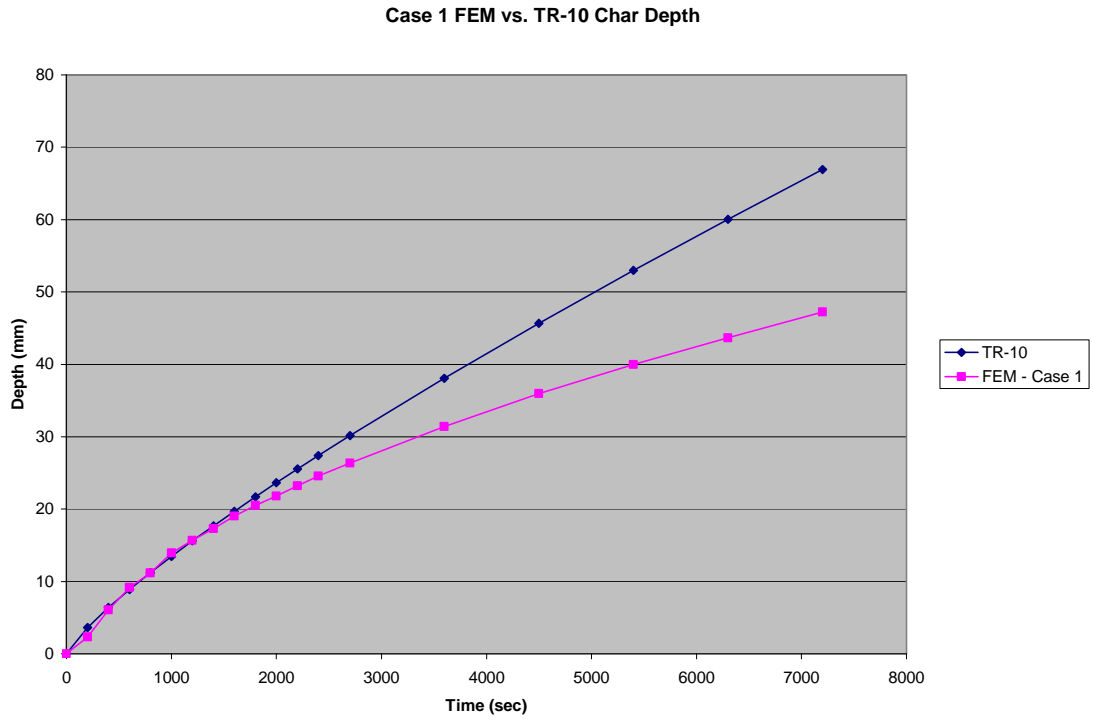


Figure 25 - FEM Case 1 vs. TR-10 Char Depth
 Constant Density, Constant Specific Heat, Constant Thermal Conductivity

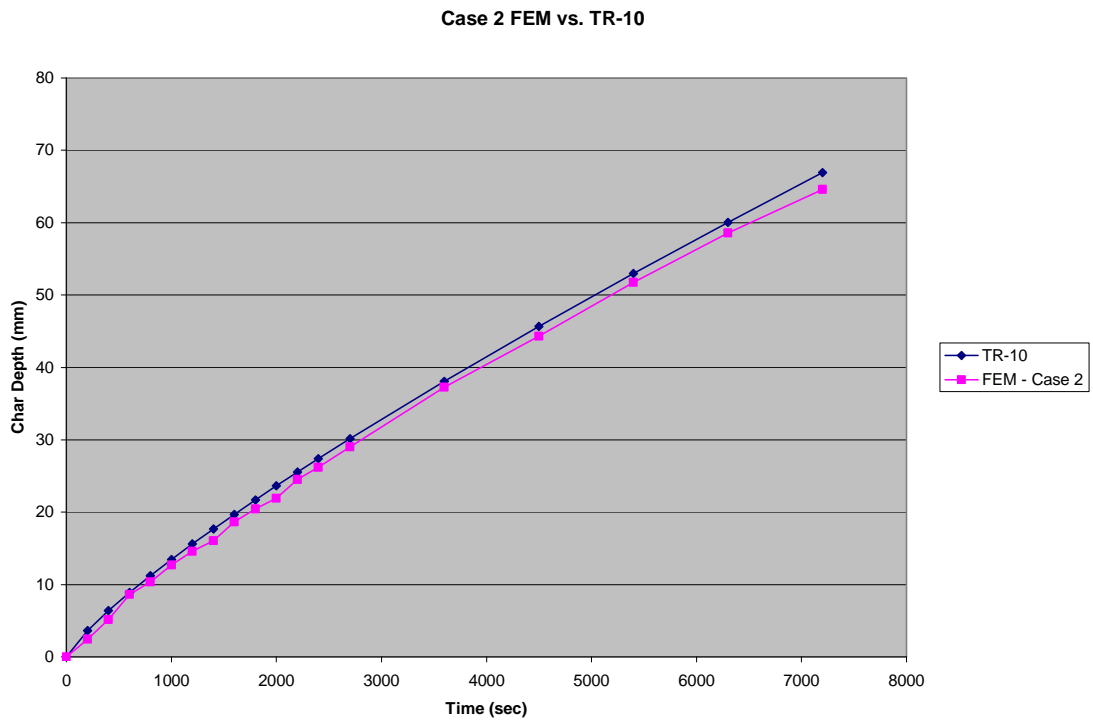


Figure 26 - FEM Case 2 vs. TR-10 Char Depth
 Constant Density, Constant Specific Heat, Non-Linear Thermal Conductivity

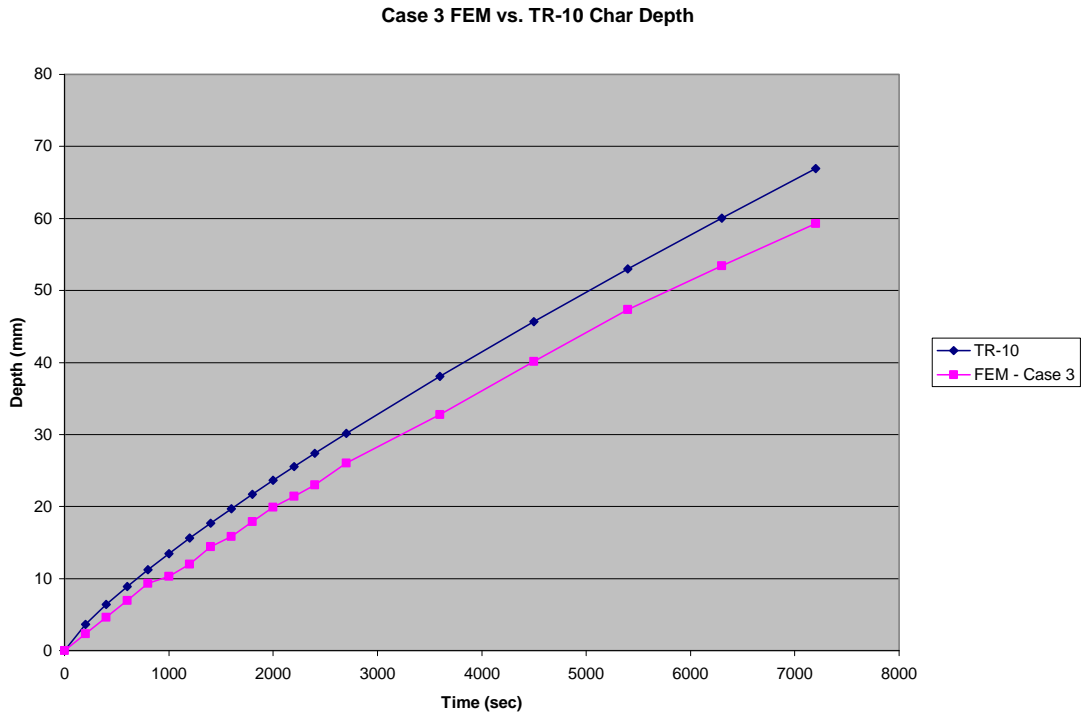


Figure 27 - FEM Case 3 vs. TR-10 Char Depth
Constant Density, Non-Linear Specific Heat, Non-Linear Thermal Conductivity

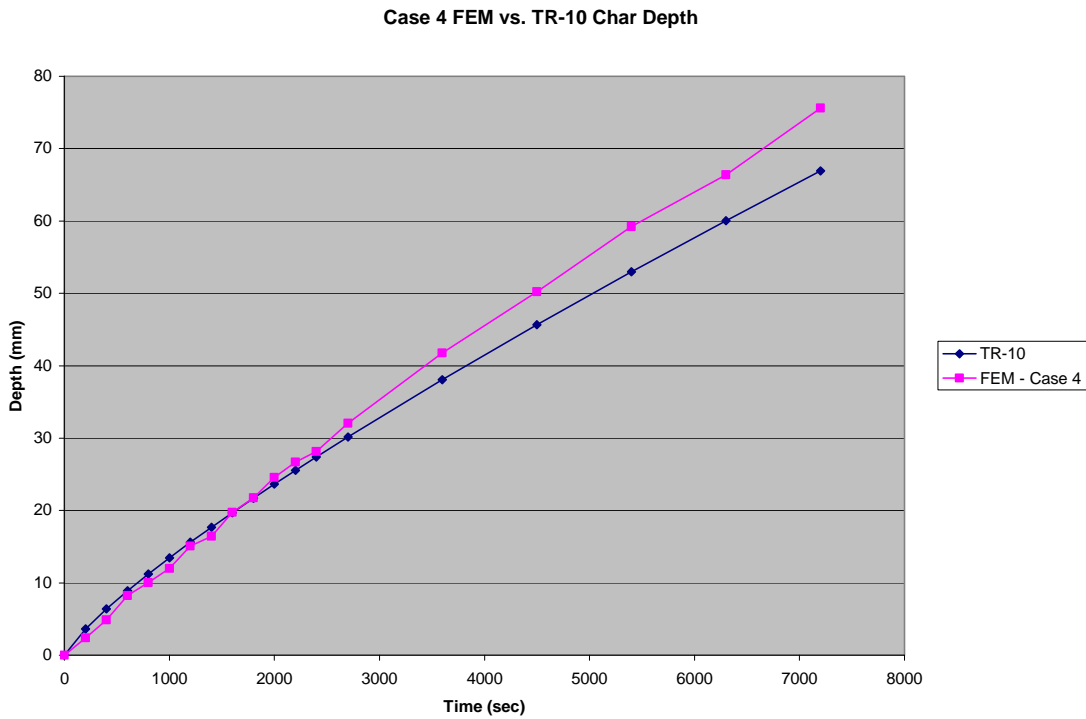


Figure 28 - FEM Case 4 vs. TR-10 Char Depth
Non-Linear Density, Non-Linear Specific Heat, Non-Linear Thermal Conductivity

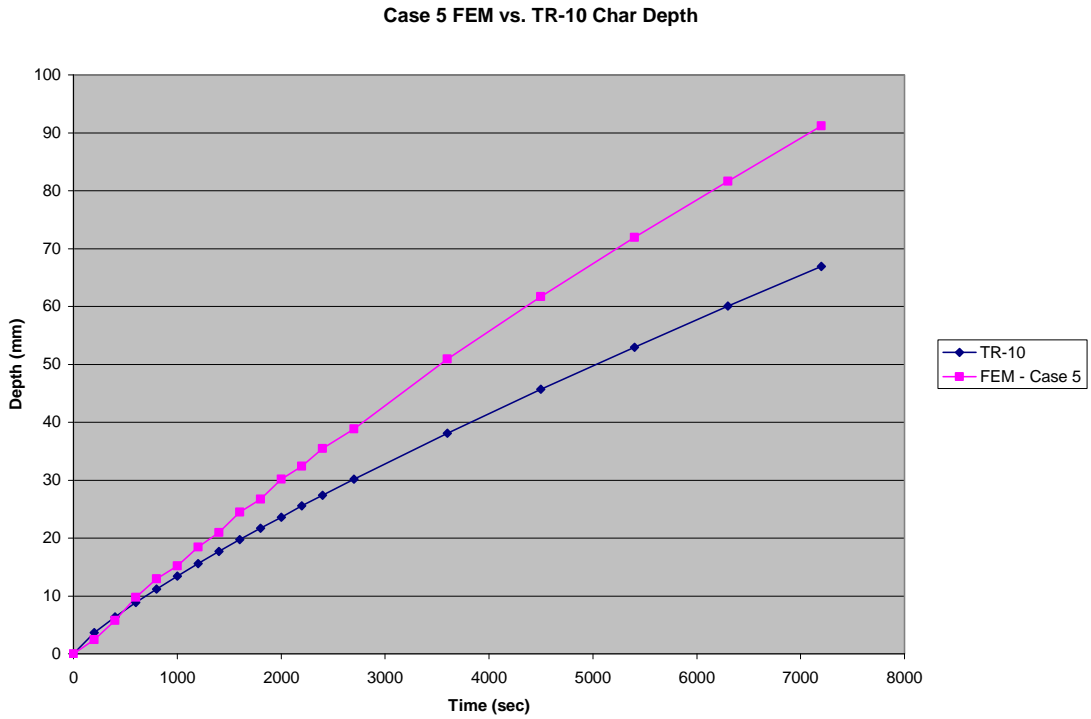


Figure 29 - FEM Case 5 vs. TR-10 Char Depth
Non-Linear Density, Constant Specific Heat, Non-Linear Thermal Conductivity

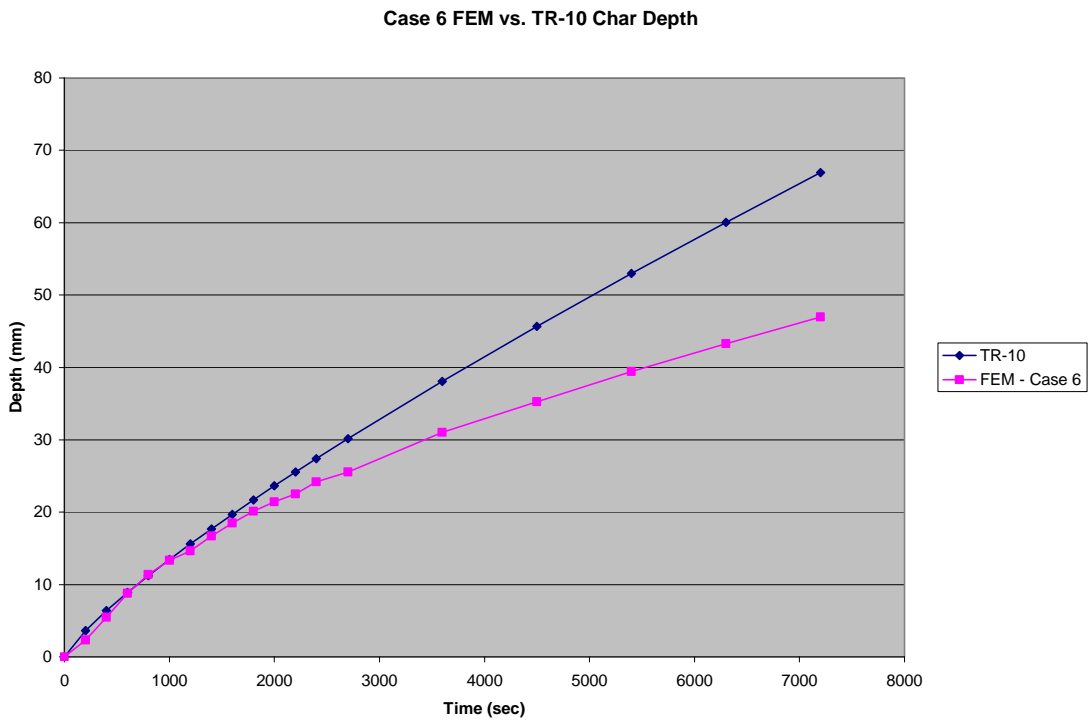


Figure 30 - FEM Case 6 vs. TR-10 Char Depth
Non-Linear Density, Non-Linear Specific Heat, Constant Thermal Conductivity

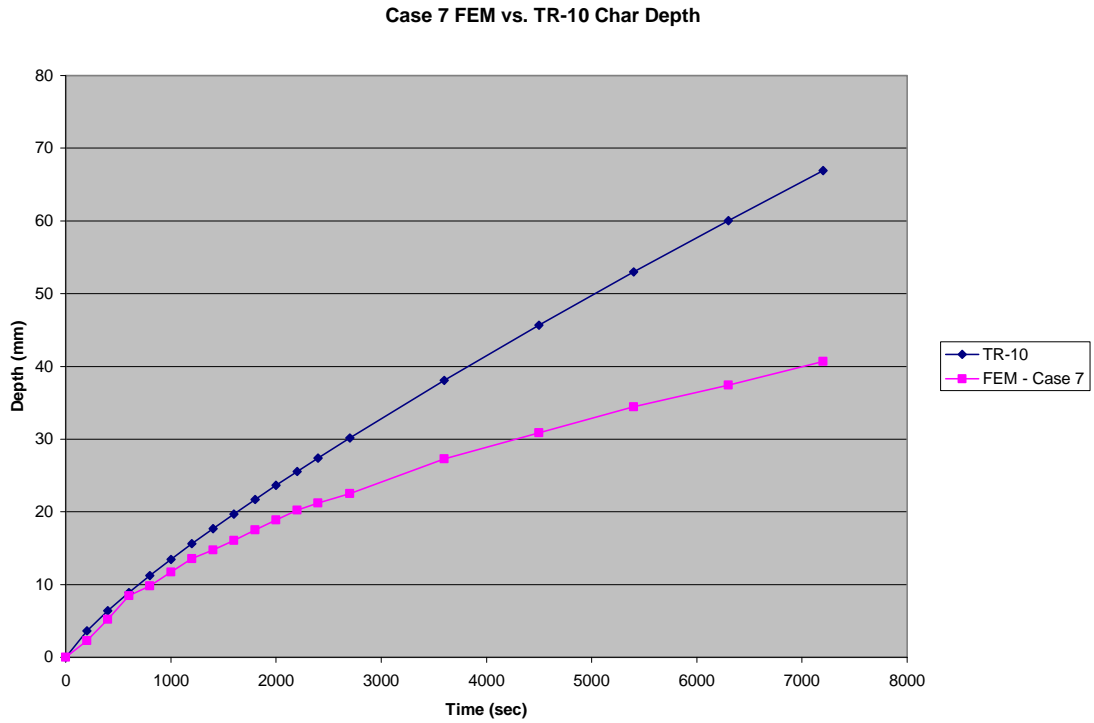


Figure 31 - FEM Case 7 vs. TR-10 Char Depth
 Constant Density, Non-Linear Specific Heat, Constant Thermal Conductivity

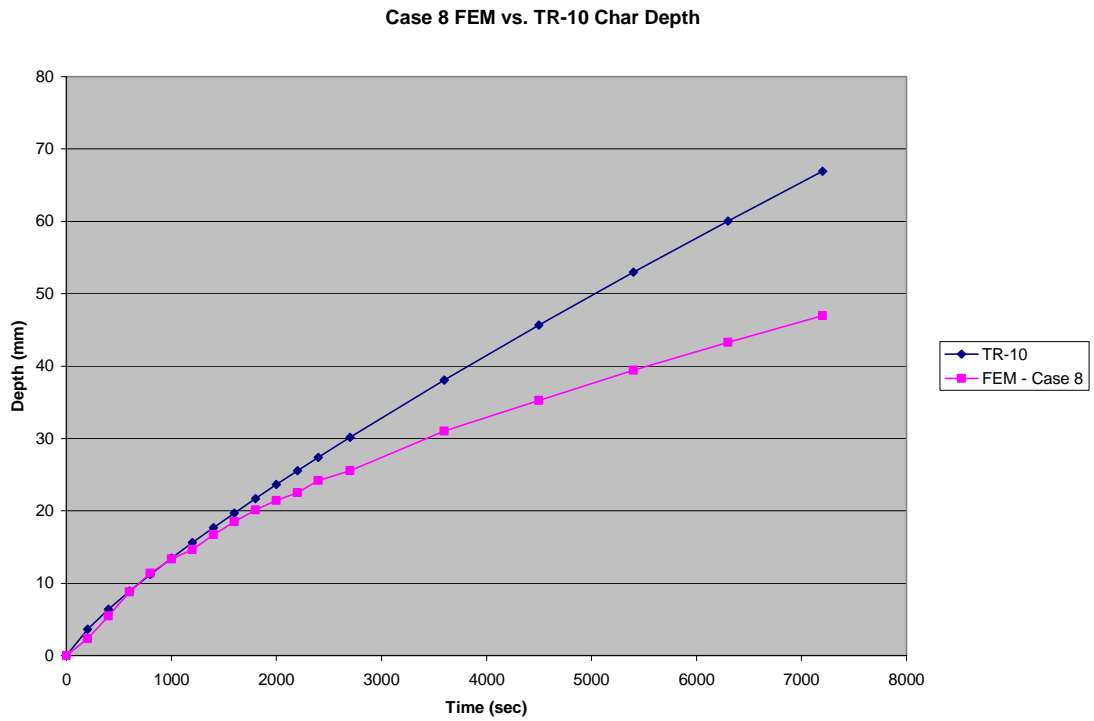


Figure 32 - FEM Case 8 vs. TR-10 Char Depth
 Non-Linear Density, Constant Specific Heat, Constant Thermal Conductivity

Each temperature-dependent expression for a material property impacted the shape of the char depth curves. Temperature-dependent density increased the magnitude of the values of the char depth curve. Temperature-dependent specific heat decreased the magnitude of the values of the char depth curve. Temperature-dependent thermal conductivity increased the magnitude of the values of the char depth curve. Temperature-dependent density and specific heat had approximate cancelling effects.

As previously discussed, models with temperature-dependent thermal conductivity were modified using Progressive Element Death. Figure 26 through Figure 29 demonstrate the modification to the shape of the char depth curve to reflect the char depth curve of the TR-10. From these four figures, it is clear that the shape of the char depth curve is sensitive to the expression of thermal conductivity as a function of temperature. Material property Case 2, shown in Figure 26, is the closest fitting char depth model to the TR-10 expression; it involves variable thermal conductivity and constant values for density and specific heat.

Following the completion of the FEM analyses for the ASTM E-119 standard fire conditions, FDM analyses using heat transfer principles were conducted. Figure 33 shows the results of the initial application of the finite difference analysis to Case 4. Clearly, the FDM analysis did not accurately represent the calculations taking place in the FEM analysis. As discussed in the Methodology, the finite difference analyses are sensitive to the time step used in the model. The suggested time step was calculated based on a relationship that was a function of the Fourier number and the three material properties: thermal conductivity, density, and specific heat. Equation 16 shows this

relationship. It was believed that the varying material properties used in Case 4 led the model to be relatively unstable and inaccurate.

$$\Delta t = \frac{(F_o \cdot \Delta x^2) \cdot (\rho \cdot C_p)}{k}$$

Equation 16

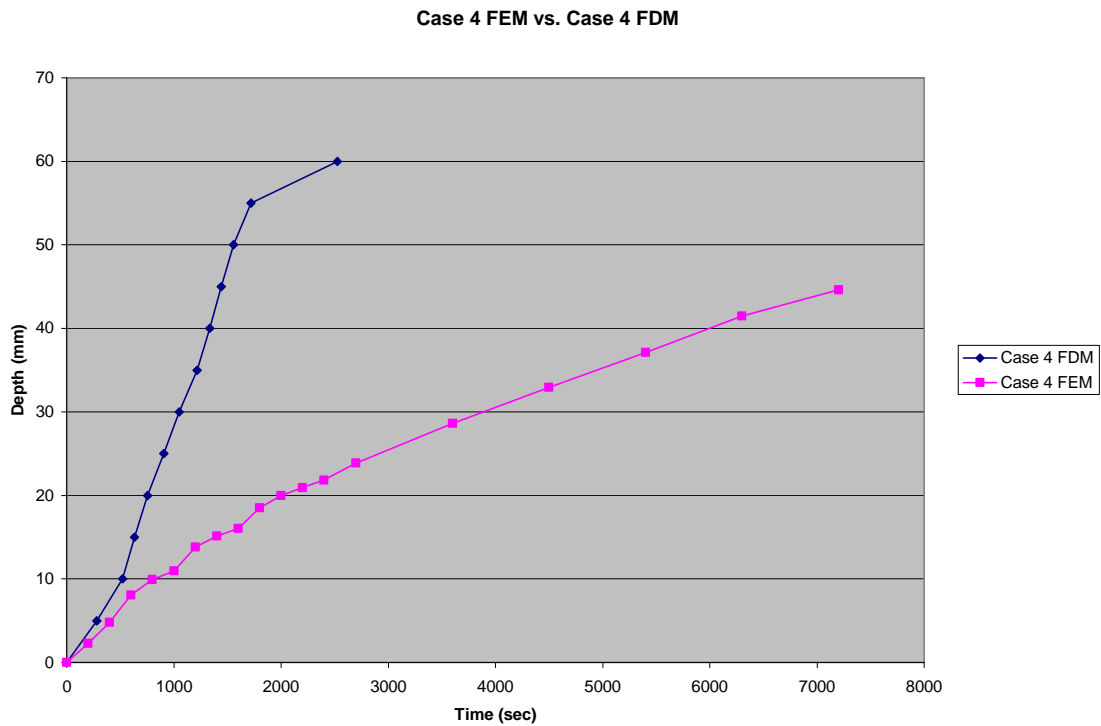


Figure 33 - Case 4 FEM vs. Case 4 FDM with Model Instabilities

Figure 34 illustrates Case 1 results for the FEM and FDM analyses. Since all of the material properties remained constant for Case 1, the time step remained constant and resulted in the closest agreement between the FEM and FDM analyses for any of the eight cases. Case 1 should have resulted in a FDM char depth curve that was similar to the FEM Case 1 curve if the analytical approach could be considered valid. Ultimately, there was still a substantial difference between the two char depth curves for Case 1.

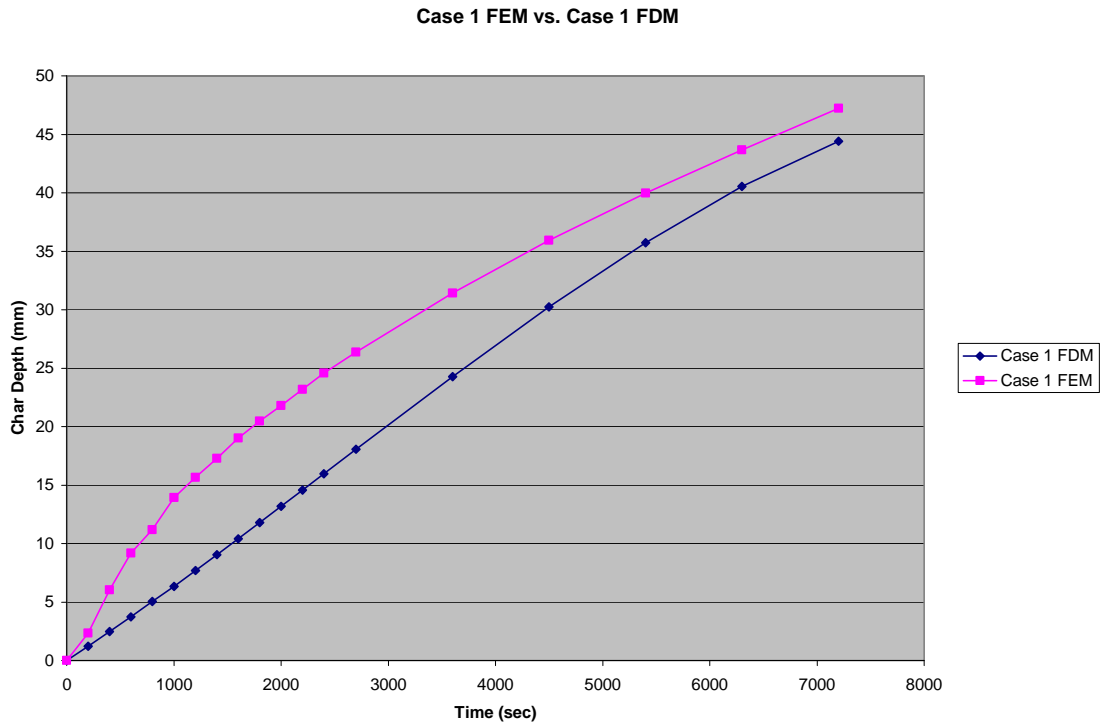


Figure 34 - Case 1 FEM vs. Case 1 FDM Char Depth

An alternative finite difference approach to transient heat transfer problems was devised and called the Adaptive Time Step method. This approach takes the average temperature of the two adjoining nodes to calculate the nodal temperature, and uses Equation 16 to calculate the most appropriate time step based changes in the Fourier number and material properties.

The results of the Case 1 FDM Adaptive Time Step method char depths and those of the FEM and TR-10 methods are shown in Figure 35. The Adaptive Time Step method follows the FEM results quite accurately. These results validate the conceptual approach for this heat transfer model.

FDM - Case 1 Adaptive Time Step Method vs. FEM - Case 1

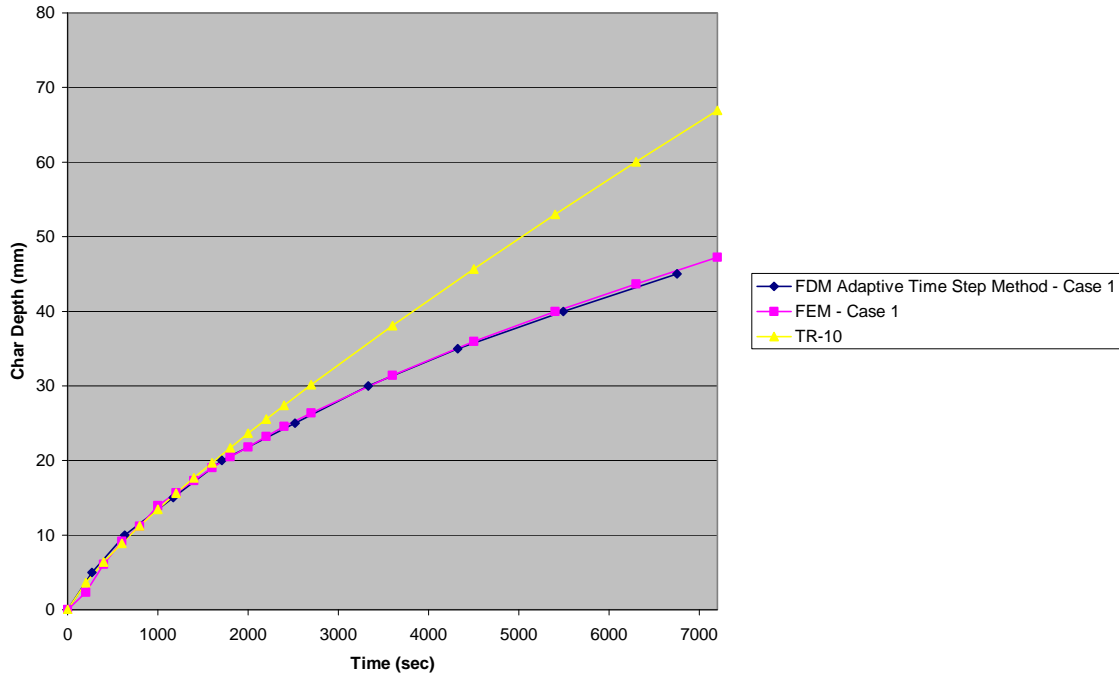


Figure 35 - Case 1 FEM vs. FDM Adaptive Time Step Method

Discrepancies between the FEM and FDM analyses start to arise when material properties change with temperature. Since the FDM model is dependent on the time step and the time step is a function of the thermal properties of the wood, calculated time steps from Equation 16 are different for each node for every time step because the temperature of the wood and its thermal properties varied with depth into the cross-section. Thus, a range of time steps were calculated for each time increment. Figure 36 illustrates how taking the average of the calculated time steps for each node leads to FDM results that differ from FEM results for Case 2.

Case 2 - FEM vs. FDM Adaptive Time Step Method

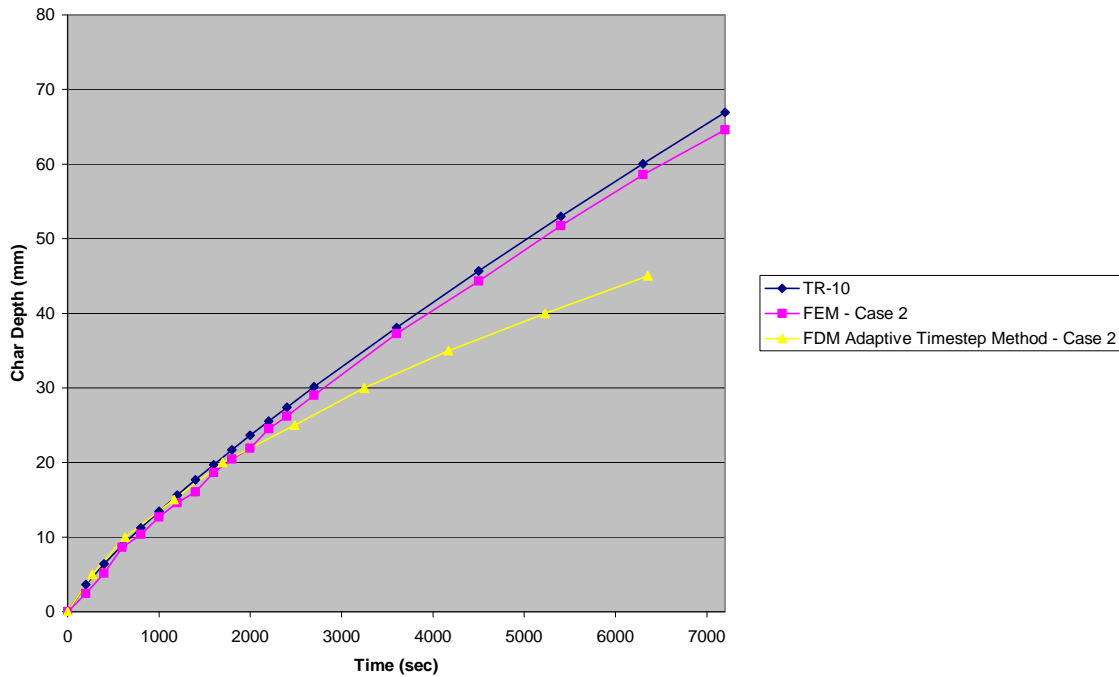


Figure 36 - Case 2 FEM vs. FDM Adaptive Time Step Method

Since ANSYS uses complex algorithms to calculate appropriate time steps for non-linear material property conditions, replicating the distinct selection of the ANSYS time steps with the finite difference method would be an unreasonable computational burden for a desk-top tool. To maintain its simplicity, various manipulations of the calculated time steps for each node of the FDM model were investigated. Calculating the mean time increment at each time step, and calculating the mean of the mean and the minimum time increment at each time step led to the most representative FDM models. Various percentile values for time steps were also investigated. As shown in Figure 37 and Figure 38, a time step value equal to the mean of the calculated time increment was most effective for cases where thermal conductivity was constant, and the mean of the

mean and the minimum time increments was most effective where thermal conductivity varied with temperature.

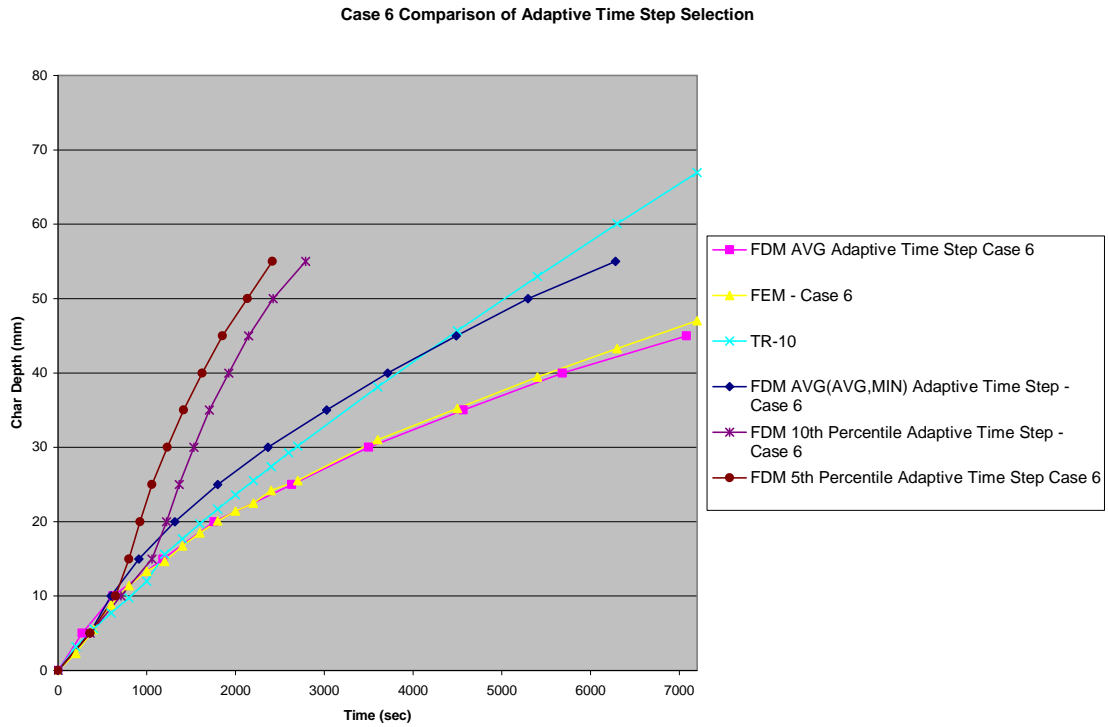


Figure 37 - FDM Adaptive Time Step Selection Comparison - Case 6

Case 4 Comparison of Adaptive Time Step Selection

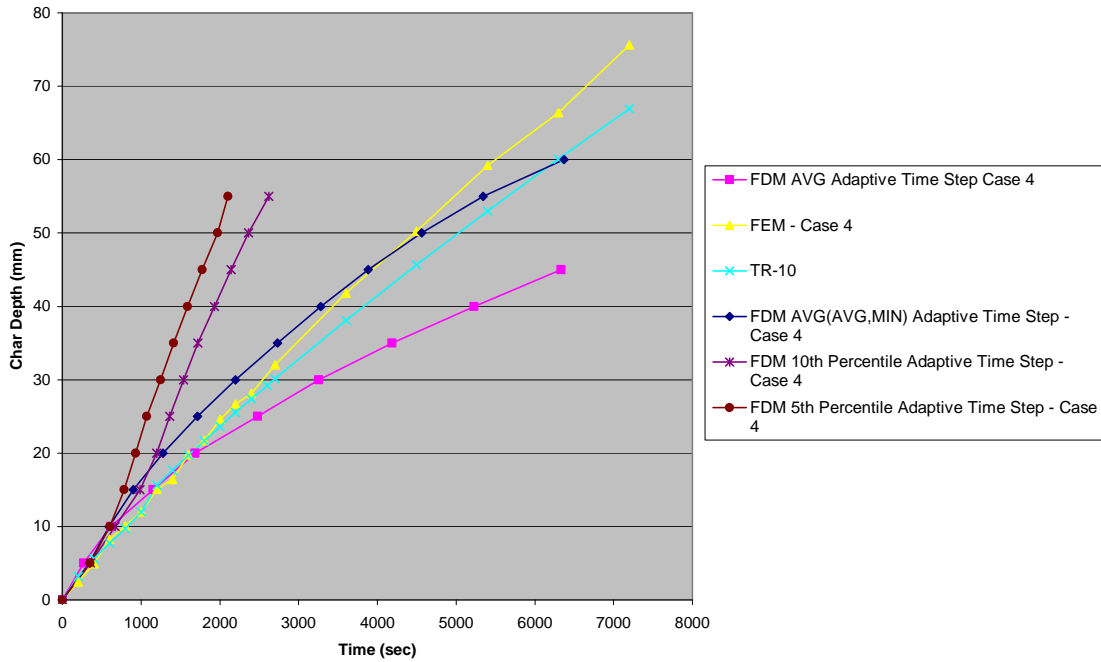


Figure 38 - FDM Adaptive Time Step Selection Comparison - Case 4

The method of using the mean of the mean and the minimum calculated time steps was applied to three representative FDM models (Case 1, 2, and 8 of Table 2). Of these three cases, Case 2 led to the char depth curve that closely matched its corresponding FEM model and the TR-10 char depth curve. The Case 2 FEM and FDM char depth curves are compared to the TR-10 curve in Figure 39.

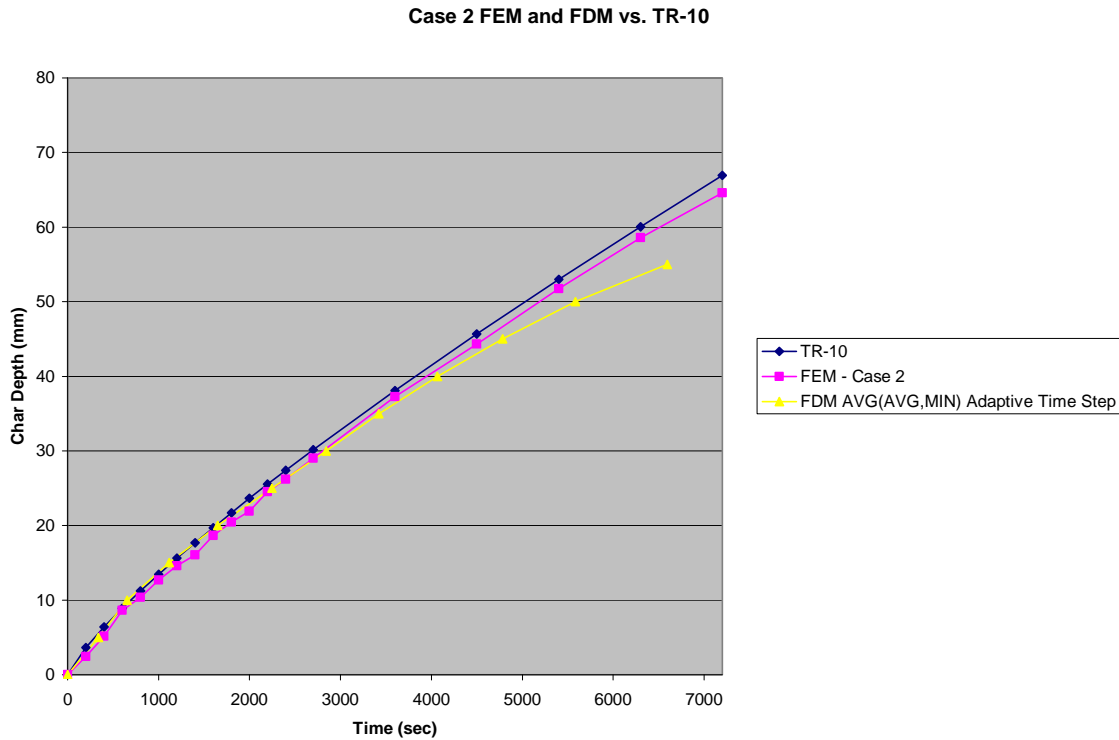


Figure 39 - Best Fit FEM and FDM Char Depth Models

5.1.2 Models of Natural Fires

Based on the results of the FEM and FDM models for ASTM E-119 analyses compared to TR-10 char data, Case 2 was further explored for application to natural design fires. As indicated in Table 2, Case 2 involved constant values for the wood's density and specific heat, and a temperature-dependent expression for thermal conductivity. Since the FEM and FDM models for Case 2 closely reflected TR-10 results for ASTM E-119 exposure, it was believed that this modeling convention would lead to most appropriate char depth predictions for natural fire exposure. Figure 40 and Figure 41 demonstrate the char depth curves for LD-MI and SD-HI exposure for FEM and FDM Case 2 models. In these figures, the char depth curves are plotted with the time-

temperature curves for the fire exposures to illustrate continued charring after fire cool down.

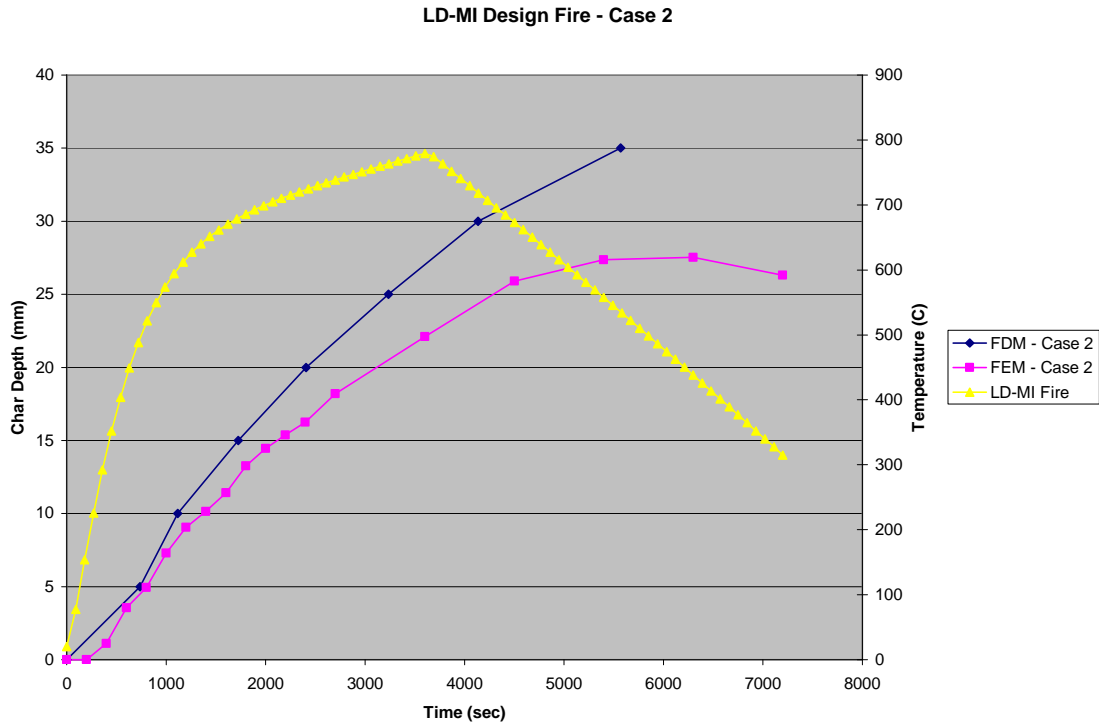


Figure 40 - FDM and FEM Char Depth - LDMI Fire - Case 2

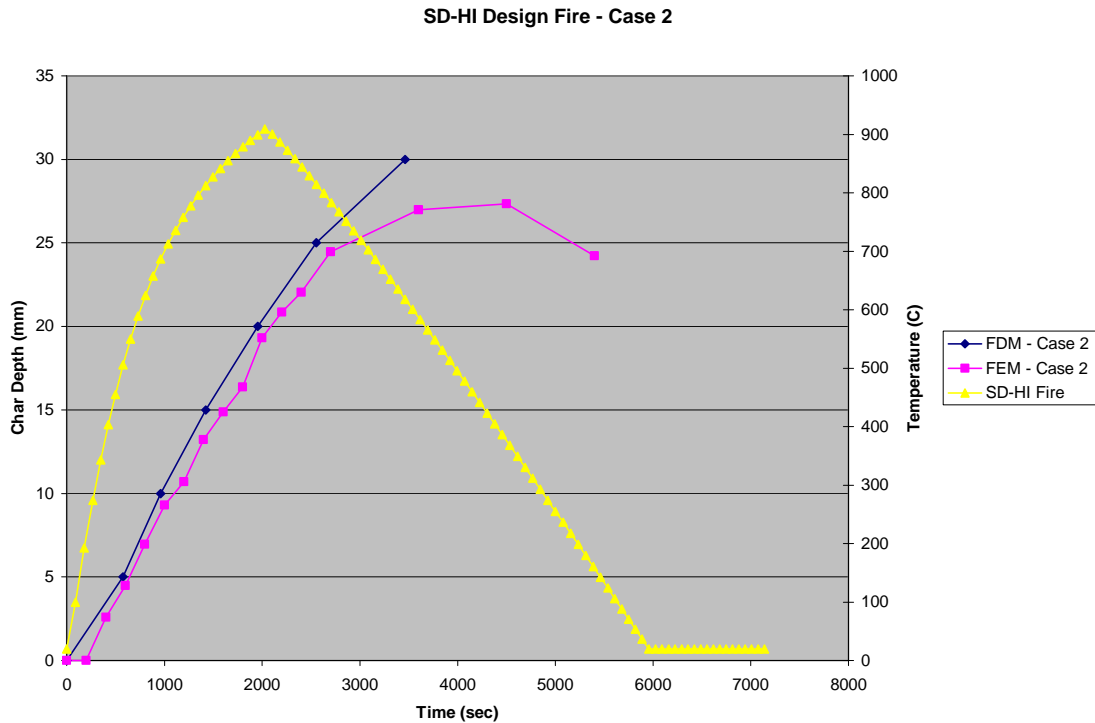
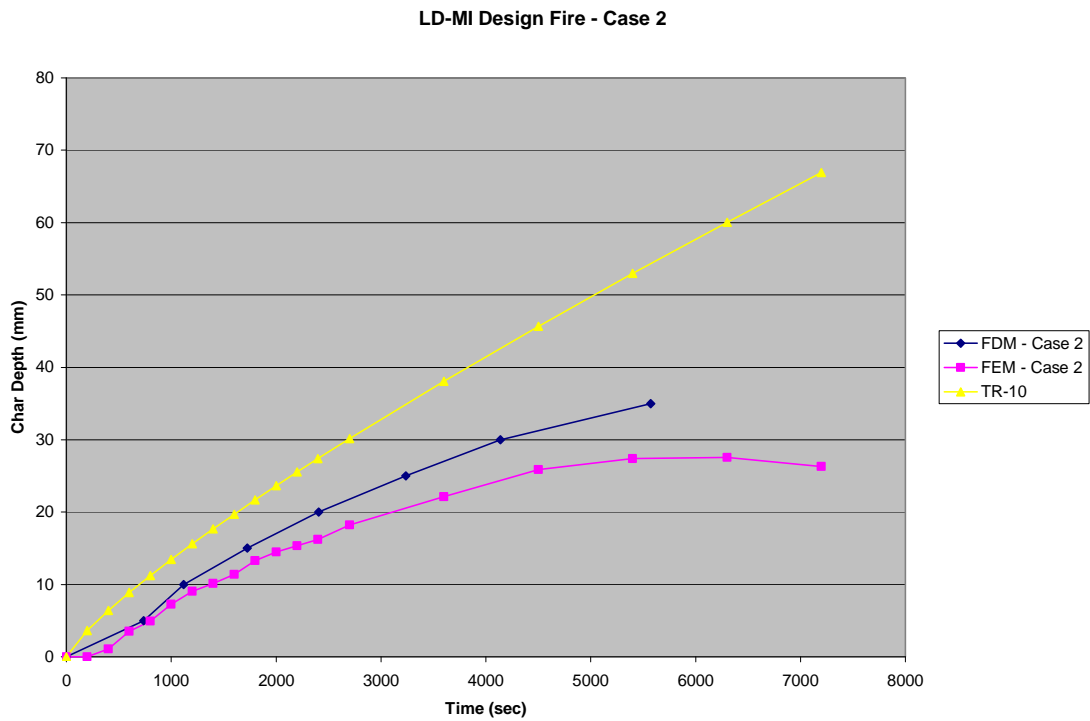


Figure 41 - FDM and FEM Char Depth - SD-HI Fire - Case 2

The FEM and FDM models displayed similar behavior for natural fire exposure. Although the char depths values deviated by about 15% to 30%, the shape of the curves for FEM and FDM models followed similar shapes. Additionally, both FEM and FDM models demonstrated the potential for continued charring after the fire began to cool down. This continuation is likely due, in part, to latent heat stored in the material after the fire reached its maximum temperature. The fire cool down portion of the FEM and FDM models are discussed further in the Conclusions chapter.

The impact of the severity and duration of fire exposure becomes apparent when comparing the FEM and FDM char depth curves for natural fires to the ASTM E-119 standard fire, as represented by TR-10. Figure 42 illustrates the medium intensity temperatures of the LD-MI exposure results in substantially different char depths than those predicted by use of TR-10. This separation is less obvious for the SD-HI exposure

shown in Figure 43, where the intensity of the temperature is similar to the ASTM E-119 fire during the period of growth. For both natural fires, char depths diverged from the TR-10 char depths, and ultimately halted after the fires cooled down. From these comparisons, it was believed that the differences between fire exposures would become more apparent when comparing time to failure of beams and columns.



**Figure 42 - FDM vs. FEM Case 2 - LD-MI
Compared to TR-10 Char Depth for ASTM E-119 Exposure**



**Figure 43 - FDM vs. FEM Case 2 - SD-HI
Compared to TR-10 Char Depth for ASTM E-119 Exposure**

5.2 Mechanics-Based Analysis to Predict Time to Failure

With a representative numerical method for calculating char depth as a function of material properties, time, and temperature conditions, member performance can be analyzed in terms of a calculated time to failure. The mechanics-based analysis to calculate time to failure considers failure to occur when the cross-section of the member has been reduced, such that the member can no longer resist the intended structural loads. The following sections use the results of char depth models to calculate time to failure of various beams and columns exposed to ASTM E-119, LD-MI, and SD-HI time-temperature conditions.

5.2.1 ASTM E-119 Fire

Figure 44 through Figure 47 present time to failure results for member sizes and loadings described in the TR-10 document and subjected to the ASTM E-119 standard fire exposure. These TR-10 beams and columns are substantially larger than those considered to be lightweight. Since limited physical test data is available to study time to failure, the results presented in the TR-10 were used to validate the analytical char depth models previously discussed. It is believed that if analytical models reflect the actual charring and time to failure performance of large members, the analytical models should extend to the analysis of lightweight members.

Figure 44 through Figure 47 show the remaining ultimate capacity of beams and columns plotted against time. As time increases cross-sectional material is lost to char, and a member's ability to carry load diminishes. Eventually the beam or column is unable to carry its original design load and the remaining capacity goes to zero. The remaining capacity is based on the original loading, as a percentage of the ultimate capacity of the member, as a function of time. As the cross-section is reduced, the ultimate capacity is reduced and the original loading will exceed the ultimate capacity, and the remaining capacity will drop to zero. The relationship of actual load, member capacity as a function of time, and remaining ultimate capacity percentage is shown in Equation 17.

$$\text{Remaining Capacity}_{\text{ultimate}} = 1 - \frac{\text{Actual Load}}{\text{Member Capacity}(t)_{\text{ultimate}}}$$

Equation 17

The time associated with the remaining capacity going to zero is considered the time to failure. Figure 22

TRADA Beam Comparison

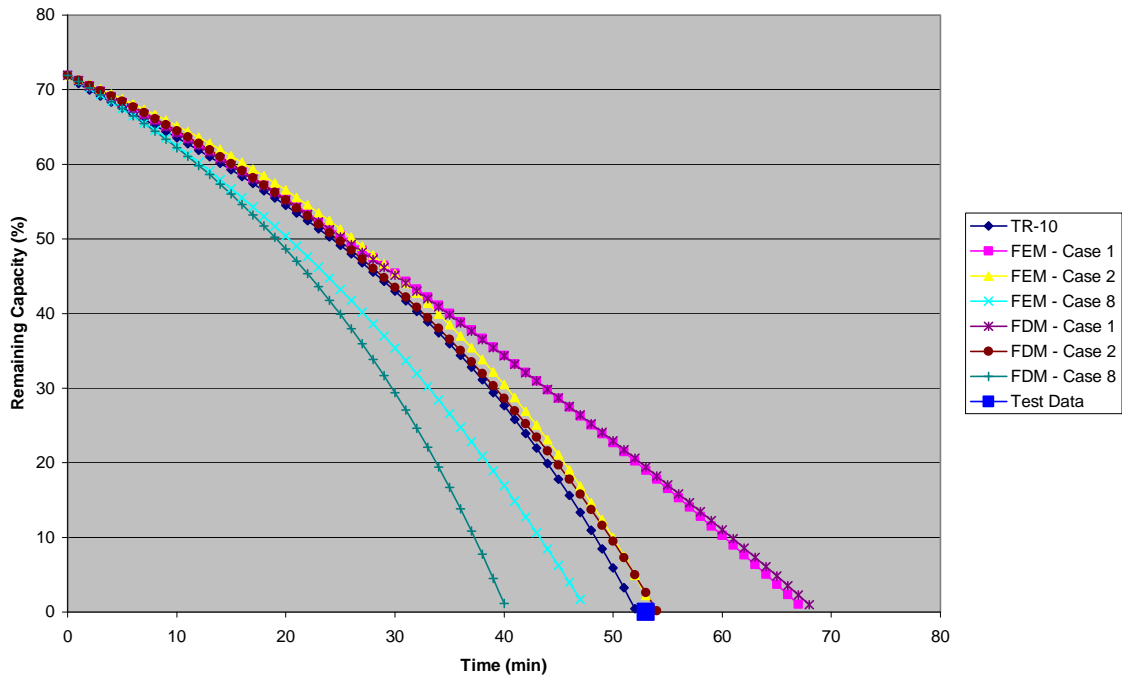


Figure 44 - TRADA Beam TR-10 vs. FEM and FDM

FCNSW-BB Beam Comparison

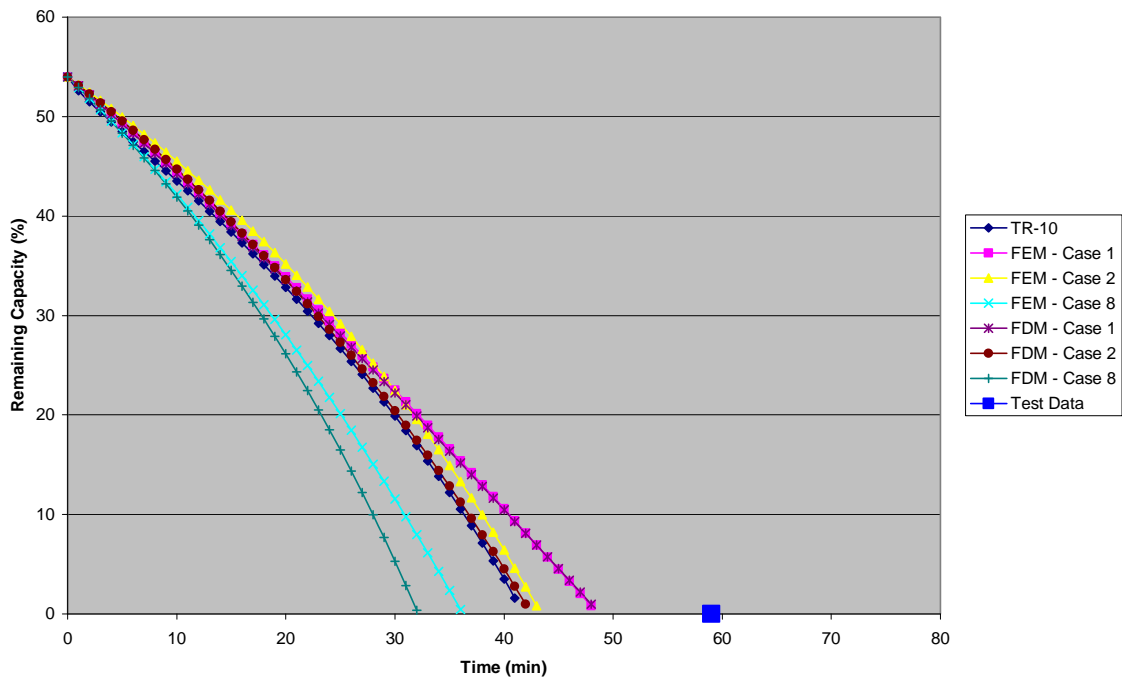


Figure 45 - FCNSW-BB Beam TR-10 vs. FEM and FDM

Figure 44 demonstrates the ability of the TR-10 and some of the FEM and FDM models to predict a time to failure that is consistent with physical test data. Figure 45, on the other hand, shows that all of the models, including TR-10, predict a similar time to failure, but do not accurately reflect the physical test data. Figure 46 and Figure 47 show time to failure results for columns presented in the TR-10. The analyses for beams and columns suggests that time to failure predictions are much closer between char depth models when the models predict a short time to failure.

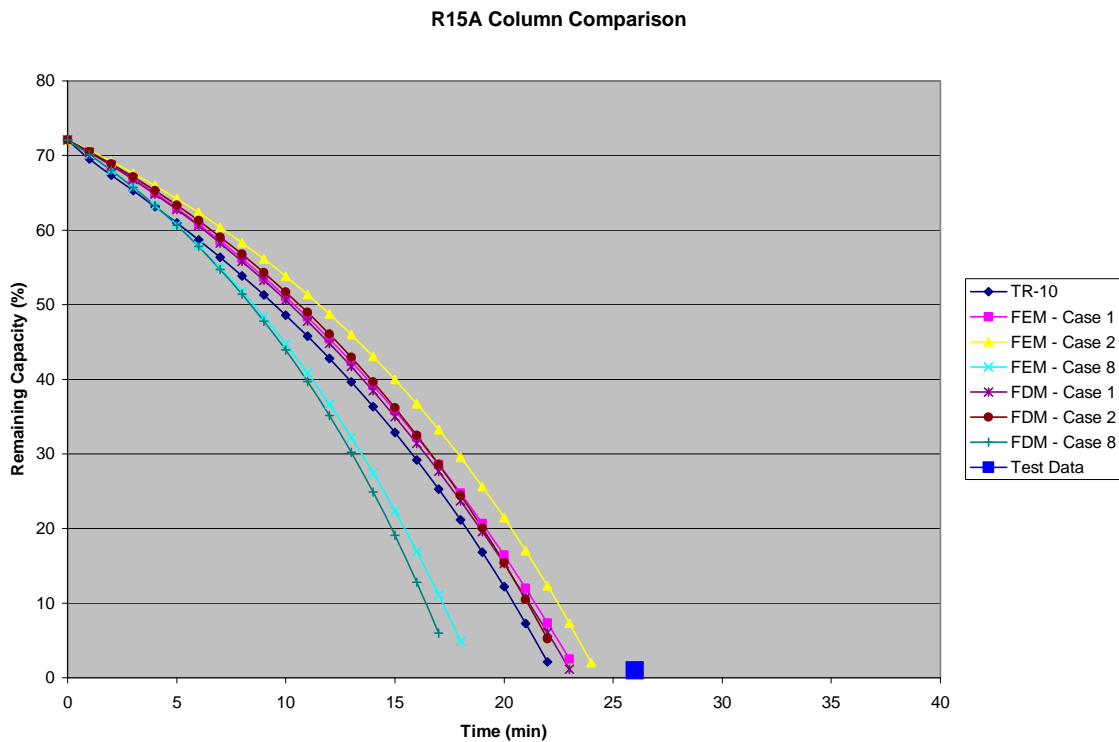


Figure 46 - R15A Column TR-10 vs. FEM and FDM

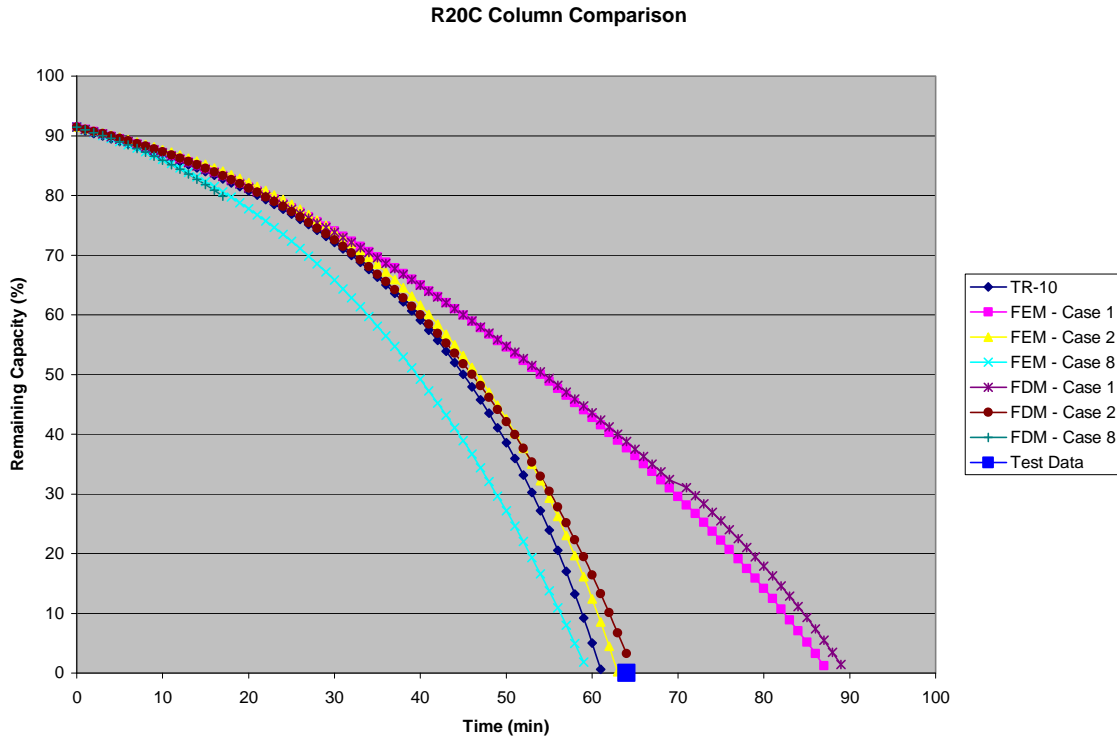


Figure 47 - R20C Column TR-10 vs. FEM and FDM

As seen with the char depth models, FEM and FDM Case 2 calculated values that were most similar to the TR-10. The failure times were within about 5 to 10% of the TR-10 values. Since these models predicted reasonably accurate failure times for TR-10 beams and columns, similar analyses were conducted for representative lightweight beams and columns. A 2x10 beam and 2x6 column with various loadings were investigated.

Figure 48 compares the remaining ultimate capacity vs. time data for a 2x10 beam loaded to 75 percent of its design capacity. The time to failure of this beam configuration varied less than five minutes amongst the TR-10, FEM, and FDM models; moreover, the numerical methods varied no more than three minutes from the TR-10 time to failure.

2x10 Beam Loaded 75% to Design Capacity - Exposed to ASTM E-119

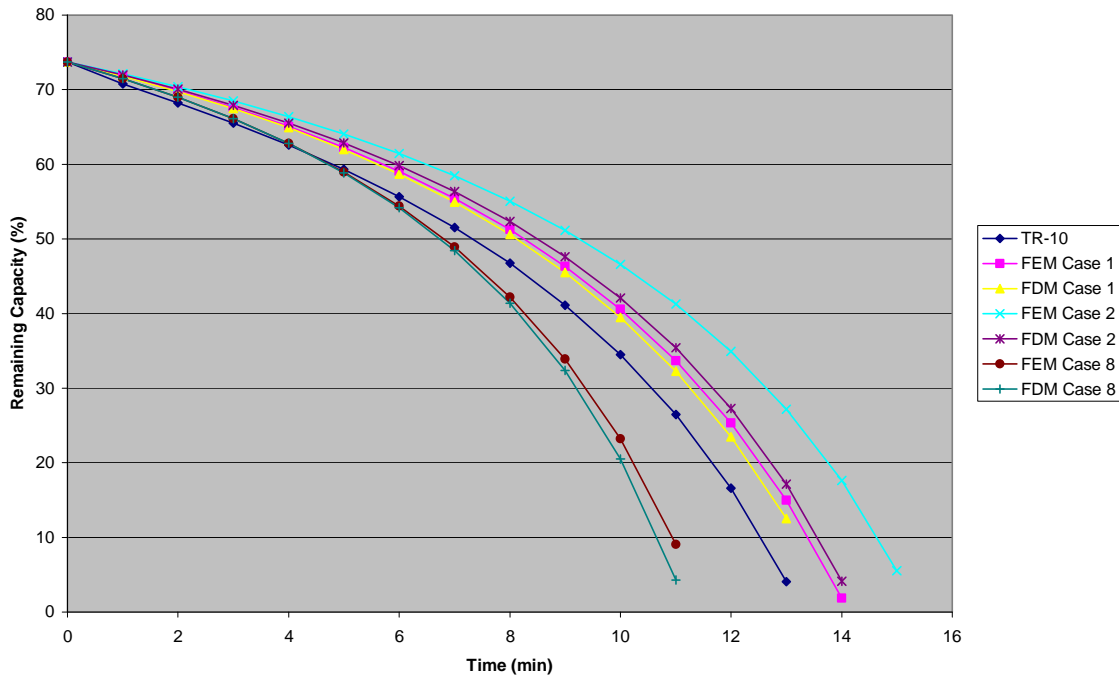


Figure 48 - Lightweight Beam TR-10 vs. FEM and FDM

Figure 49 illustrates the impact of the loading on time to failure calculation. The beam configuration for this comparison remained the same, while the level of loading, expressed as a percentage of design capacity, was changed. The data suggests that the predicted time to failure is more sensitive to the level of loading than the analytical model used. Similar correlations were observed in the study of with lightweight columns. Results of column analyses can be seen in Appendix F.

2x10 Beam FDM Case 2 - Exposed to ASTM E-119

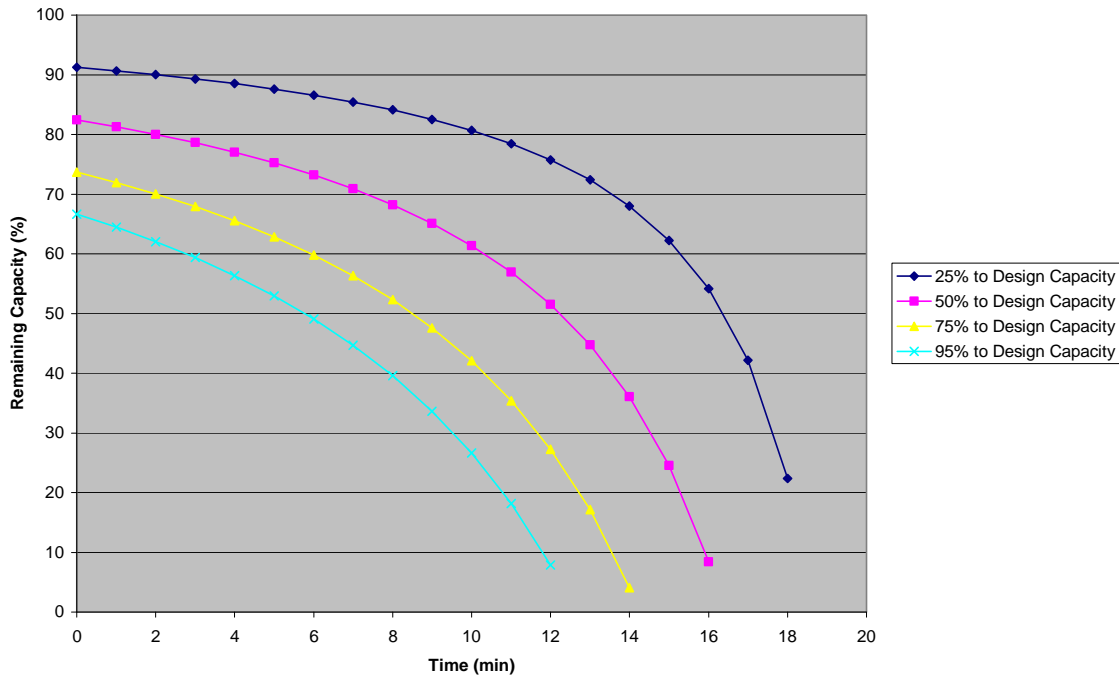


Figure 49 - Lightweight Beam FDM Case 2 - % to Design Capacity Variation

5.2.2 Models of Natural Fires

Analyses for natural fires were conducted for the same lightweight beam and column scenarios as the ASTM E-119 exposure. For natural fire exposures, Cases 1,2, and 8 from Table 2 were used with both the FEM and FDM char depth models to predict time to failure, and the results from the numerical models were compared to predictions from use of TR-10. Figure 50 shows the LD-MI exposure time to failure curves from the FEM and FDM models compared to the TR-10 prediction. Beam and column time to failure curves for other loadings and SD-HI exposure are developed further in Appendix E and Appendix F.

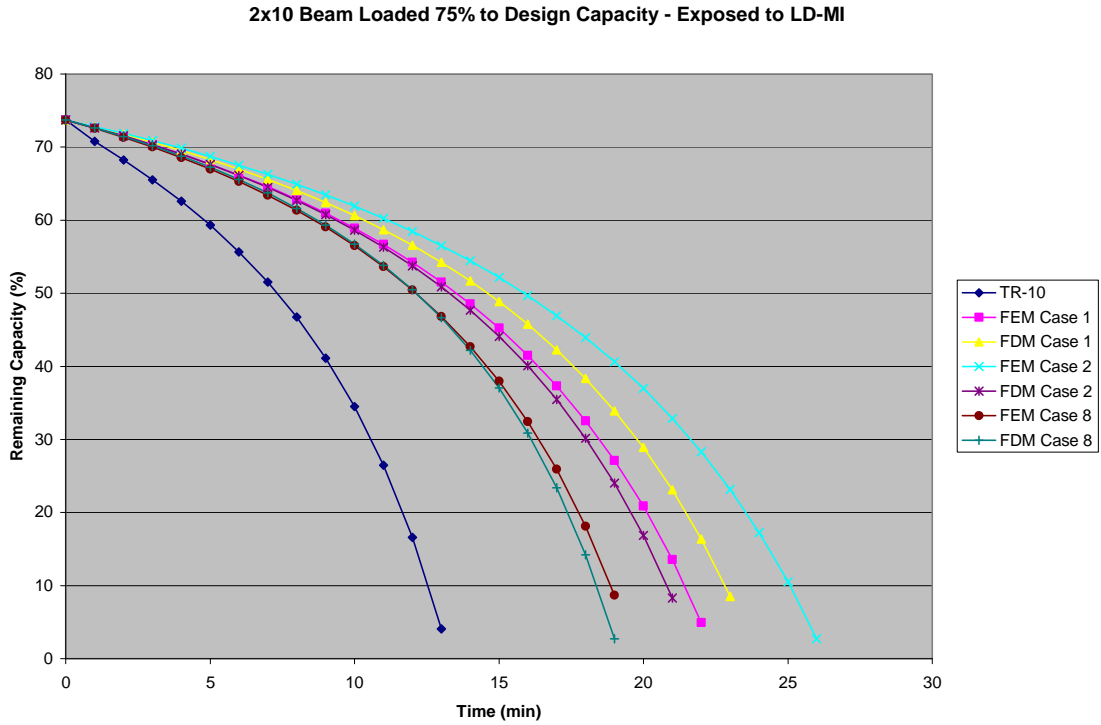


Figure 50 - 2x10 Beam Loaded to 75% of Design Capacity - LD-MI

The beam and column time to failure analysis curves exhibited similar trends to the ASTM E-119 results. The level of loading greatly affected the time to failure of the members.

One of the most notable observations is that TR-10 predictions prematurely predict time to failure for natural fires that are less intense than the ASTM E-119 standard fire exposure. Figure 51 illustrates the impact that the three different fire exposures has on the time to failure for a 2x10 beam loaded to 75% of design capacity. FDM Case 2 was used to predict char depth for the ASTM E-119, LD-MI, and SD-HI fires.

ASTM E-119 vs. LD-MI vs. SD-HI 2x10 Beam Loaded 75% to Design Capacity

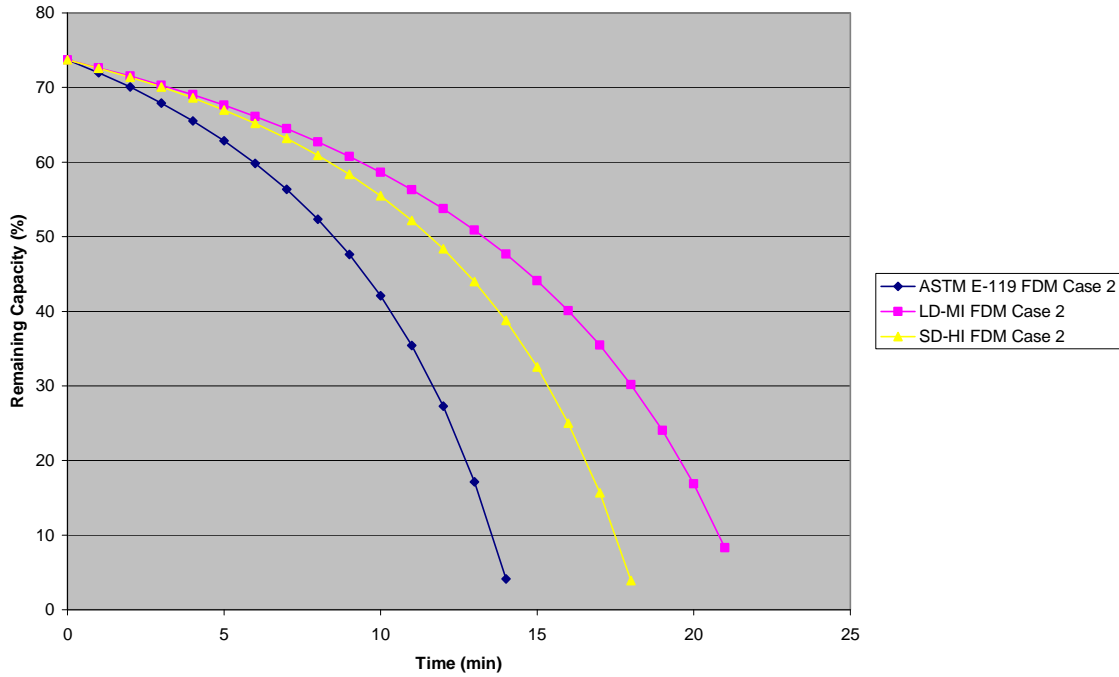


Figure 51 - 2x10 Beam Loaded 75% - Exposure Comparison

The predicted times to failure for these three fire exposures vary by as much as seven minutes. This difference in time is a substantial percentage of the predicted time. This variation demonstrates the importance of establishing an appropriate fire exposure for evaluating performance, even for members that have relatively short times to failure.

6 Conclusions

Lightweight wood and engineered wood products are some of the most commonly used materials in residential construction. Unprotected lightweight wood structural members are extremely sensitive to the elevated temperatures often experienced in fire conditions. Although building codes require protective coverings in most living spaces, some areas of structures are not required to have protection. Whether or not protective coverings are necessary, building codes and the approval process does not require analytical or engineering calculations to evaluate the fire performance of a structure.

The American Wood Council provides an analytical approach for assessing the time to failure of unprotected wood elements (although it is not required by building codes in the US). This approach is founded on empirical equations, and as a result is limited in its application by the bounds of physical test data from which the equations are derived. The empirical equations for this method were developed for exposure to the ASTM E-119 standard fire, and “adequately address fire design of large, exposed wood members.”⁷²

The objective of this thesis was to develop a reliable and transparent calculation method, not bounded by empirical equations, that could be used by a structural engineer to assess the time to failure of lightweight wood structural elements. The primary component of the analytical methods was the assessment of loss of cross section due to wood charring. As a result, a large portion of the development of this analytical method was comprised of modeling char depth of wood when exposed to fire conditions. Once

⁷² “Calculating the Fire Resistance of Exposed Wood Members: Technical Report 10,” p.23

these models for char depth were developed and validated, they were used to develop an analytical tool to determine time to failure for lightweight wood members.

6.1 Modeling the Performance of Wood

The method of analysis presented in the TR-10 is a straightforward approach to evaluating the char rate of one specific family of wood exposed to the ASTM E119 design fire. The TR-10 method of char assessment is not valid for predicting char depths in natural fires because it is based on empirical equations. The FEM models were shown to provide char depths that reflected the equations provided in the TR-10 for ASTM E-119 exposure. Although some of the FEM models were more representative of the TR-10 data than others, the less representative results illustrated some of the sensitivities of the modeling technique. Ultimately, some of the FEM models were highly representative of the TR-10 char depths for ASTM E-119 exposure, thus validating the conceptual application of numerical models for char depth calculations.

FDM models for char depth were developed as an alternative numerical technique to the FEM models. FDM models for char depth are relatively straightforward to develop in spreadsheet format, and once established, easy to use. In contrast, FEM modeling using a finite element program has a steep and time-consuming learning curve to successfully produce a reliable char depth model. Developing FDM models required a basic understanding of finite difference equations for transient heat transfer problems, and an experienced understanding of spreadsheet programming. FDM calculations were shown to serve as an effective substitute for FEM models -- they predicted similar char depth curves for the same model parameters.

After validating both numerical approaches for calculating char depth due to ASTM E-119 exposure, the FEM and FDM models were used to investigate performance of wood members in natural fire exposure. The influence of natural fire exposure on wood elements becomes increasingly evident when comparing the time to failure results of natural fire exposure for beams and columns with those obtained from exposure to the ASTM E-119 standard fire. When the intensity and duration of the natural fire exposure vary from those of the standard fire, the calculated times to failure are vastly different. This indicates the overall model sensitivity to the time-temperature relationship for its environment, and shows the importance of accurately representing the intensity and duration of fire exposures for analyzing structural performance during fire conditions.

For the three fire exposure conditions investigated in this thesis, lightweight beams and columns were analyzed. Initially, heavy and lightweight beams and columns were analyzed for ASTM E-119 exposure. Columns tended to predict more consistent time to failure between models than beams, for long durations of time to failure. When beams and columns failed quickly, the variation in time to failure prediction between models was similar for beams and columns. Only lightweight members were analyzed for the natural fire exposures. The variation of predicted time to failure between beams and columns was similar because of the relatively quick failure time. Ultimately, fire exposure and the initial loading condition played the most critical roles in predicting time to failure for lightweight members.

6.2 Analysis in Practice

Following the development of char depth expressions, the performance of lightweight wood members can be calculated based on the fundamental mechanics

principles with which structural engineers are comfortable. If a comprehensive, but straightforward method of evaluating char depth as a function of fire exposure is established and adopted by the structural engineering community, evaluating the fire performance of lightweight wood elements could become an integral part of the analysis of lightweight wood structures. By being able to adequately predict time to failure, engineers could design buildings more appropriately for fire conditions, and possibly improve the safety of lightweight wood structures exposed to fire conditions.

Finite Element Method analysis can be an effective tool in evaluating the char depth of various woods and design fires. When compared to the results predicted by TR-10, the finite element model for char is quite similar. TR-10 is limited to ASTM E-119 fire exposure, and therefore the need for a tool to accommodate fires of varying intensity and duration exists. However, the development of finite element models for heat transfer problems is likely outside the expertise of most structural engineers, and application of finite element programs beyond structural analysis in most design offices is limited. For this reason, the finite difference method is more appealing to the engineering practice because it can be developed in a spreadsheet and model equations are relatively straightforward to assess. Spreadsheets also allow the user to visualize the progression of the heat transfer through the wood cross section. The finite difference models are sensitive to time step parameters and could be poorly representative if incorrectly assembled. With proper treatment of time step parameters, finite difference models can lead to reliable and transparent analysis of time to failure of lightweight wood members exposed to fire conditions.

6.3 Recommendations for Future Work

The following lists recommendations for further study in the area of lightweight wood members exposed to fire conditions:

1. The moisture content of wood ultimately affects the rate of char and strength properties of wood cross-sections. The FEM and FDM models utilized in this thesis neglected the effects of moisture content to maintain a simplified, yet representative model. Although moisture content was neglected in this thesis, the numerical char depth models were in agreement with published test data. The inclusion of this material property may impact the calculation of time to failure of wood members.
2. 1-dimensional heat transfer analyses were conducted to predict char depths for this thesis. In the 1-dimensional analyses, elements were assumed to be semi-infinite, meaning the boundary conditions of the opposite face would not interfere with the heat transfer analysis of the near face. For lightweight wood members, the heat transfer model may be impacted by fire exposures on opposing or adjacent faces. Further development of FEM and FDM models, investigating 2-dimensional heat transfer may improve the prediction of char depth models for lightweight wood members.
3. As the temperature of wood rises above ambient temperature, strength properties begin to deteriorate. Although the char was modeled to have no material strength, material with temperatures below 288°C was assumed to have strength properties equal to those at ambient temperatures. The mechanics-based model assumed a twenty percent increase in char depth to account for strength property degradation and other effects as suggested in the TR-10. An analytical approach would likely result in a more accurate depiction of the material strength profile of the cross-section.
4. Similar to strength property deterioration, corner rounding of the cross-section was accounted for in the twenty percent increase of char depth as suggested by the TR-10. Following Buchanan's calculation (Buchanan, 2002) directly including corner rounding in the calculation of section modulus, would likely lead to a better representation of what the remaining cross-section actually looks like.
5. The FEM and FDM models of char depth for this thesis account for char layer degradation by changing material properties. Additionally, the material properties are solely a function of material temperature. If a natural fire were to have temperatures that dropped below 288°C during fire decay, the material properties used by both numerical techniques would revert to values of those seen in uncharred wood. Realistically this would not occur after the material has already

charred. To investigate the propagation of char depth after fire cool down, it would be advantageous to develop a better representation of the cool-down phase of charring for FEM and FDM models so that the material does not “unchar” below 288°C.

6. When researching physical fire test data, it became apparent that the availability of the data was limited for wood beams and columns (especially lightweight sections). Additionally, the description of the fire tests did not always seem consistent with the data presented for the tests (as seen in the TR-10). Investigation of the consistency of the presentation of physical test data may have some value in validation of numerical modeling. Additionally, test data should be extended in the TR-10 for application of its method to other types of wood.
7. Further development of FEM and FDM char depth models to incorporate the effects of fire resistive insulation would have additional value for study of design situations. The pre-ignition phase of insulated wood member exposure relates to the loss of moisture and strength as discussed previously in recommendations 1 and 2. Investigating the interaction of insulation and wood for both pre- and post-ignition conditions of protected lightweight wood members would aid structural engineers in understanding the performance of protected lightweight wood members.

7 Bibliography

Albano, Leonard D., “CE 534 - Structural Design for Fire Conditions”, class notes, Class 5, February 9, 2006.

American Wood Council, National Design Specification For Wood Construction, American Forest & Paper Association, Washington, DC, 2001.

ANSYS University Advanced, Version 9.0, ANSYS Inc.

Beall, F.C and H.W. Eickner, “Thermal Degradation of Wood Components: a review of the literature,” USDA Forest Service, Forest Products Laboratory. Madison, WI. 1970.

Benichou, Nouredine and George Hadjisophocleous, “Fire Safety Design Guidelines For Federal Buildings,” National Research Council of Canada, A4409.2.

Buchanan, Andrew H., Structural Design for Fire Safety. John Wiley & Sons, Ltd. West Sussex, England. 2002.

“Calculating the Fire Resistance of Exposed Wood Members: Technical Report 10,” American Wood Council, Washington D.C., 2003.

Croft, David R., Heat Transfer Calculations Using Finite Difference Equations, Applied Science Publishers, Ltd., London, 1977.

“Design for Code Acceptance 3 – Fire Rated Wood Floor and Wall Assemblies” American Wood Council, 2002.

“Fatal Fires,” U.S. Fire Administration/ National Fire Data Center, Topical Fire Research Series, Vol. 5 – Issue 1, Department of Homeland Security, March 2005.

“Fire in the United States 1992 – 2002,” U.S. Fire Administration/ National Fire Data Center, Thirteenth Edition, FA-286, October 2004.

“First Law of Thermodynamics,” <<http://hyperphysics.phy-astr.gsu.edu/hbase/thermo/firlaw.html>>, page viewed: April 27, 2007.

Freitag, J.K., The Fire-proofing of Steel Buildings. John Wiley & Sons. New York. 1899.

Gewain, Richard G., “Facts for Steel Buildings – Fire,” American Institute of Steel Construction, Inc., Chicago, 2003.

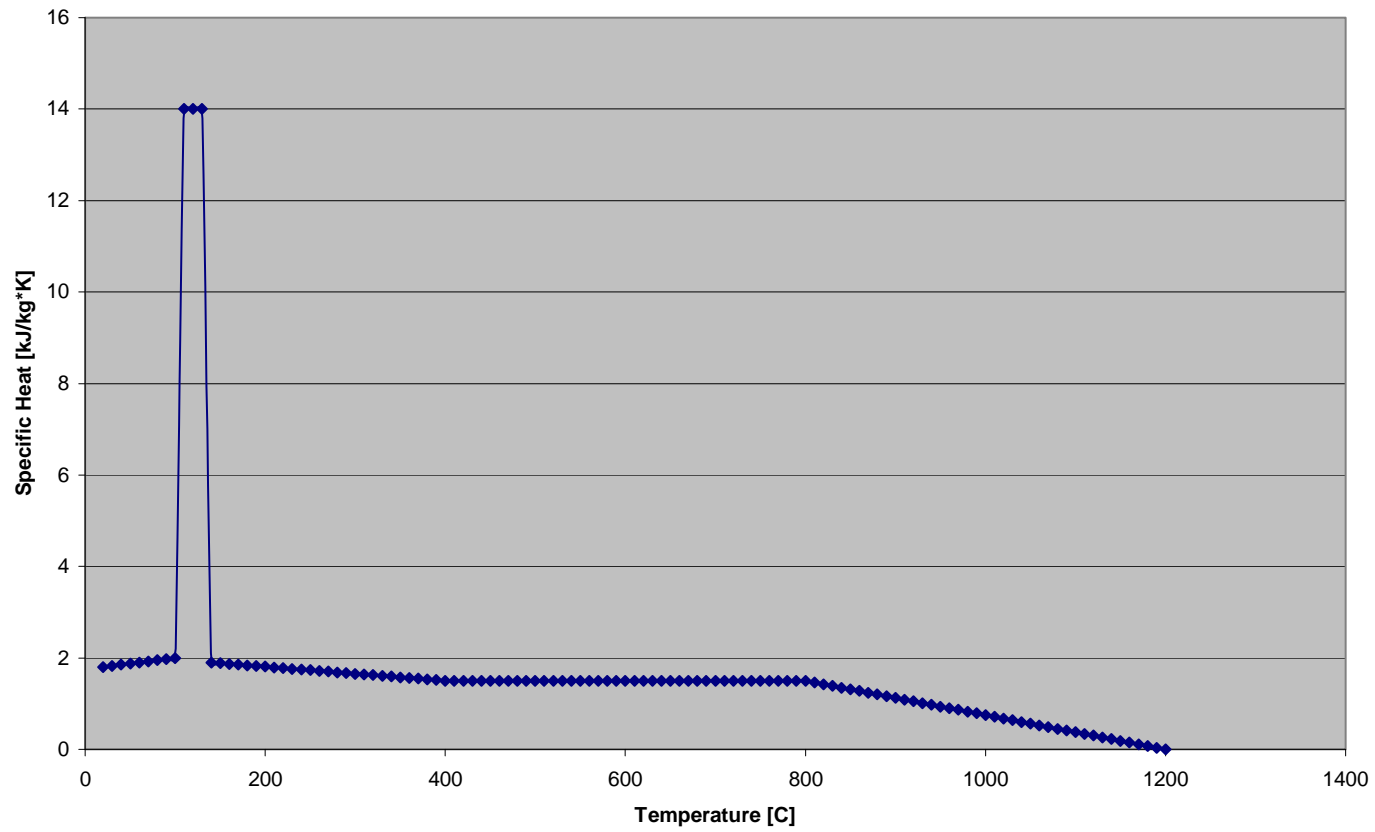
International Building Code 2006, International Code Council, Falls Church, VA. 2006.

- “International Code Adoptions,” International Code Council,
<<http://www.iccsafe.org/government/adoption.html>>, Last viewed: May 2007.
- Janssens, Marc L., “Modeling of the thermal degradation of structural wood members exposed to fire,” Fire and Materials, Vol. 28: 1997-207, John Wiley & Sons, Ltd. 2004.
- Lau, Peter W.C., Robert White, and Ineke Van Zeeland, “Modeling the Charring Behaviour of Structural Lumber,” Fire and Materials, Vol. 23, 209-216, John Wiley & Sons, Ltd. 1999.
- LeVan, S.L., “Thermal Degredation,” In: Schniewind, Arno P., ed. Concise Encyclopedia of Wood & Wood-Based Materials, 1st Edition. Elmsford, NY: Pergamon Press: 271-273, 1989.
- Lie, T.T., Structural Fire Protection, American Society of Civil Engineers, New York. 1992.
- Moaveni, Saeed, Finite Element Analysis, Second Edition, Pearson Education, Inc. Upper Saddle River, NJ. 2003.
- Moghtaderi, Behdad, “The State-of-the-Art in Pyrolysis Modelling of Lignocellulosic Solid Fuels”, Fire and Materials, John Wiley & Sons, Ltd. 2005.
- “National,” U.S. Fire Administration, Department of Homeland Security,
<<http://www.usfa.dhs.gov/statistics/national/index.shtm>>, Last Reviewed: December 28, 2006.
- “The Great Conflagration,” Chicago Historical Society and the Trustees of Northwestern University, <<http://www.chicagohistory.org/fire/conflag/>>, Lase Revised: October 8, 1996.
- White, Robert H., “Analytical Methods for Determining Fire Resistance of Timber Members”, Section Four, Chapter 11, SFPE Handbook of Fire Protection Engineering, Third Edition, National Fire Protection Association, Quincy, Massachusetts, 2002.
- White, Robert H., “Fire Resistance of Exposed Wood Members”, Wood and Fire Safety, 5th International Scientific Conference, April 2004.
- White, Robert H. and Erik V. Nordheim, “Charring Rate of Wood for ASTM E119 Exposure”, Fire Technology, Vol. 28, Number 1, 1992.

Appendix

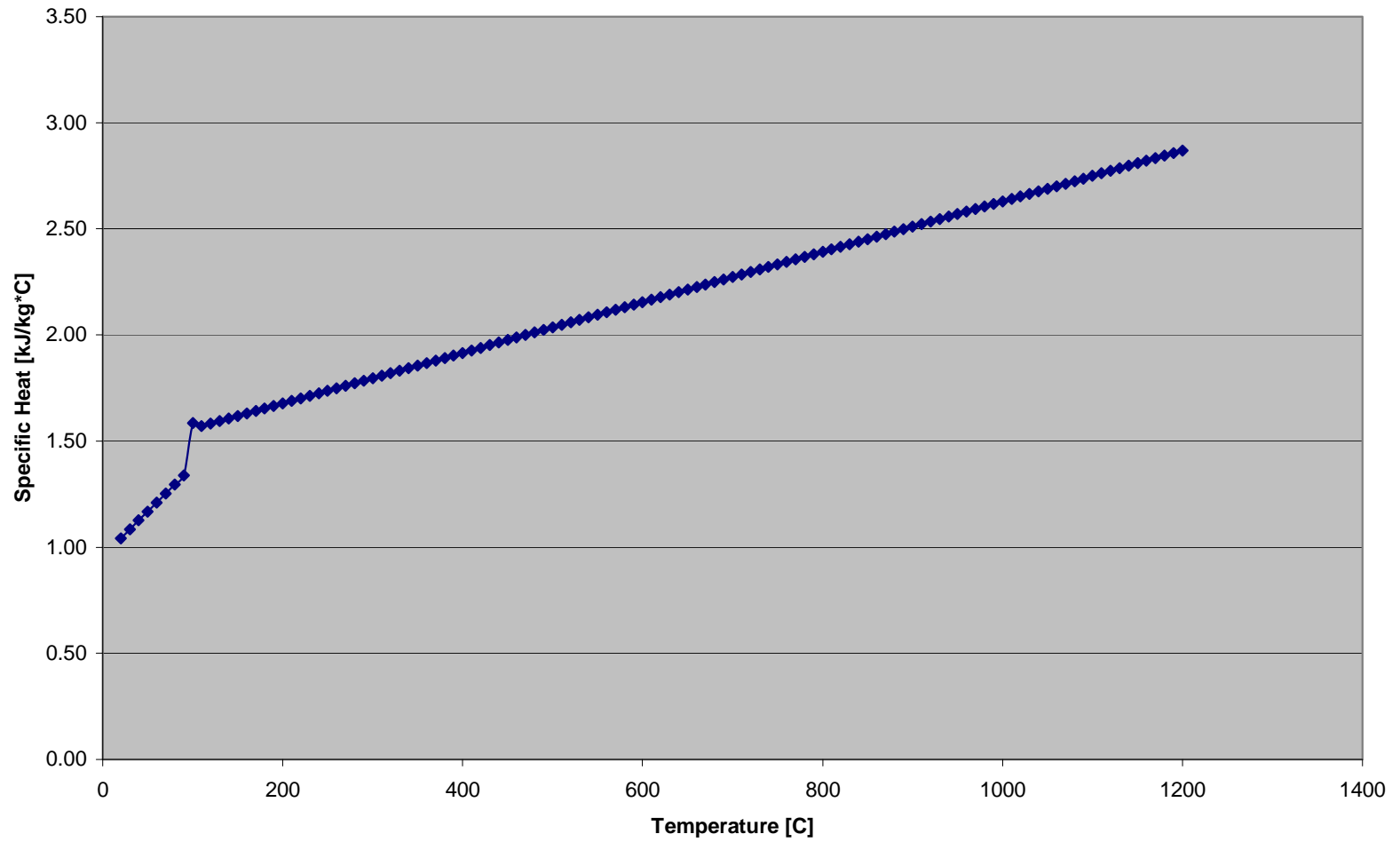
Appendix A – Specific Heat Variations

Konig and Walleij Specific Heat vs. Temperature



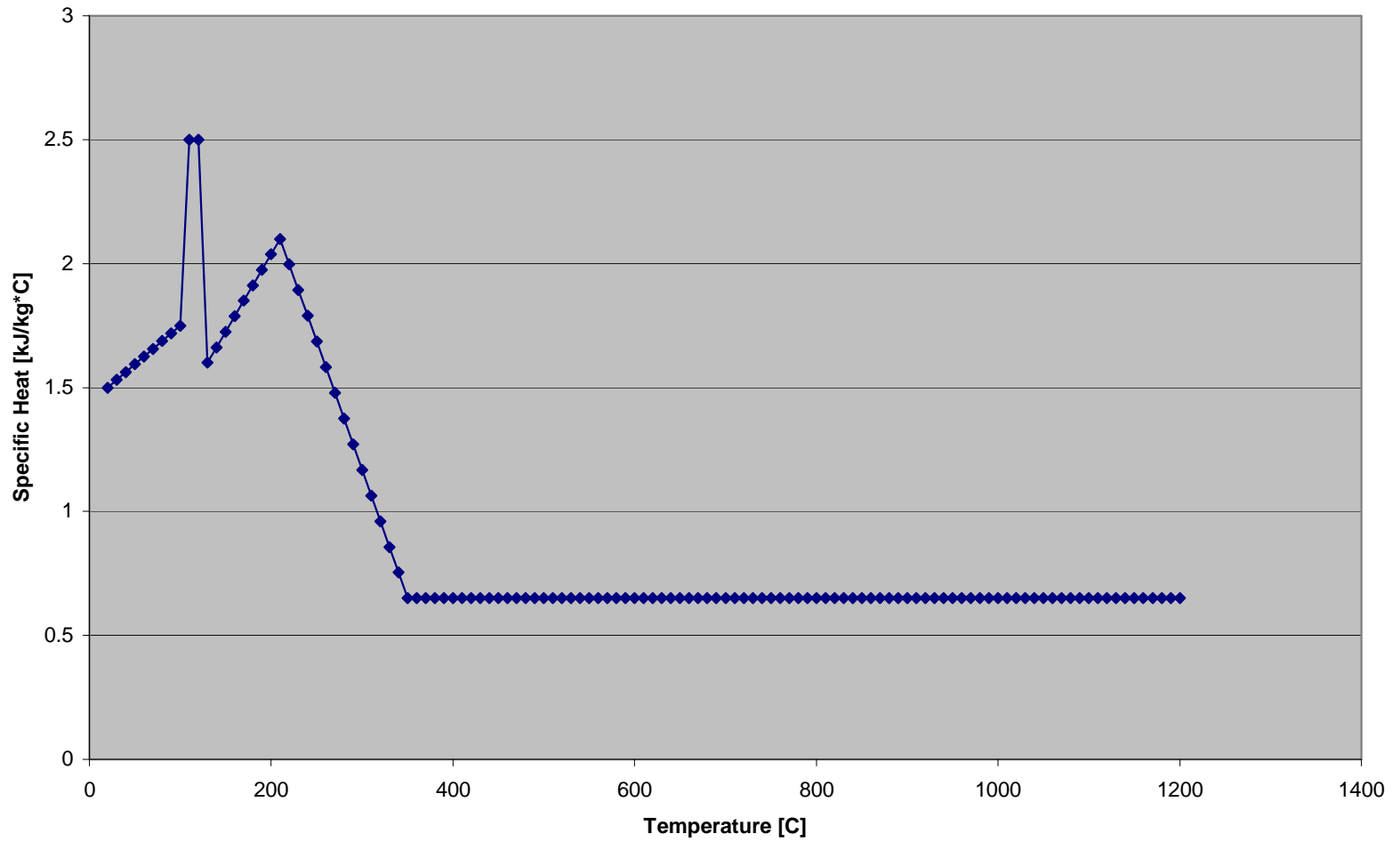
Konig and Walleij Representation of Specific Heat vs. Temperature

Gammon Specific Heat vs. Temperature



Gammon's Representation of Specific Heat vs. Temperature

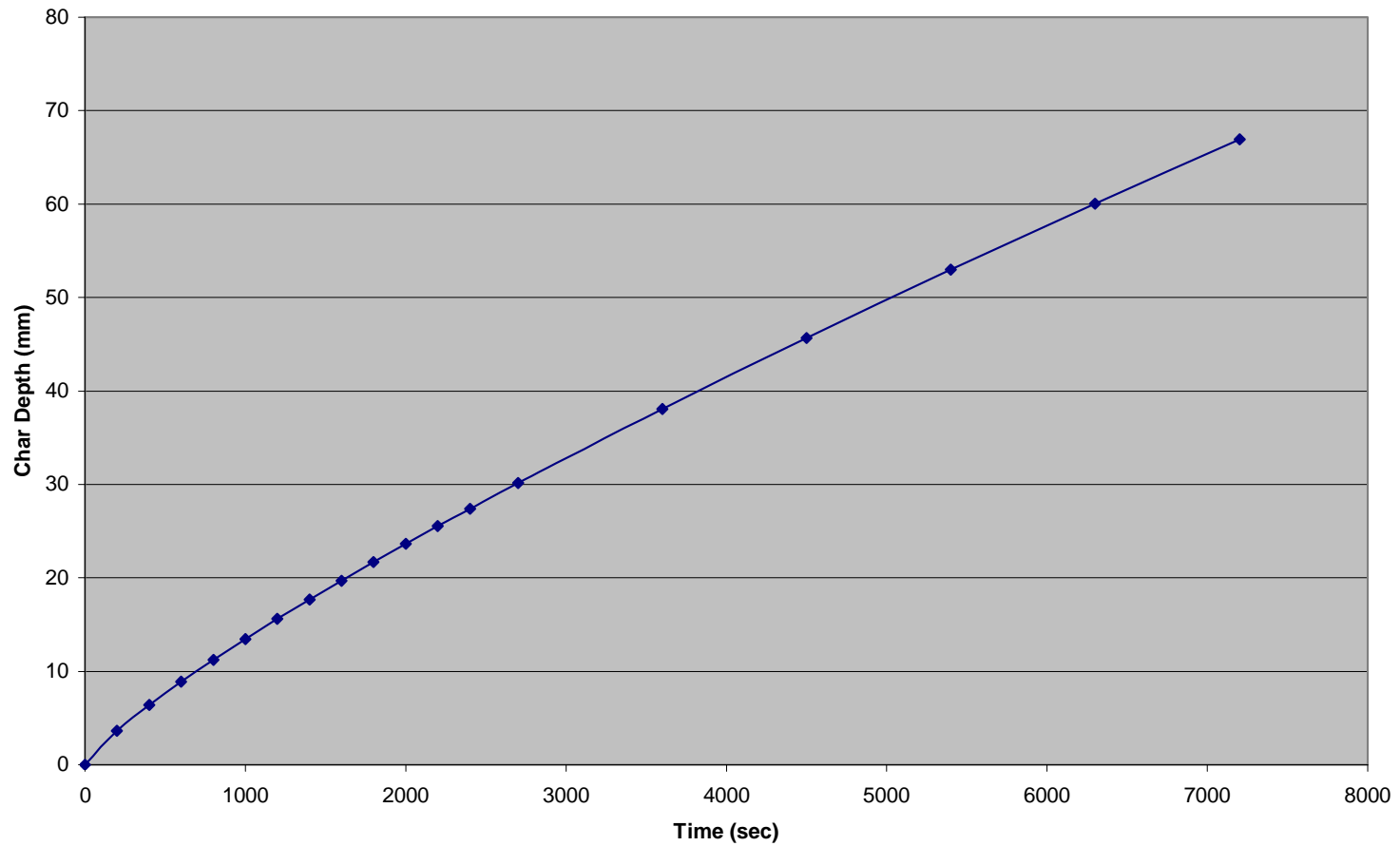
Lie Specific Heat vs. Temperature



T.T. Lie's Representation of Specific Heat vs. Temperature

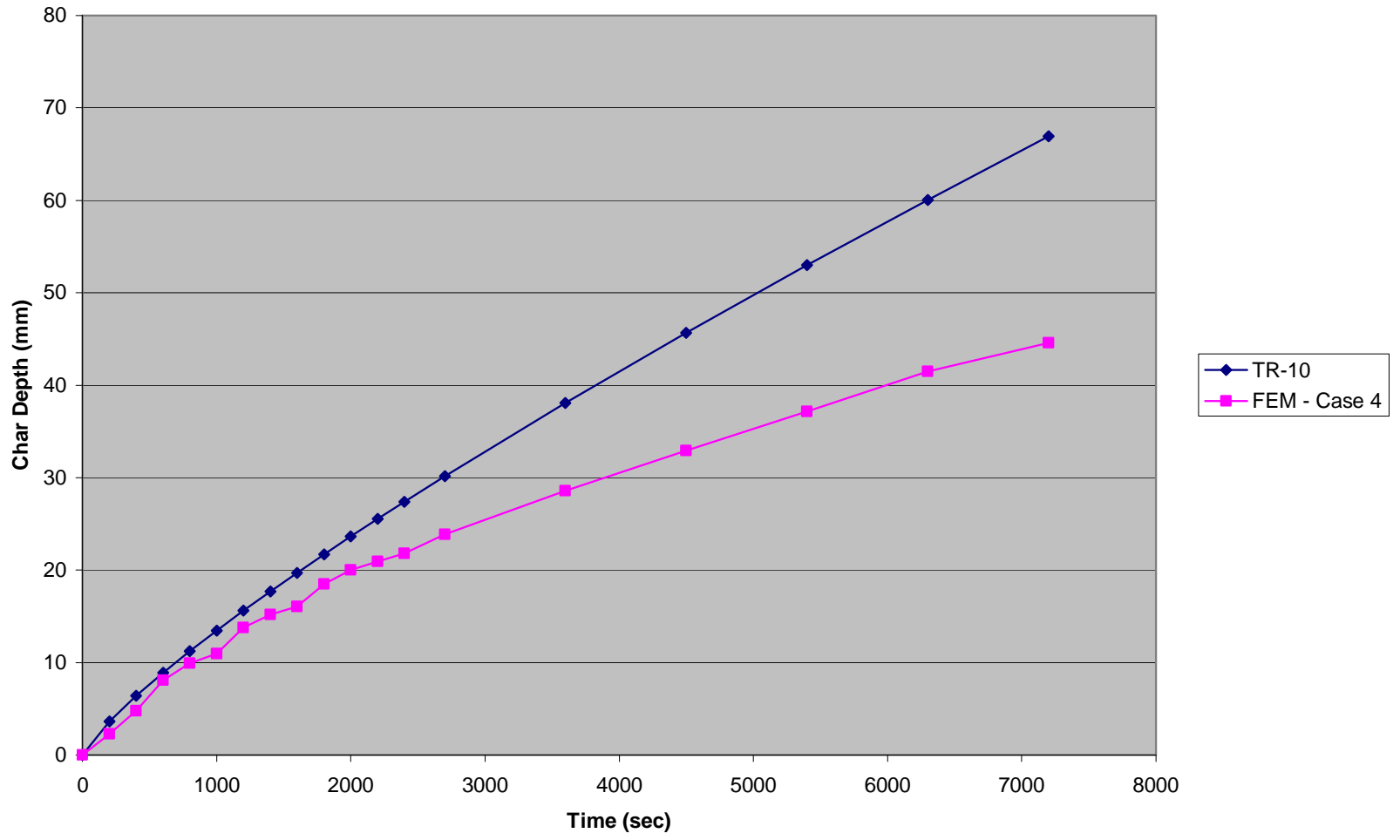
Appendix B – ASTM E-119 Char Depth Results

TR-10 Char Depth vs. Time



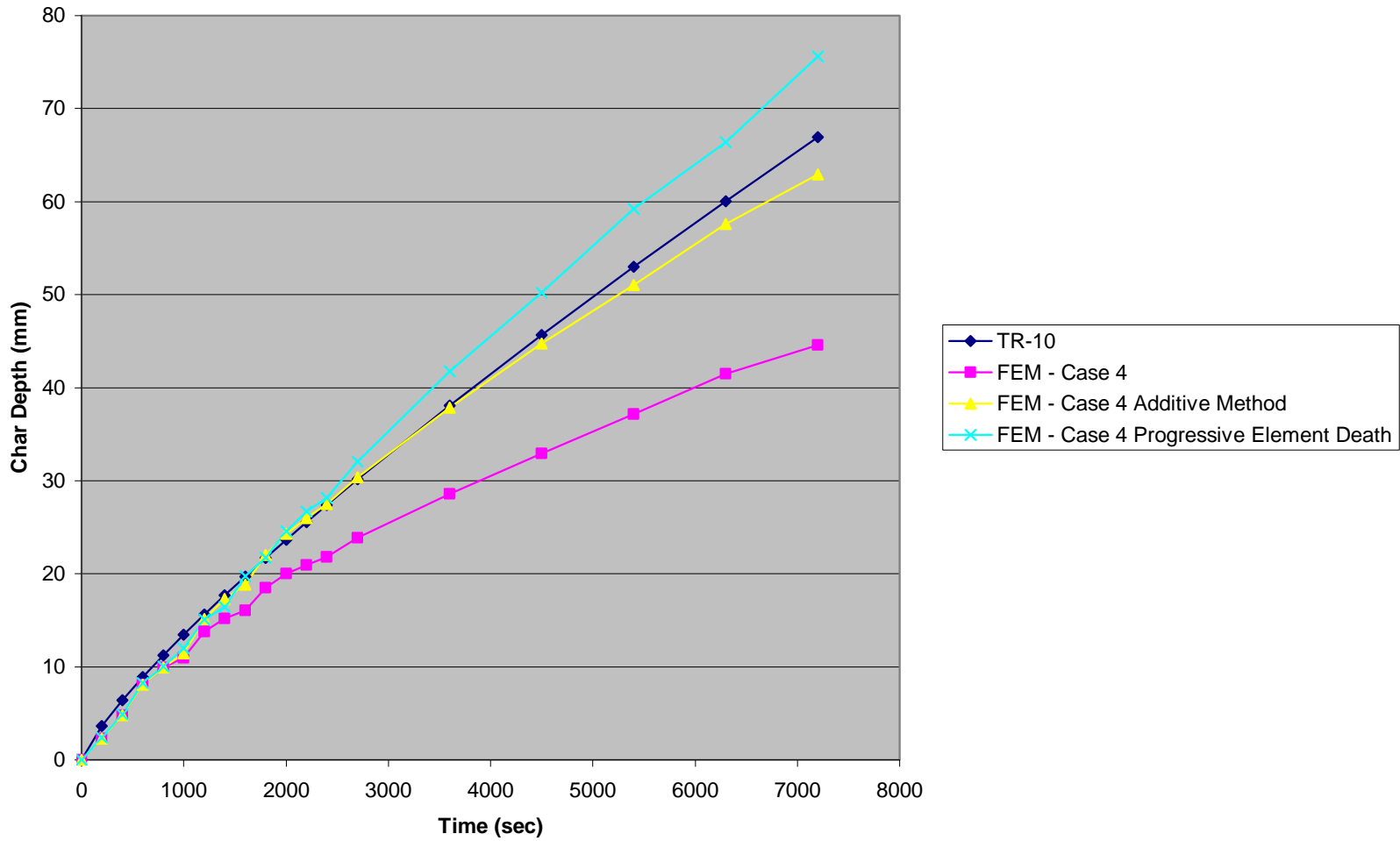
TR-10 Char Depth vs. Time

Case 4 FEM vs. TR-10 Char Depth



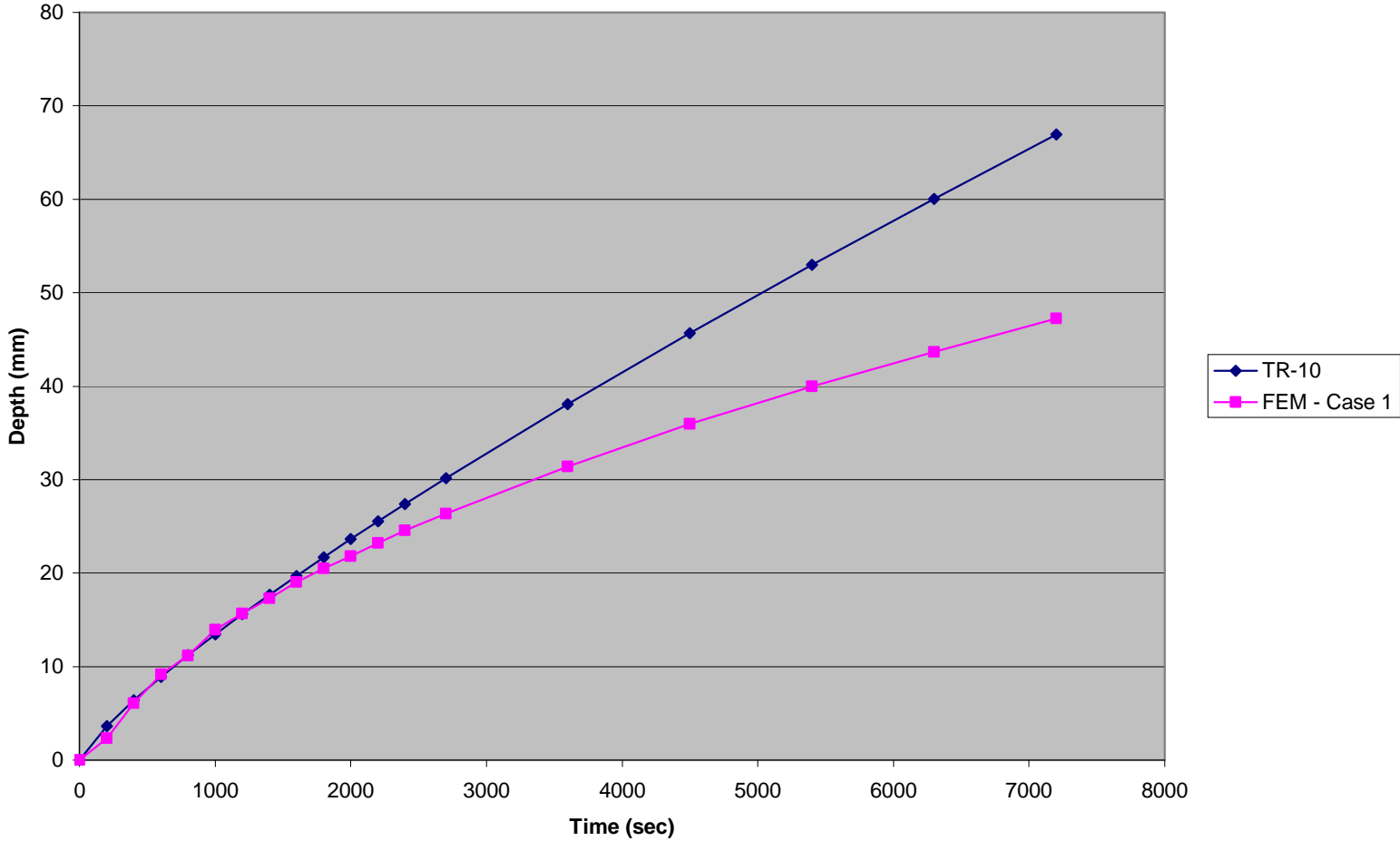
Case 4 FEM vs. TR-10 Char Depth

Case 4 FEM Variations vs. TR-10 Char Depth



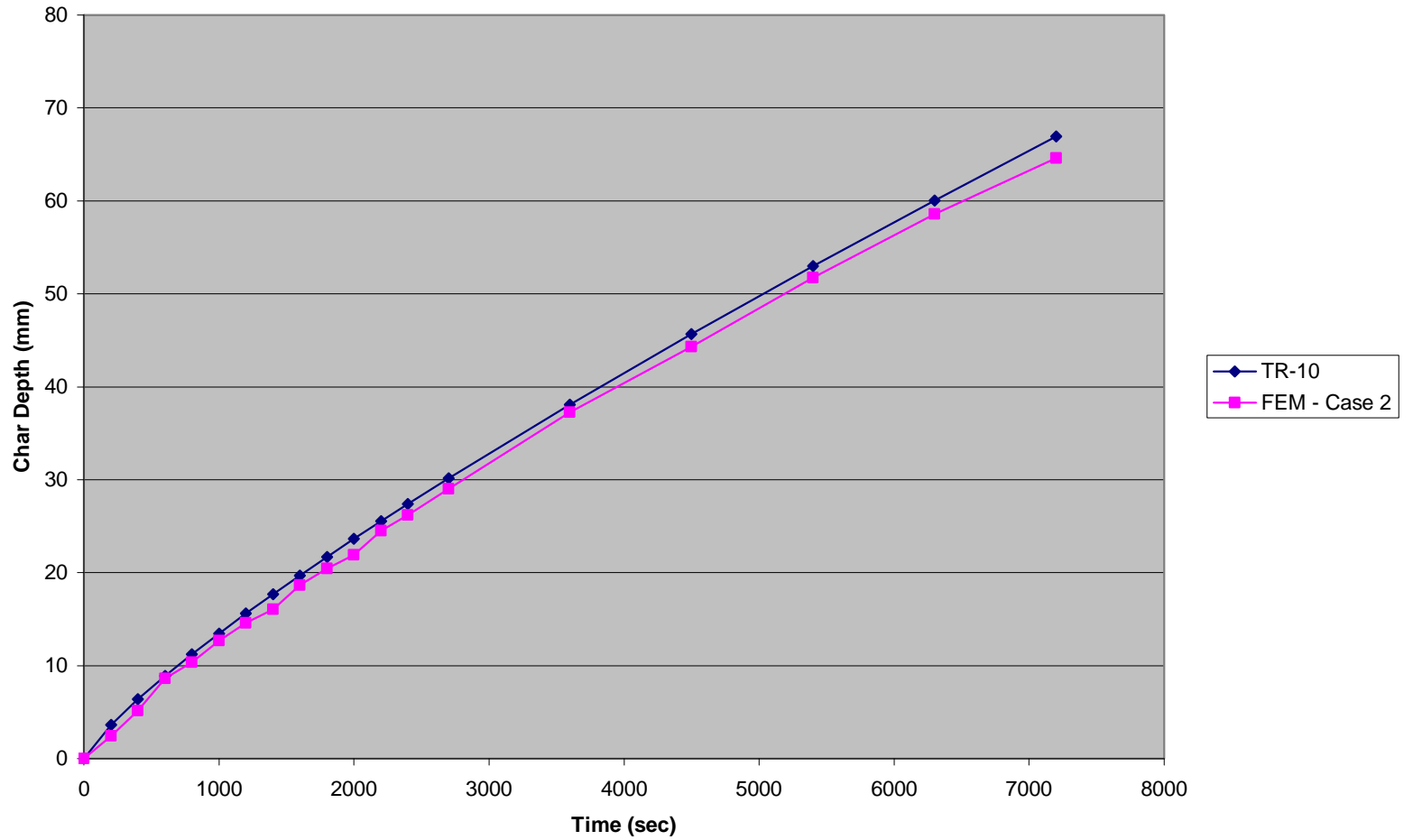
FEM Case 4 Variations vs. TR-10 Char Depths

Case 1 FEM vs. TR-10 Char Depth



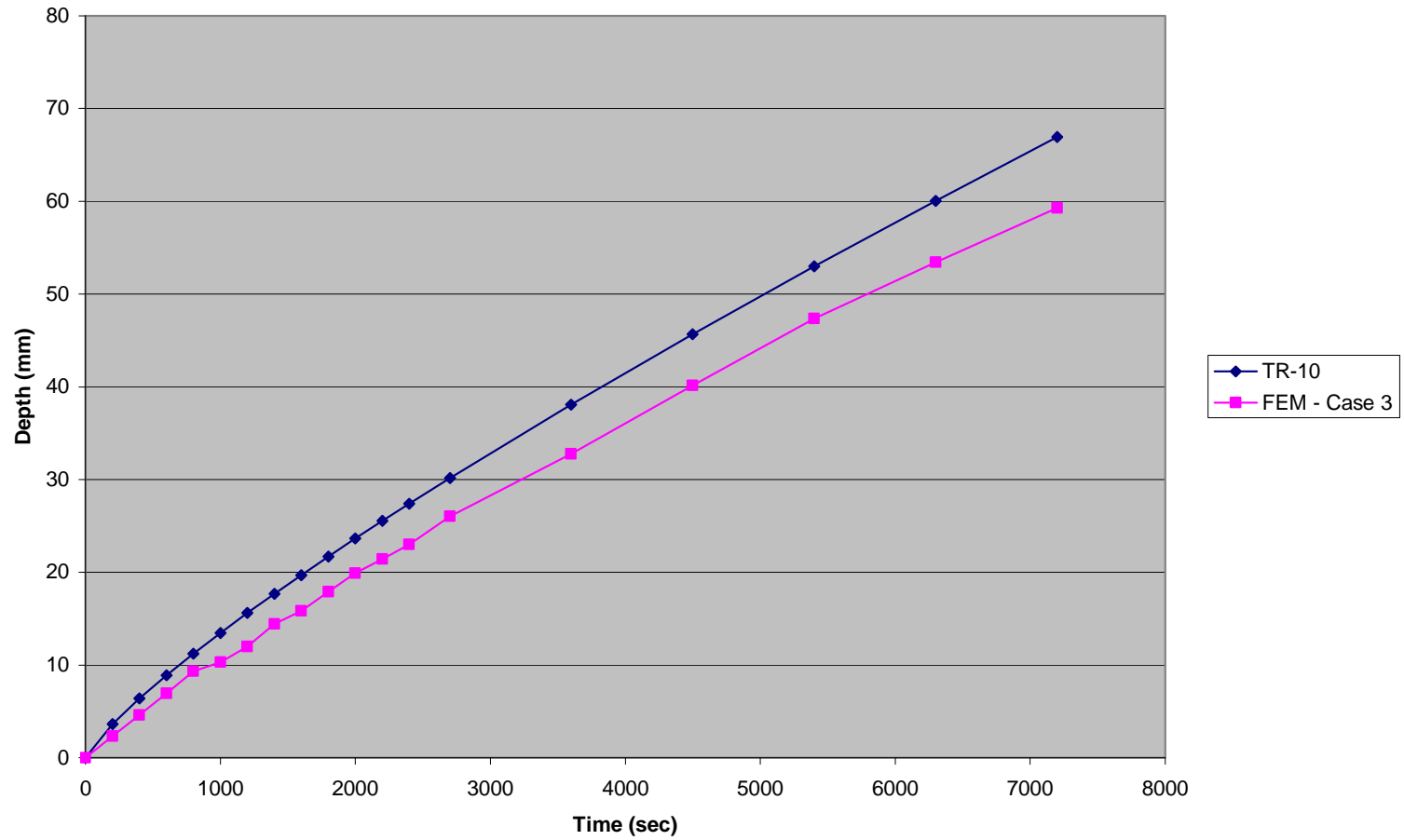
FEM Case 1 vs. TR-10 Char Depth
Constant Density, Constant Specific Heat, Constant Thermal Conductivity

Case 2 FEM vs. TR-10



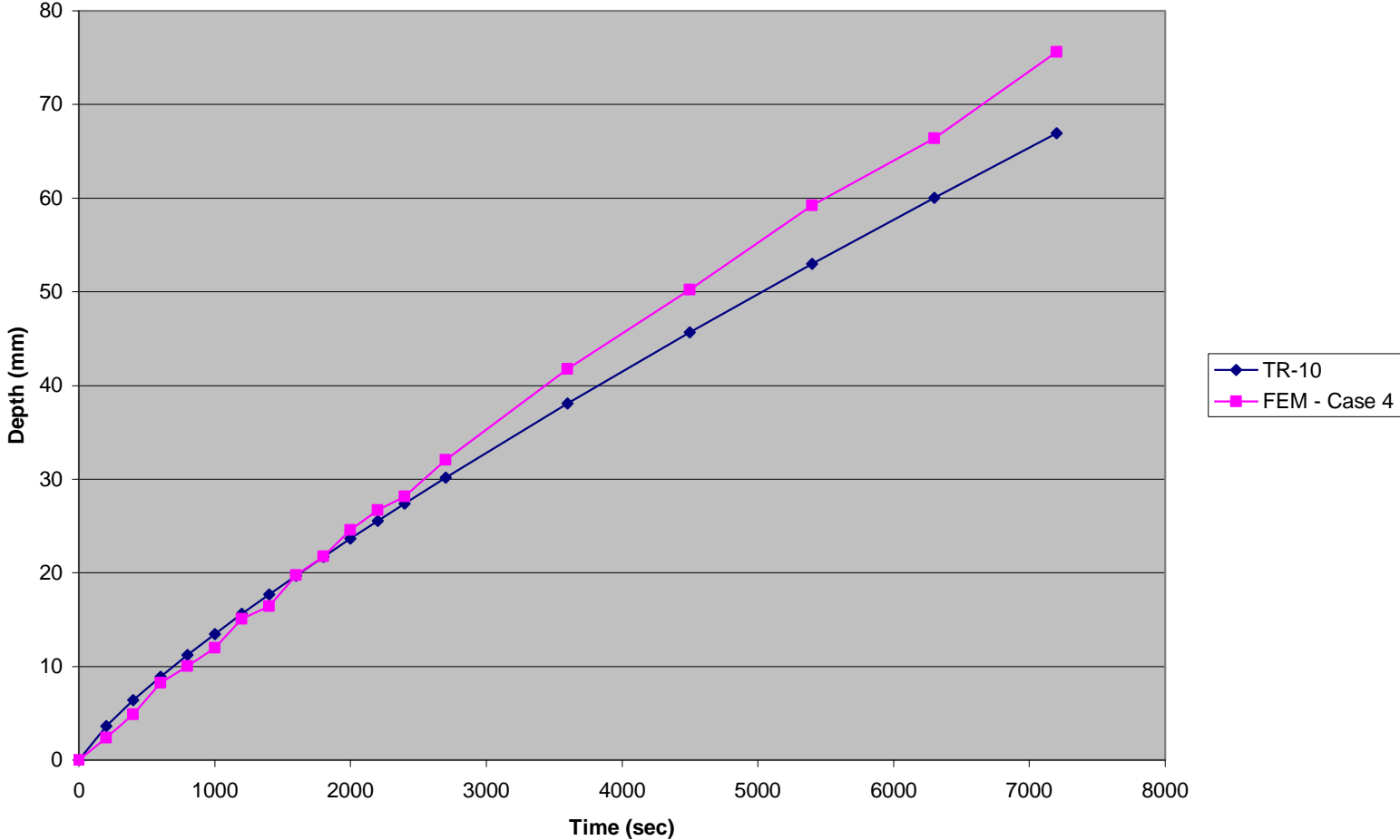
FEM Case 2 vs. TR-10 Char Depth
Constant Density, Constant Specific Heat, Non-Linear Thermal Conductivity

Case 3 FEM vs. TR-10 Char Depth



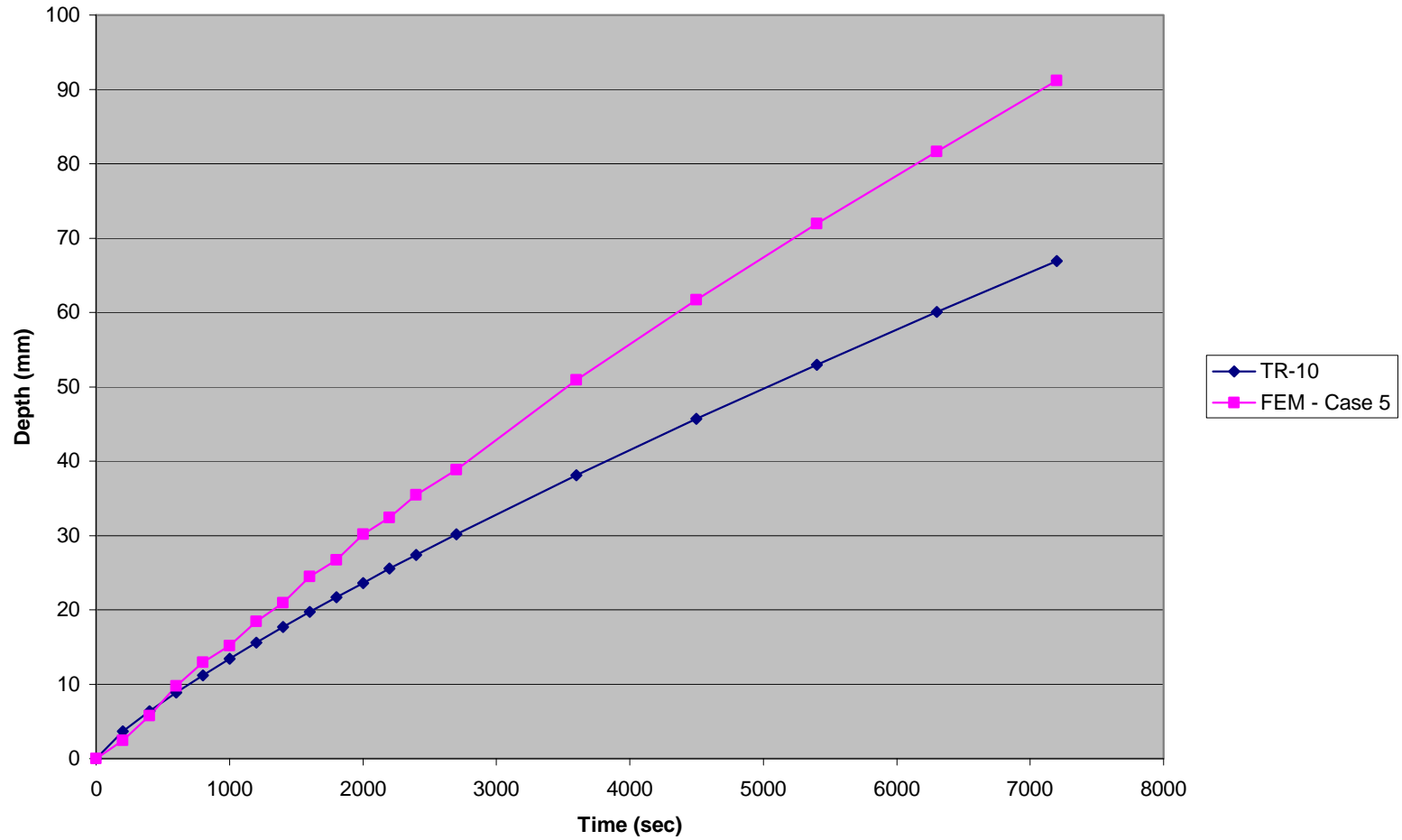
FEM Case 3 vs. TR-10 Char Depth
Constant Density, Non-Linear Specific Heat, Non-Linear Thermal Conductivity

Case 4 FEM vs. TR-10 Char Depth



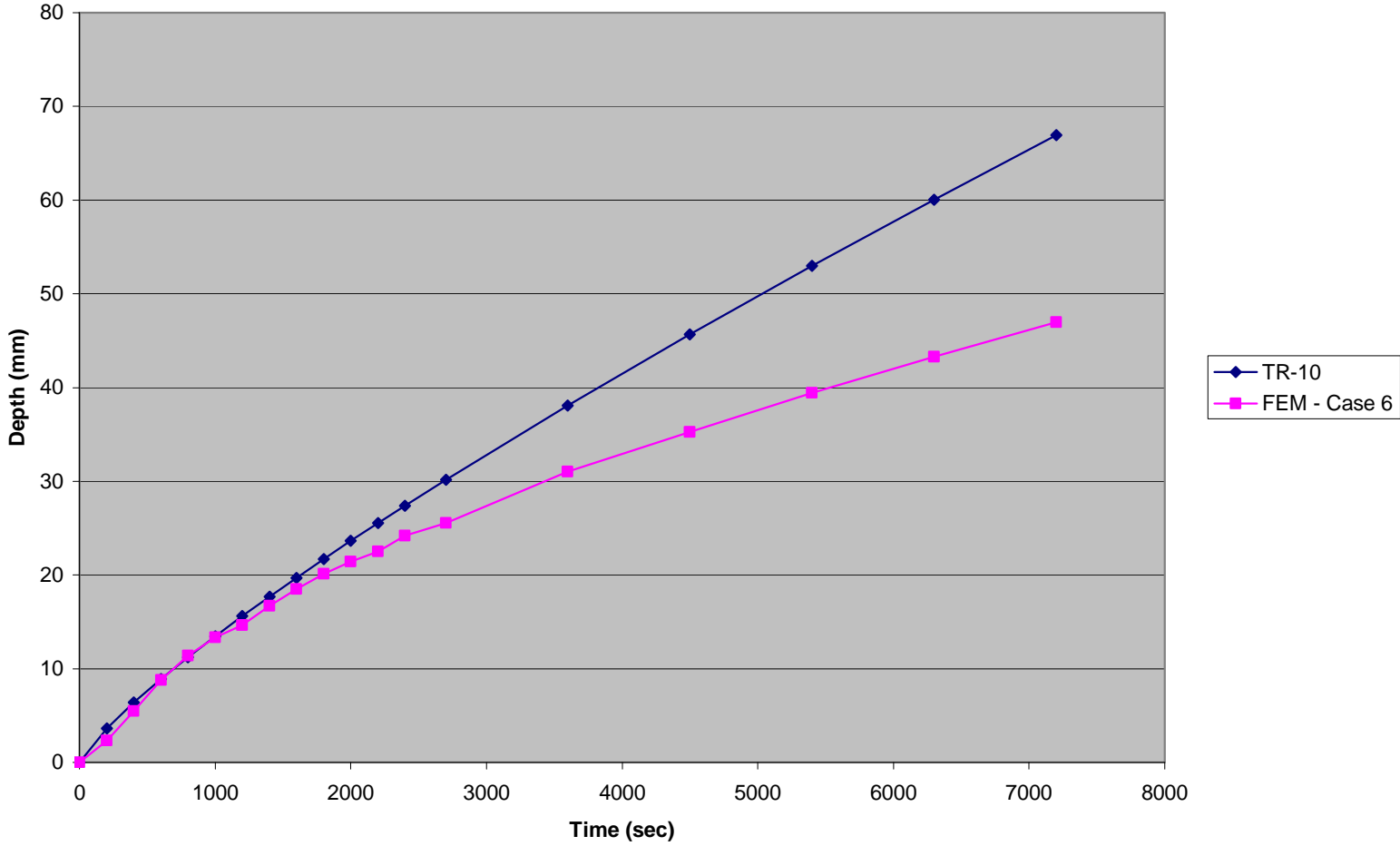
FEM Case 4 vs. TR-10 Char Depth
Non-Linear Density, Non-Linear Specific Heat, Non-Linear Thermal Conductivity

Case 5 FEM vs. TR-10 Char Depth



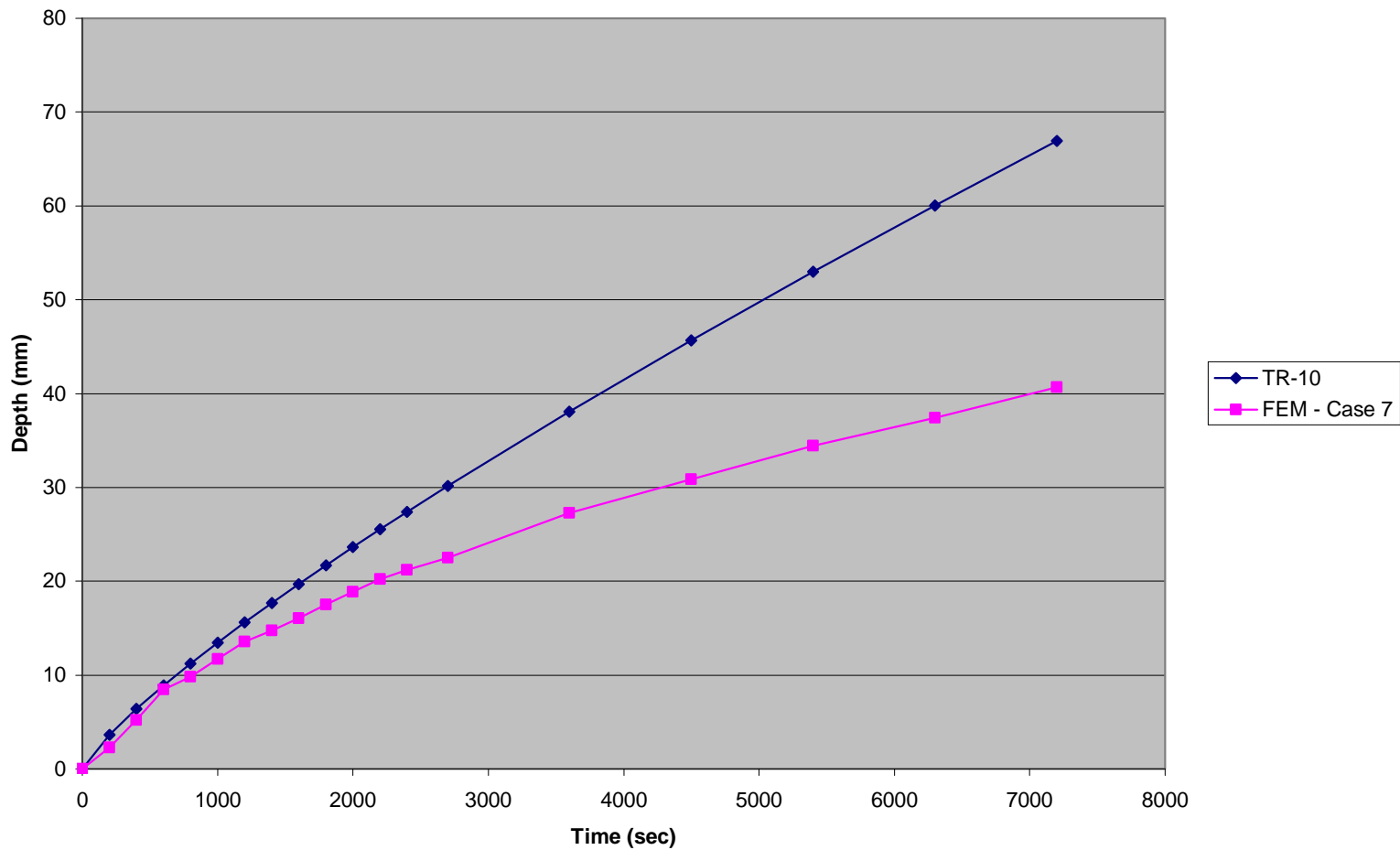
FEM Case 5 vs. TR-10 Char Depth
Non-Linear Density, Constant Specific Heat, Non-Linear Thermal Conductivity

Case 6 FEM vs. TR-10 Char Depth



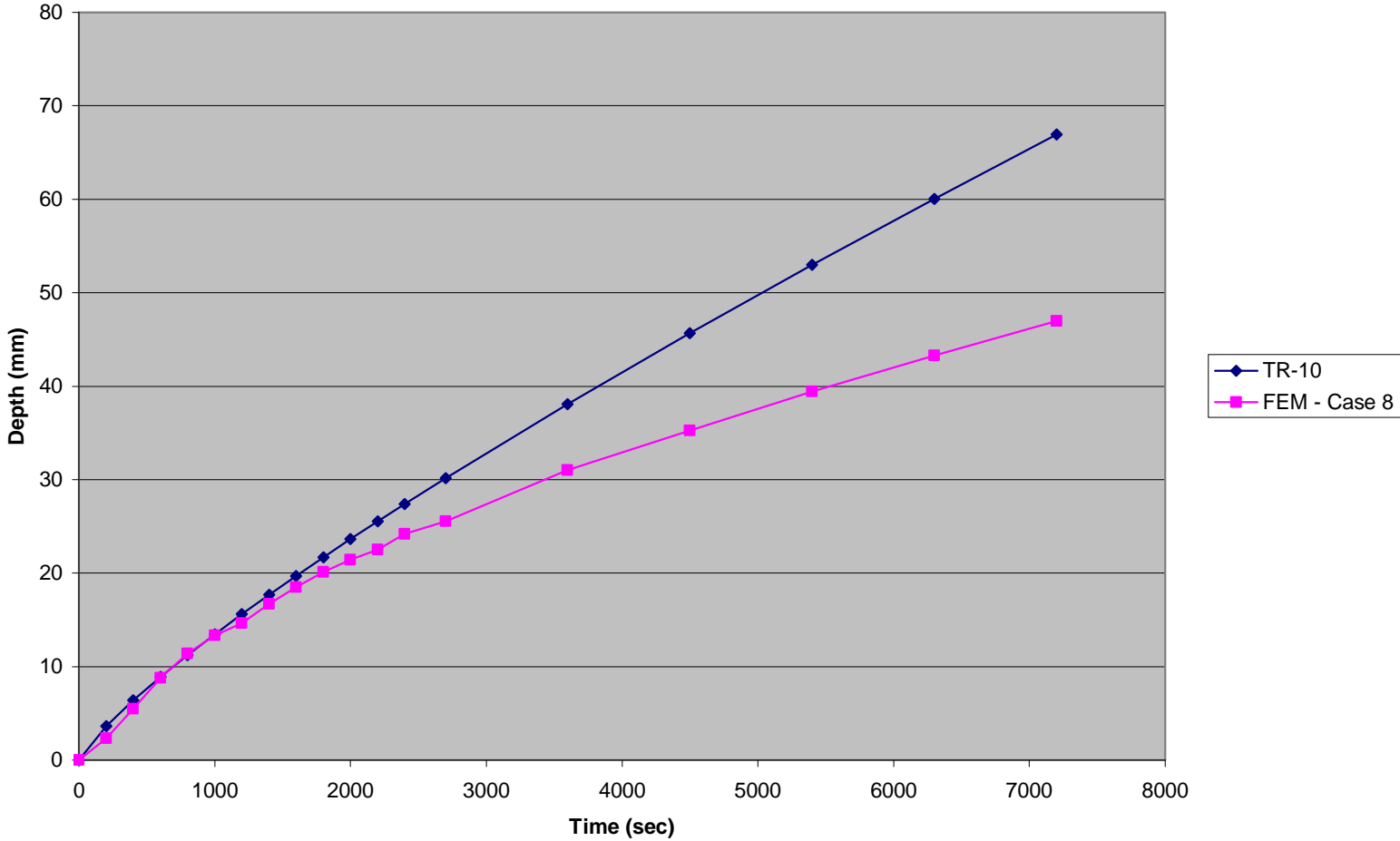
FEM Case 6 vs. TR-10 Char Depth
Non-Linear Density, Non-Linear Specific Heat, Constant Thermal Conductivity

Case 7 FEM vs. TR-10 Char Depth



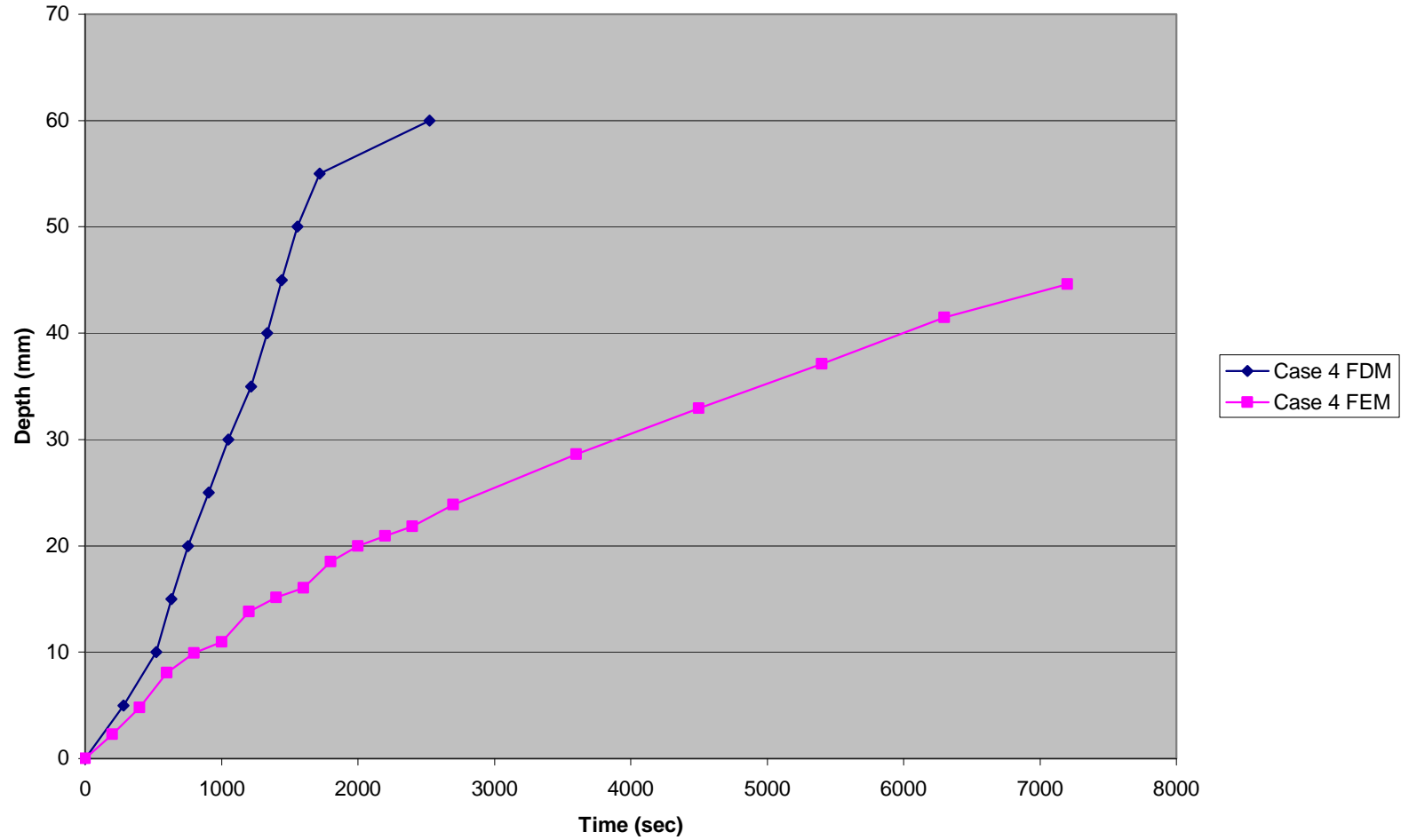
FEM Case 7 vs. TR-10 Char Depth
Constant Density, Non-Linear Specific Heat, Constant Thermal Conductivity

Case 8 FEM vs. TR-10 Char Depth



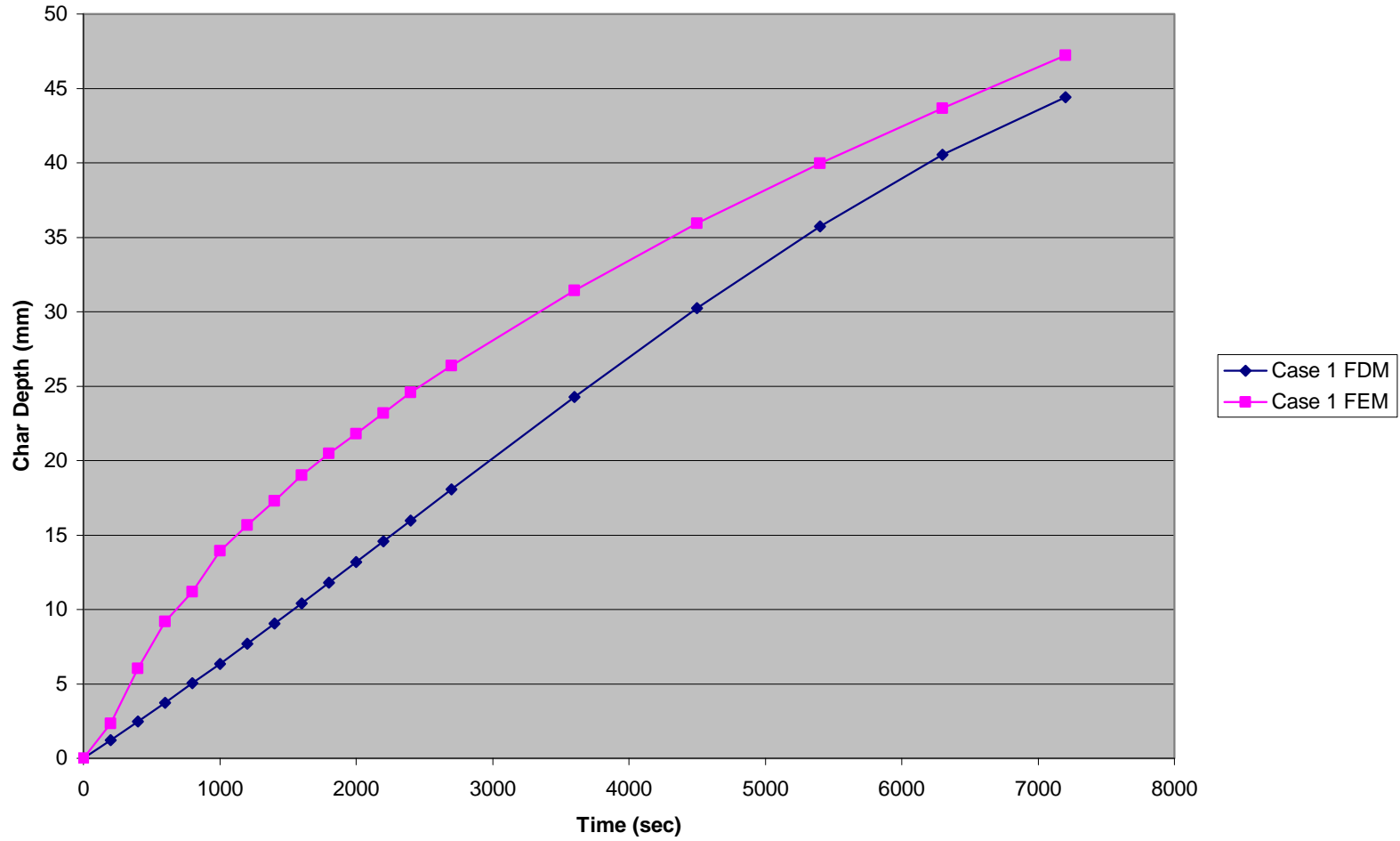
FEM Case 8 vs. TR-10 Char Depth
Non-Linear Density, Constant Specific Heat, Constant Thermal Conductivity

Case 4 FEM vs. Case 4 FDM



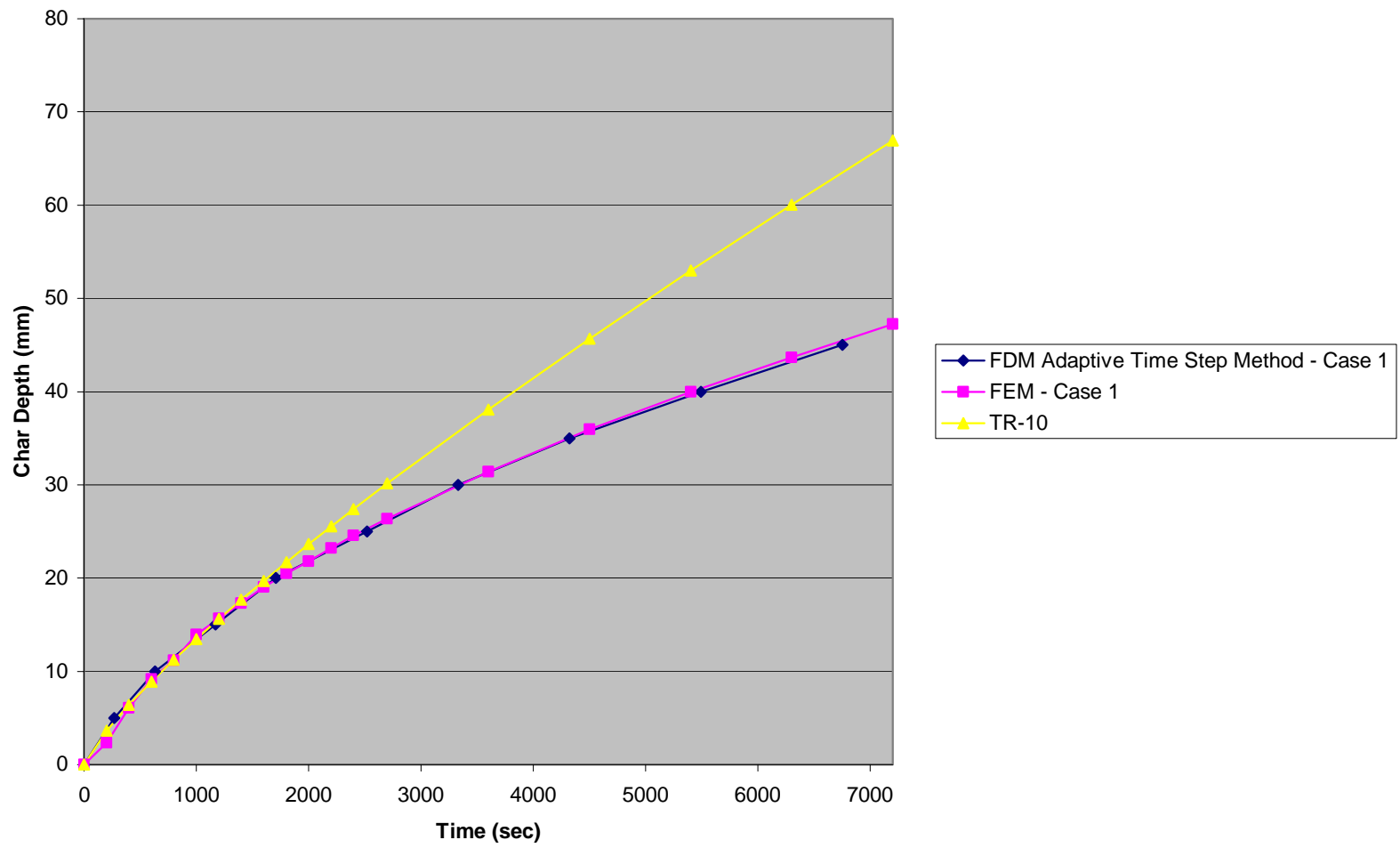
Case 4 FEM vs. Case 4 FDM with Model Instabilities

Case 1 FEM vs. Case 1 FDM



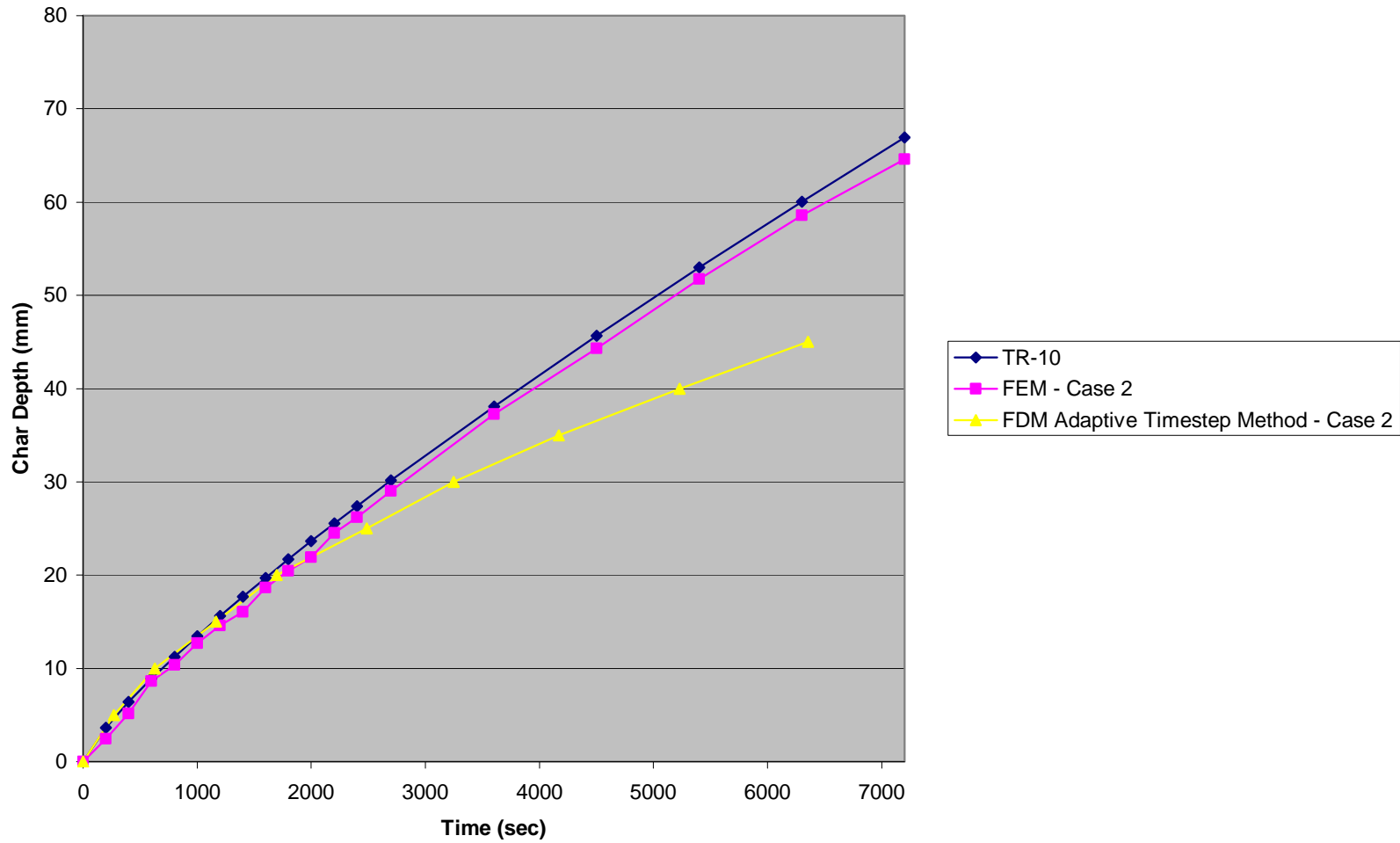
Case 1 FEM vs. Case 1 FDM Char Depth

FDM - Case 1 Adaptive Time Step Method vs. FEM - Case 1



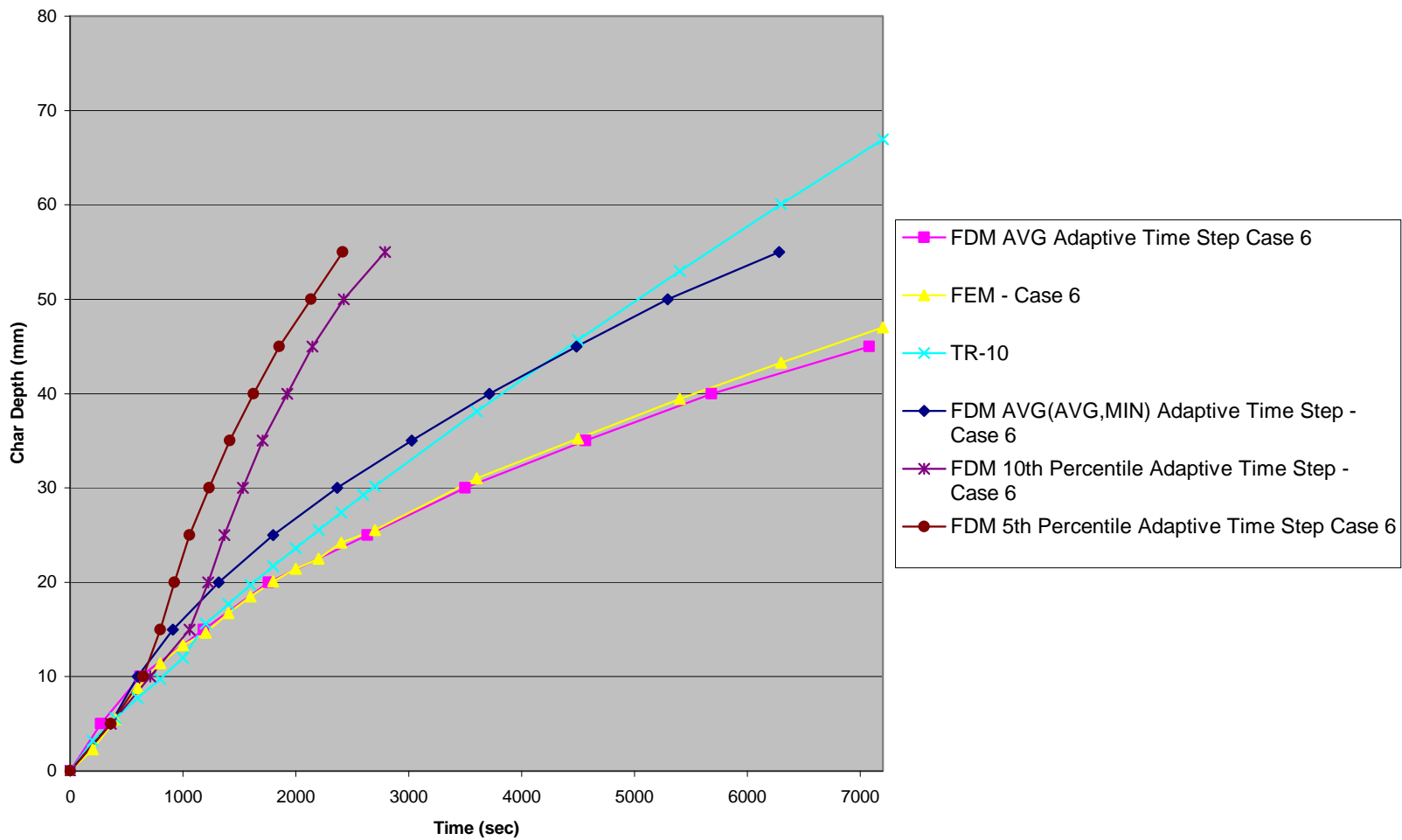
Case 1 FEM vs. FDM Adaptive Time Step Method

Case 2 - FEM vs. FDM Adaptive Time Step Method



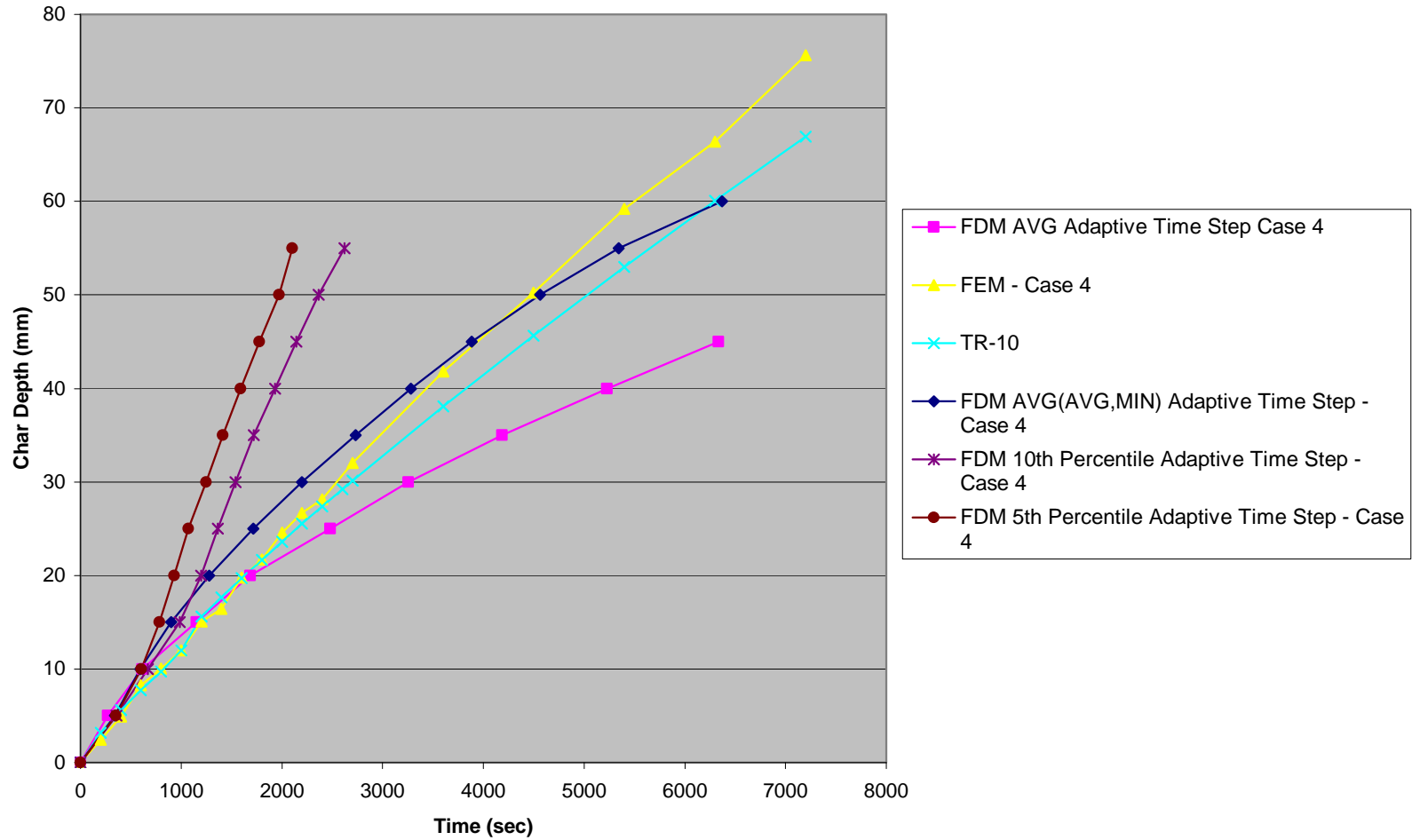
Case 2 FEM vs. FDM Adaptive Time Step Method

Case 6 Comparison of Adaptive Time Step Selection



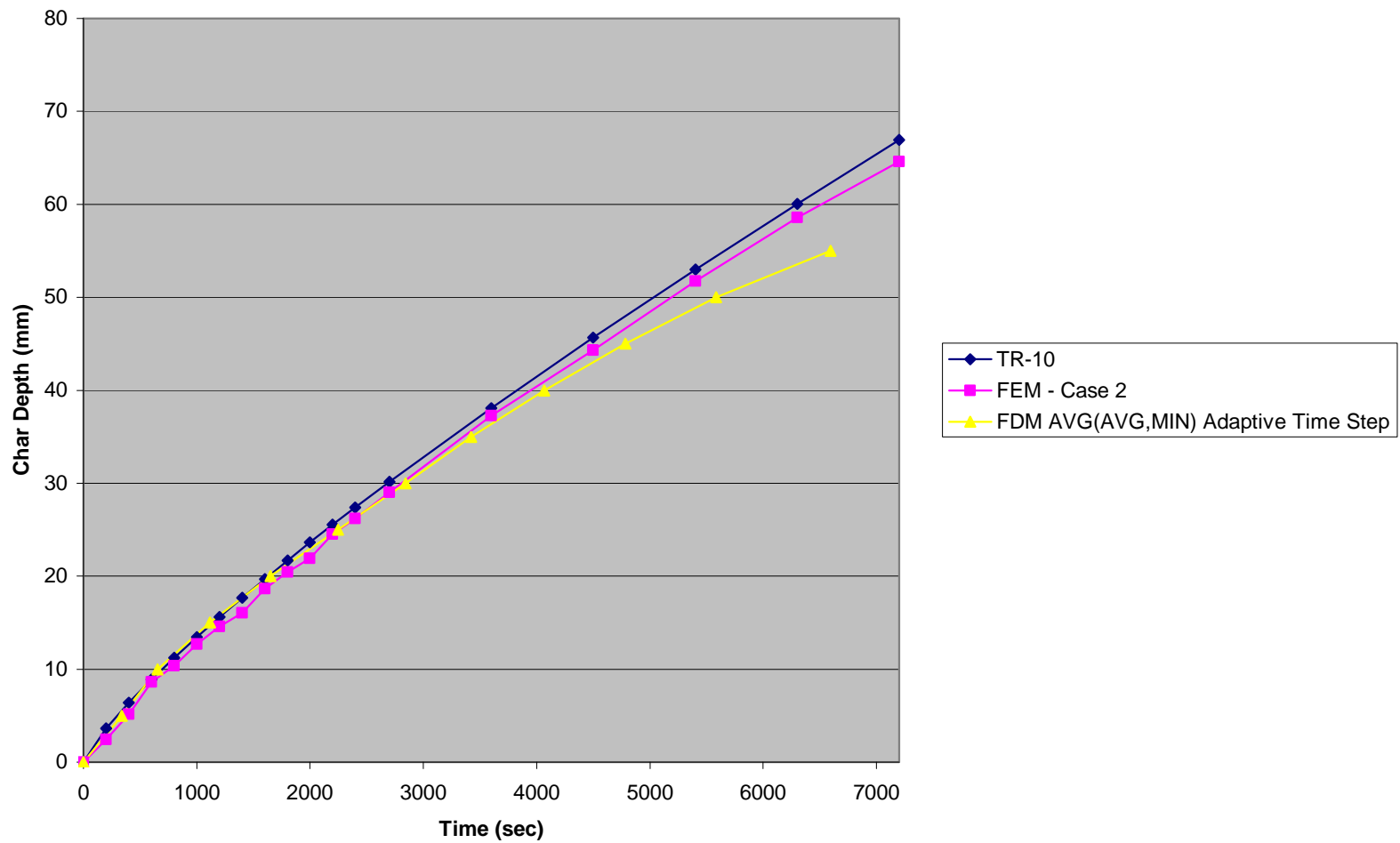
FDM Adaptive Time Step Selection Comparison - Case 6

Case 4 Comparison of Adaptive Time Step Selection



FDM Adaptive Time Step Selection Comparison - Case 4

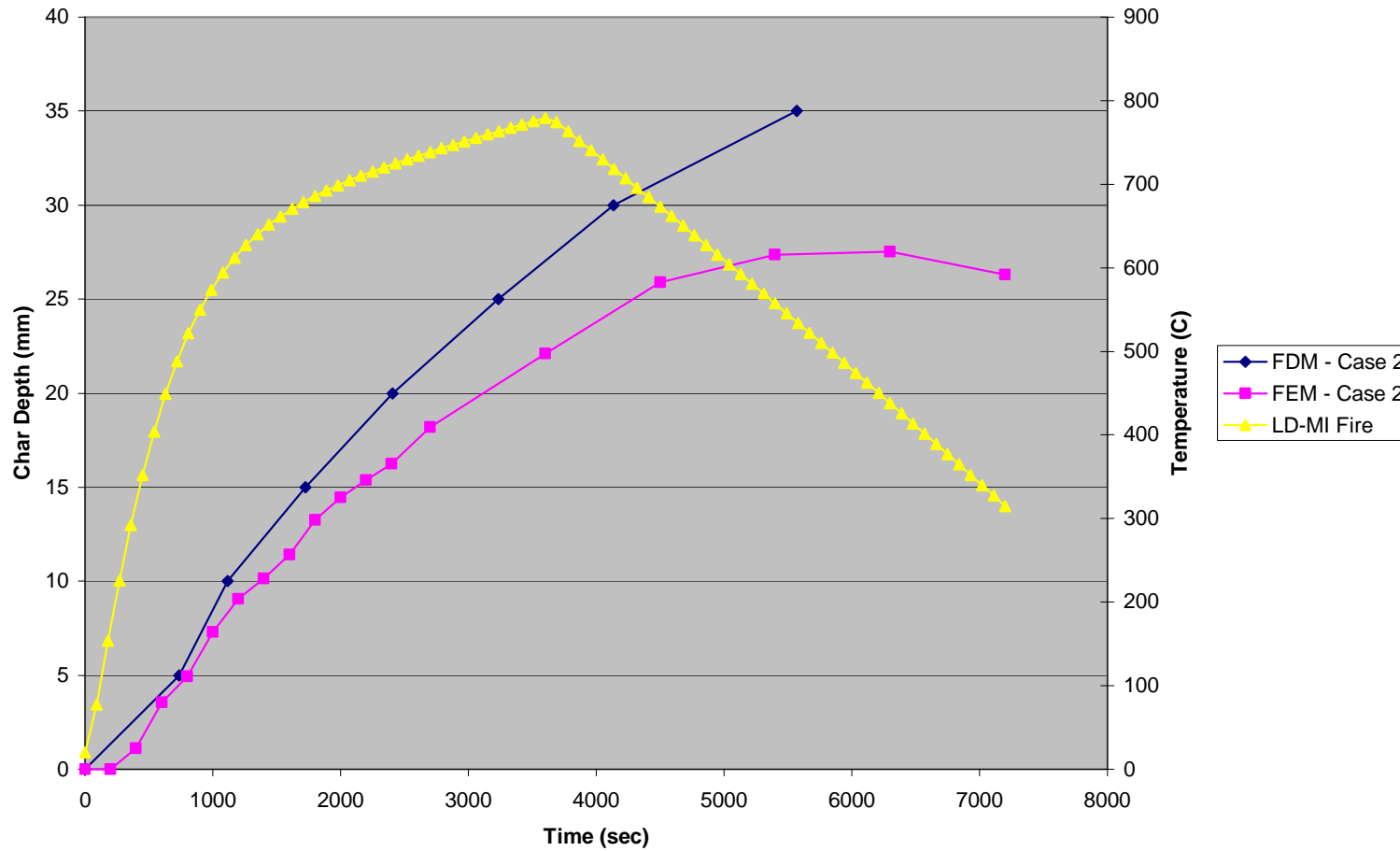
Case 2 FEM and FDM vs. TR-10



Best Fit FEM and FDM Char Depth Models

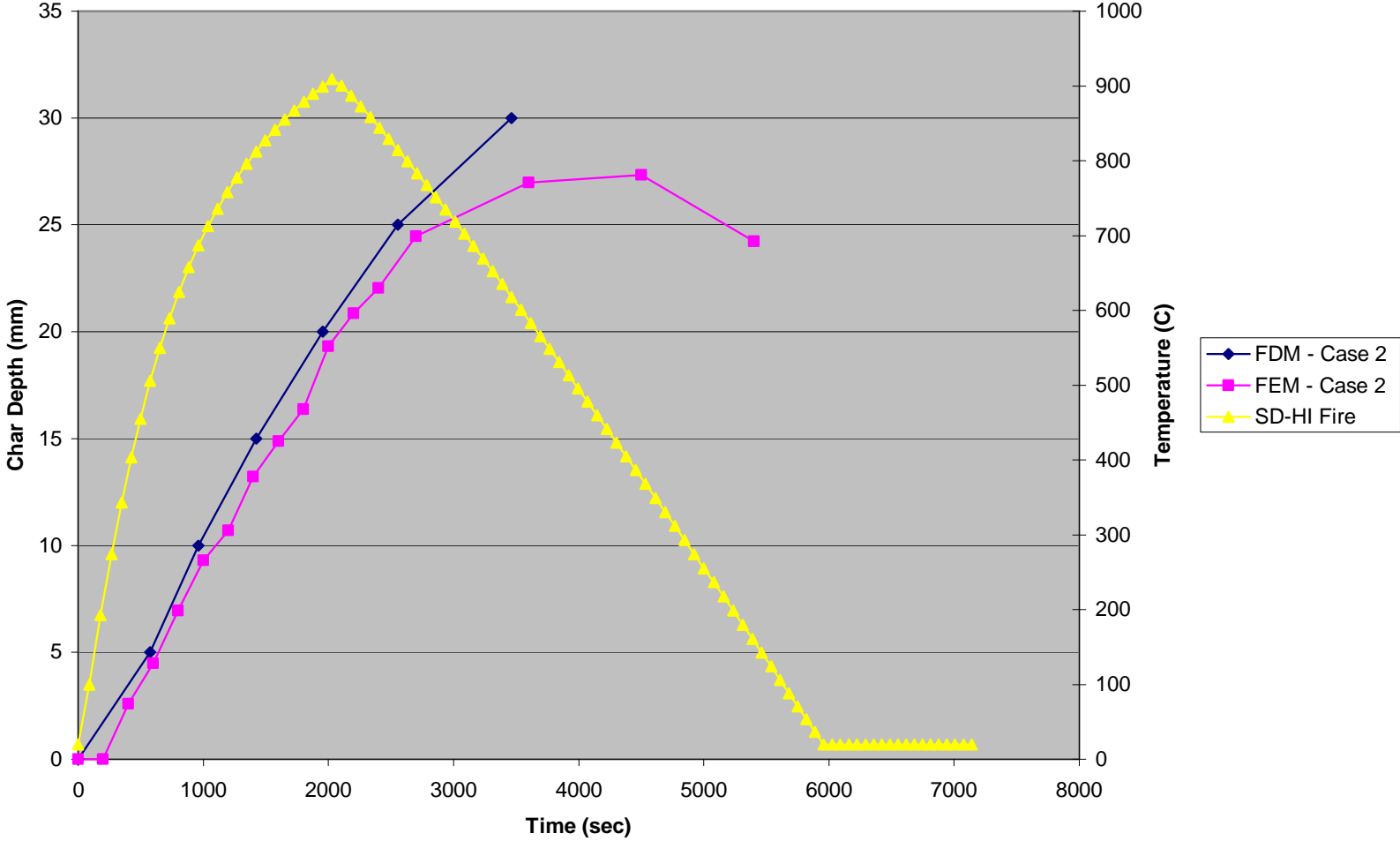
Appendix C – Natural Fire Char Depth Results

LD-MI Design Fire - Case 2



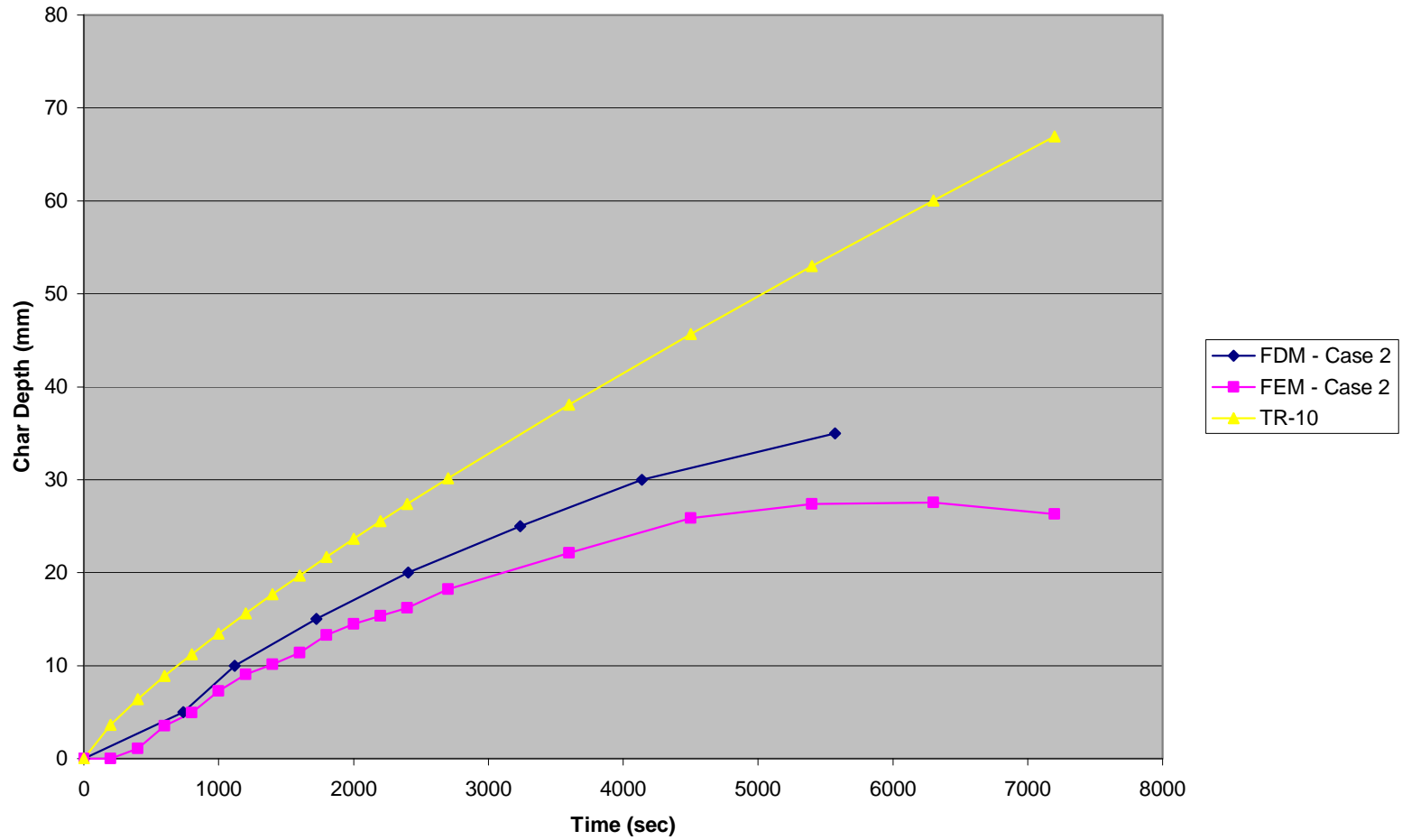
FDM and FEM Char Depth - LDMI Fire - Case 2

SD-HI Design Fire - Case 2



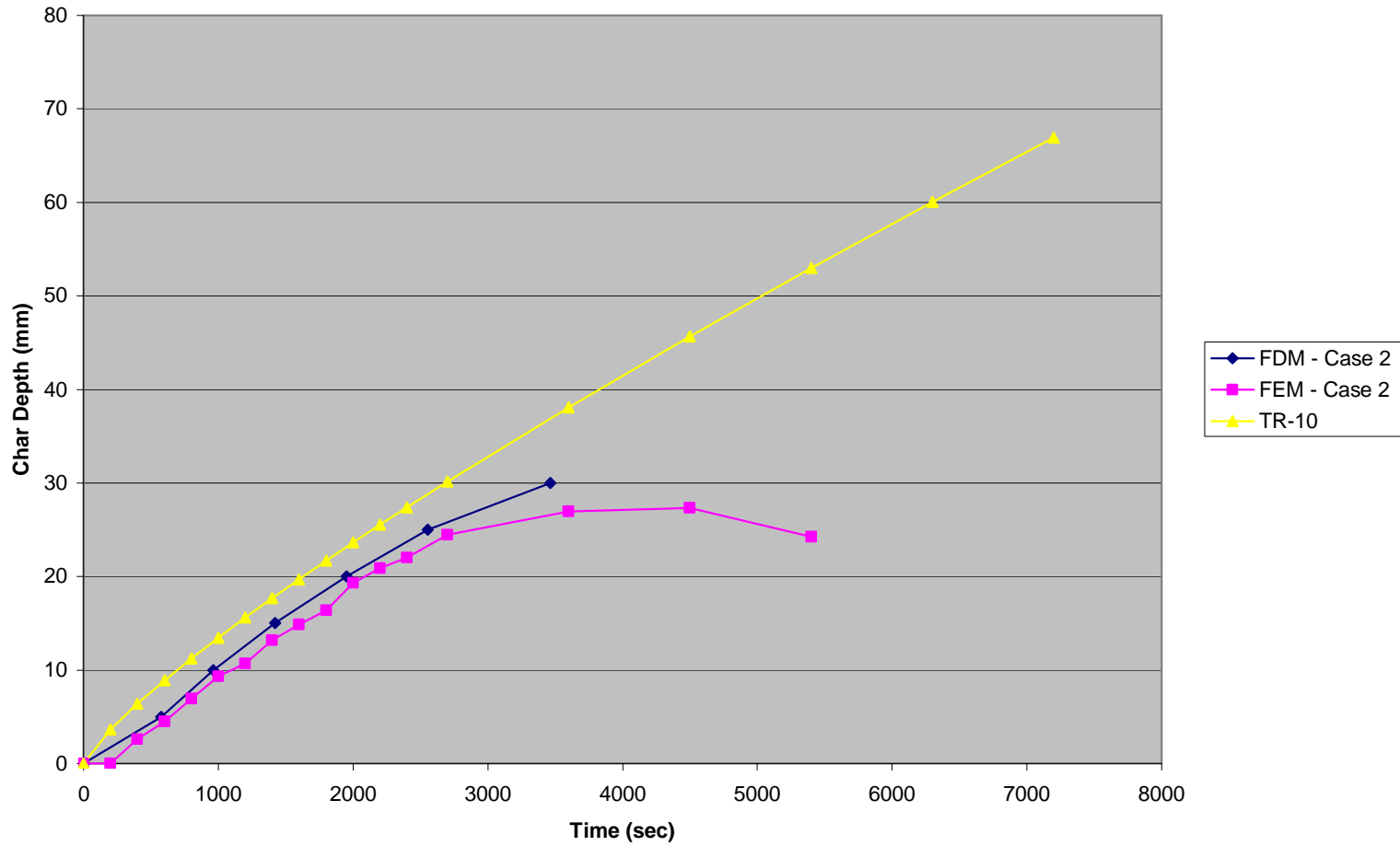
FDM and FEM Char Depth - SD-HI Fire - Case 2

LD-MI Design Fire - Case 2



FDM vs. FEM Case 2 - LD-MI
Compared to TR-10 Char Depth for ASTM E-119 Exposure

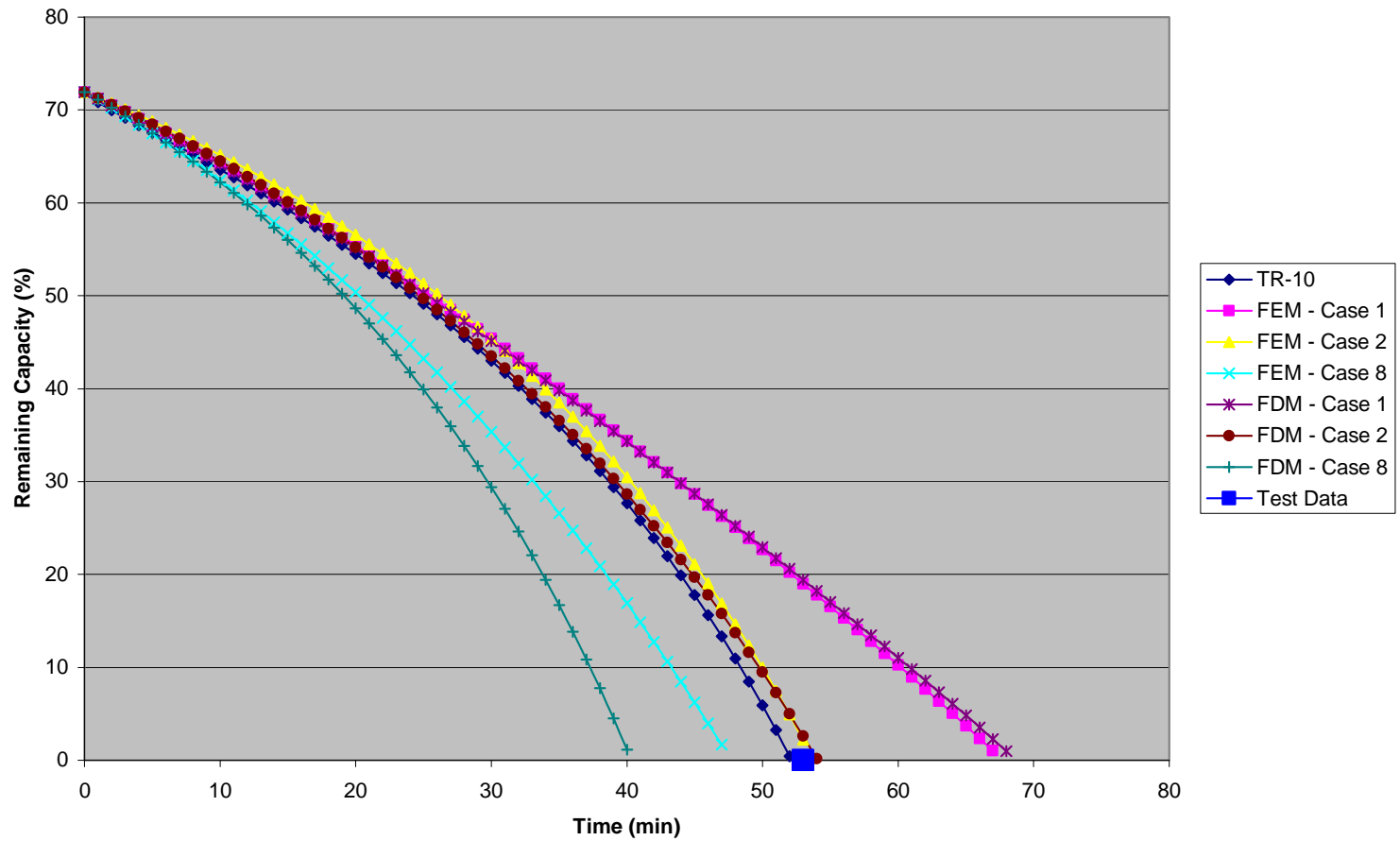
SD-HI Design Fire - Case 2



FDM vs. FEM Case 2 - SD-HI
Compared to TR-10 Char Depth for ASTM E-119 Exposure

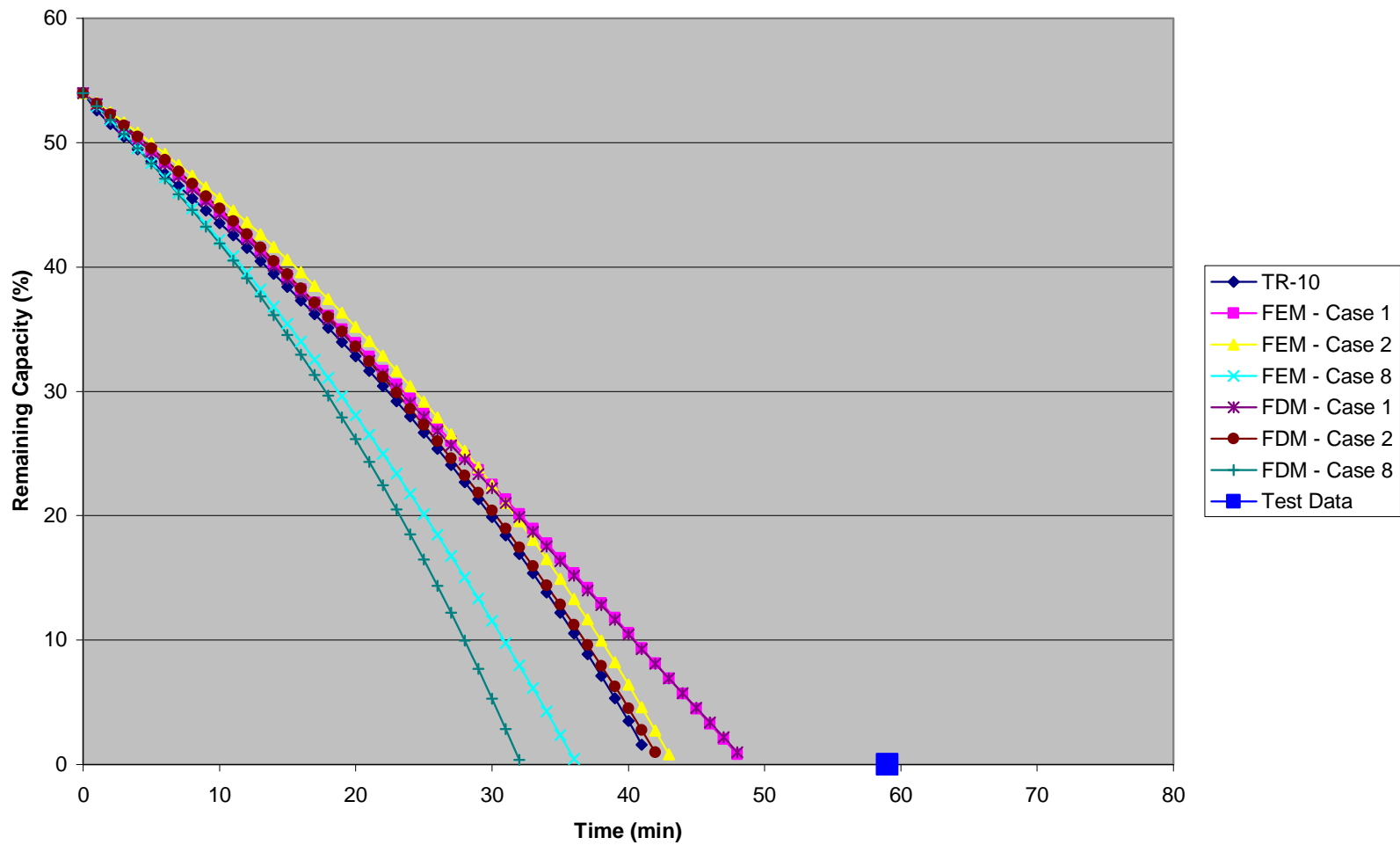
Appendix D – TR-10 Beam and Column Time to Failure Comparisons

TRADA Beam Comparison



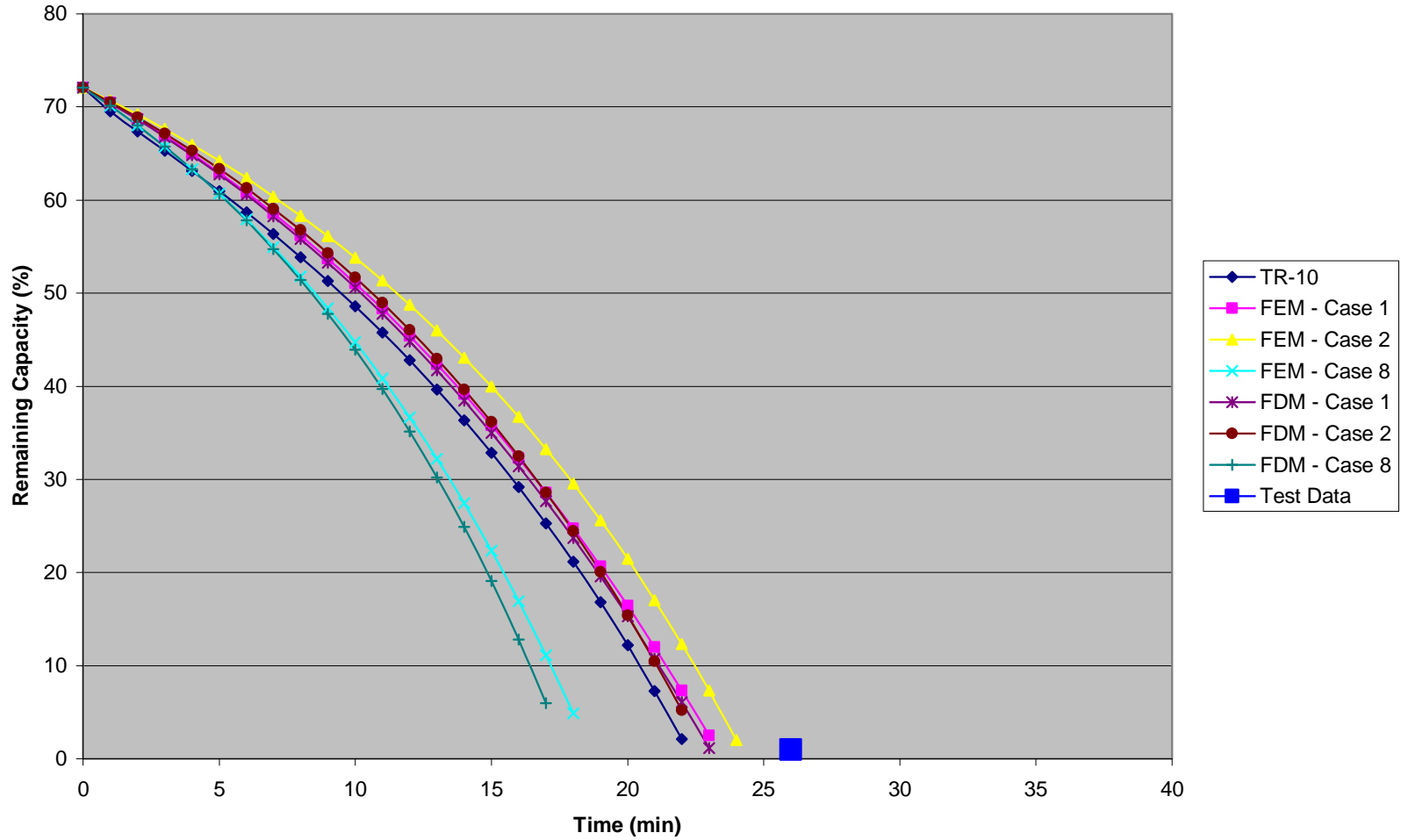
TRADA Beam TR-10 vs. FEM and FDM

FCNSW-BB Beam Comparison



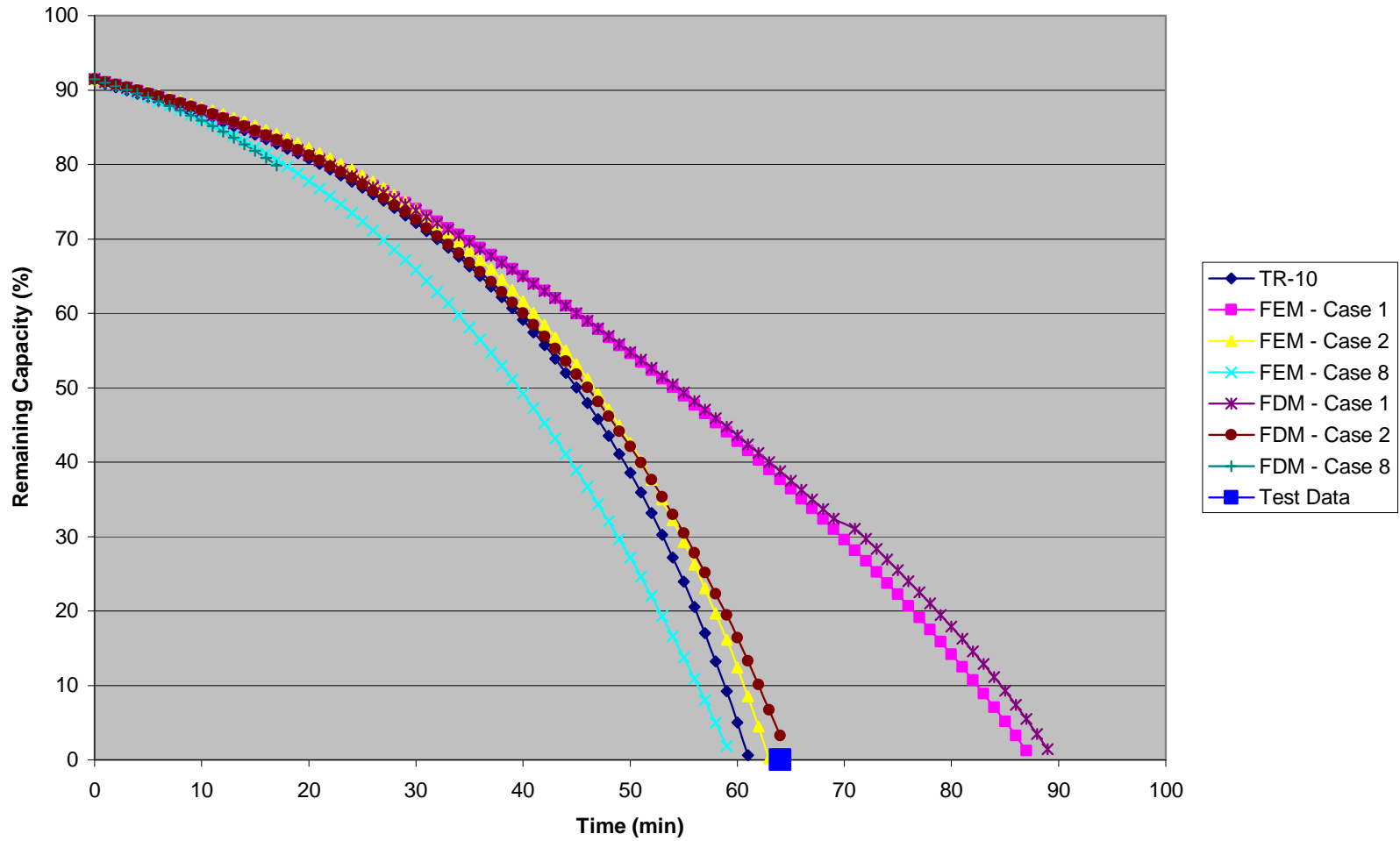
FCNSW-BB Beam TR-10 vs. FEM and FDM

R15A Column Comparison



R15A Column TR-10 vs. FEM and FDM

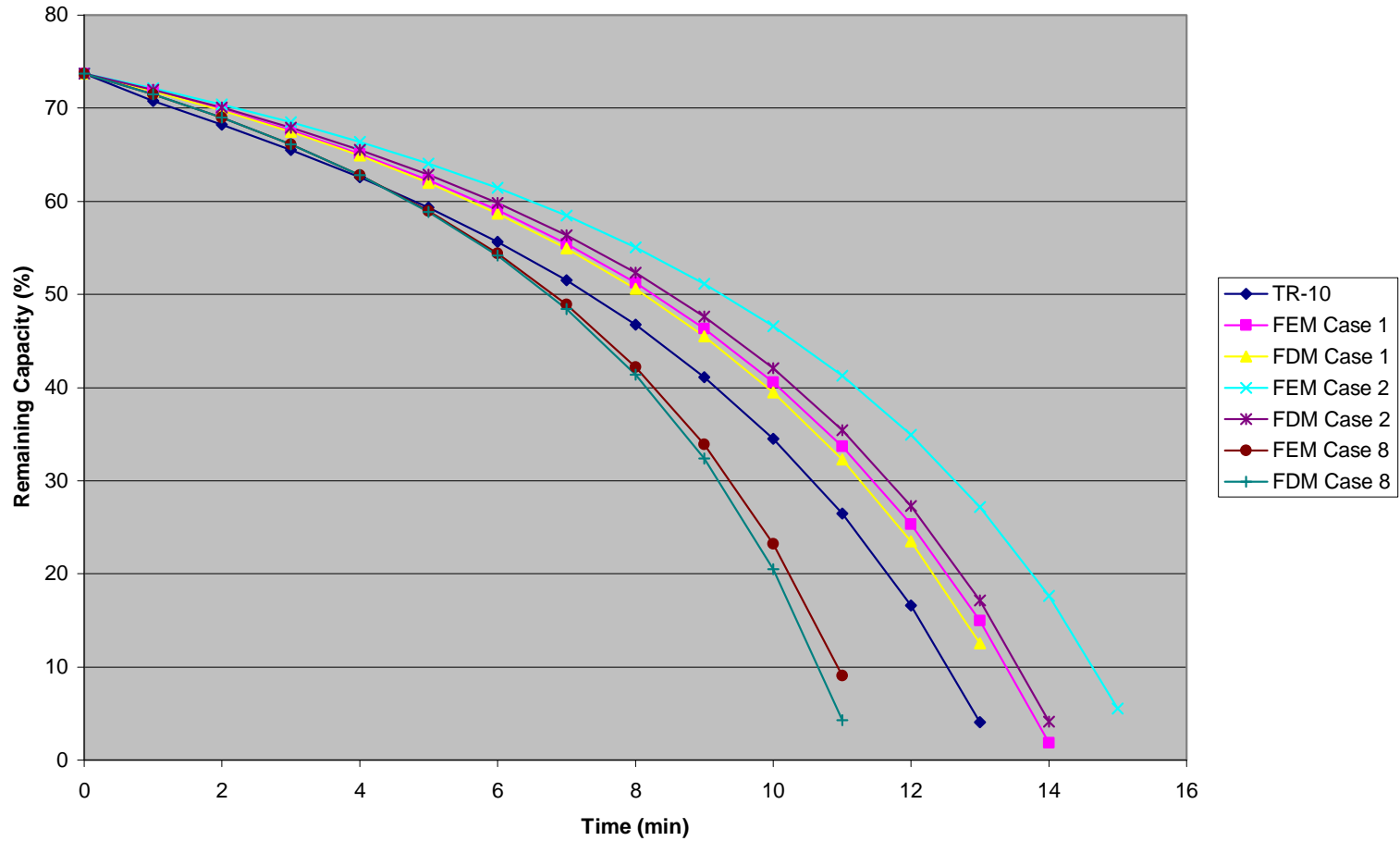
R20C Column Comparison



R20C Column TR-10 vs. FEM and FDM

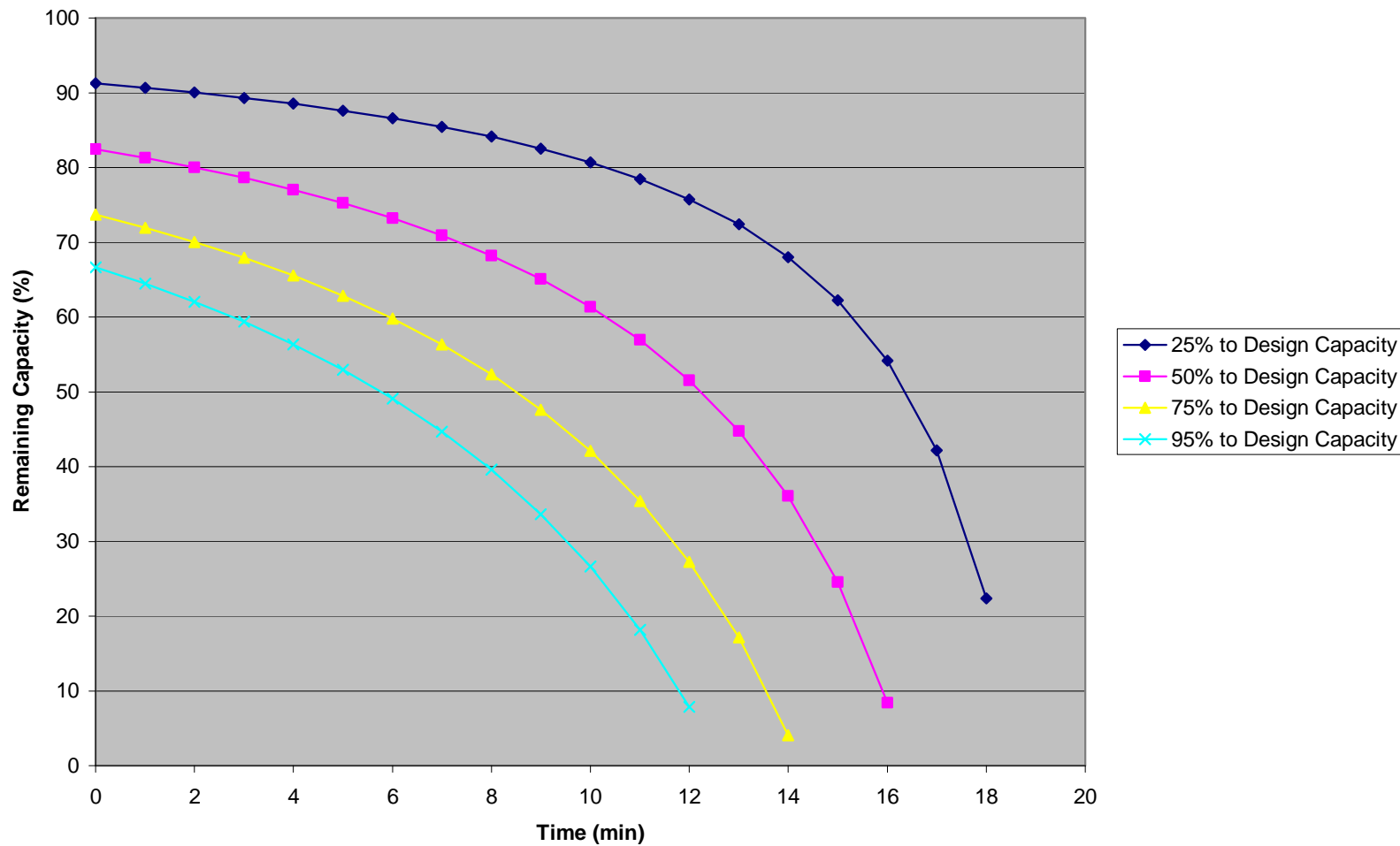
Appendix E – 2x10 Beam Time to Failure

2x10 Beam Loaded 75% to Design Capacity - Exposed to ASTM E-119



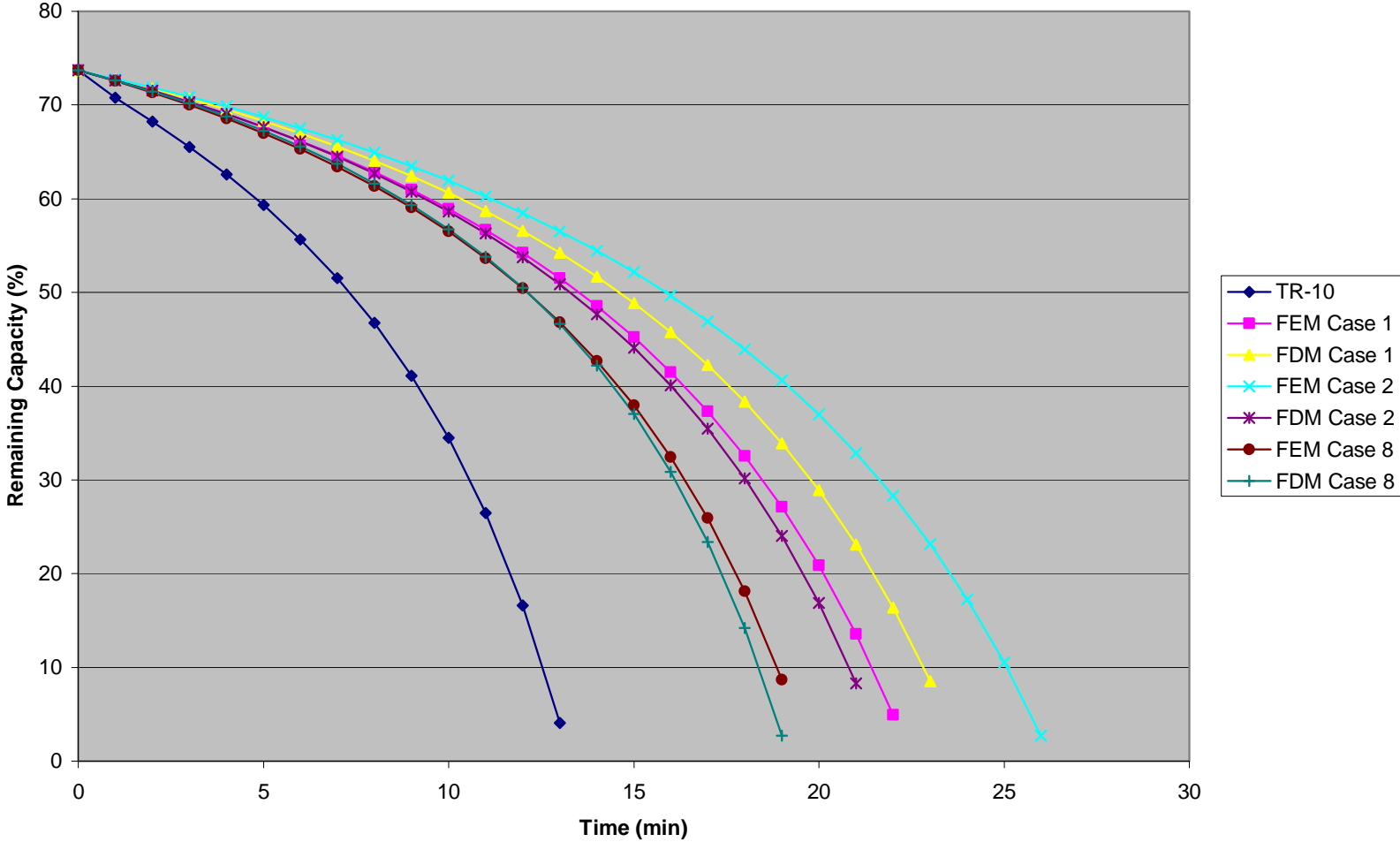
Lightweight Beam TR-10 vs. FEM and FDM – ASTM E-119

2x10 Beam FDM Case 2 - Exposed to ASTM E-119



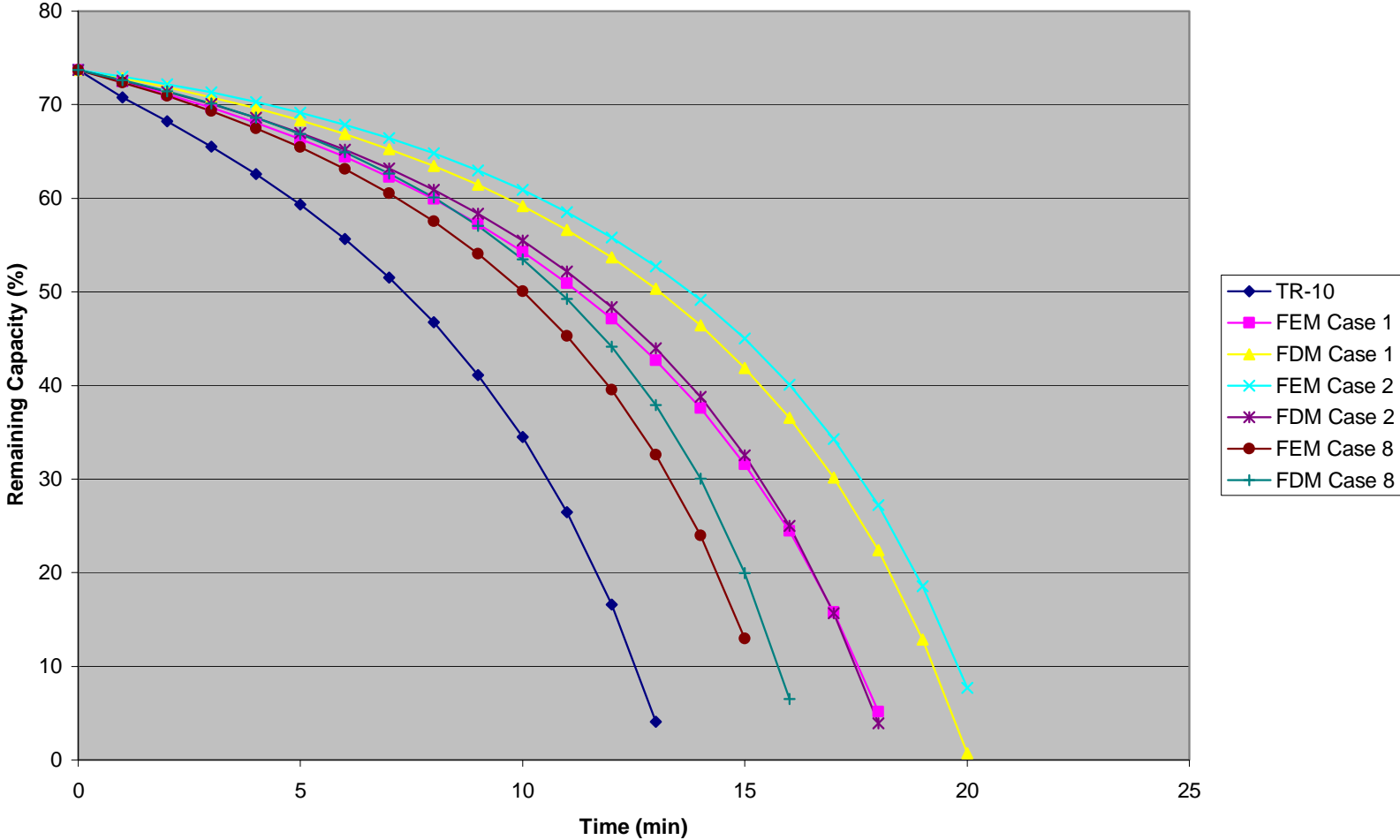
Lightweight Beam FDM Case 2 - % to Design Capacity Variation - ASTM E-119

2x10 Beam Loaded 75% to Design Capacity - Exposed to LD-MI



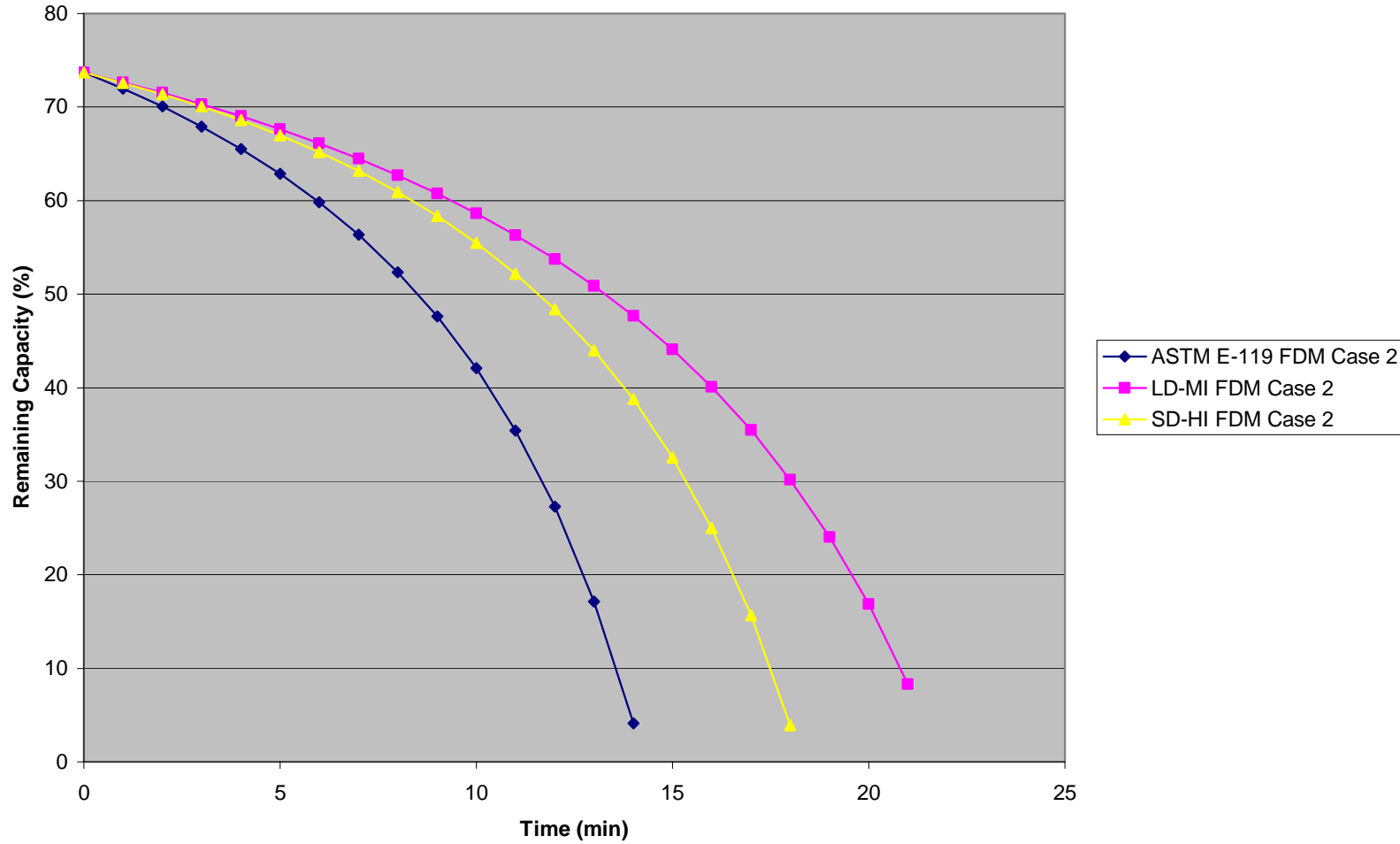
Lightweight Beam Loaded to 75% of Design Capacity - LD-MI

2x10 Beam Loaded 75% to Design Capacity - Exposed to SD-HI



Lightweight Beam Loaded to 75% of Design Capacity - SD-HI

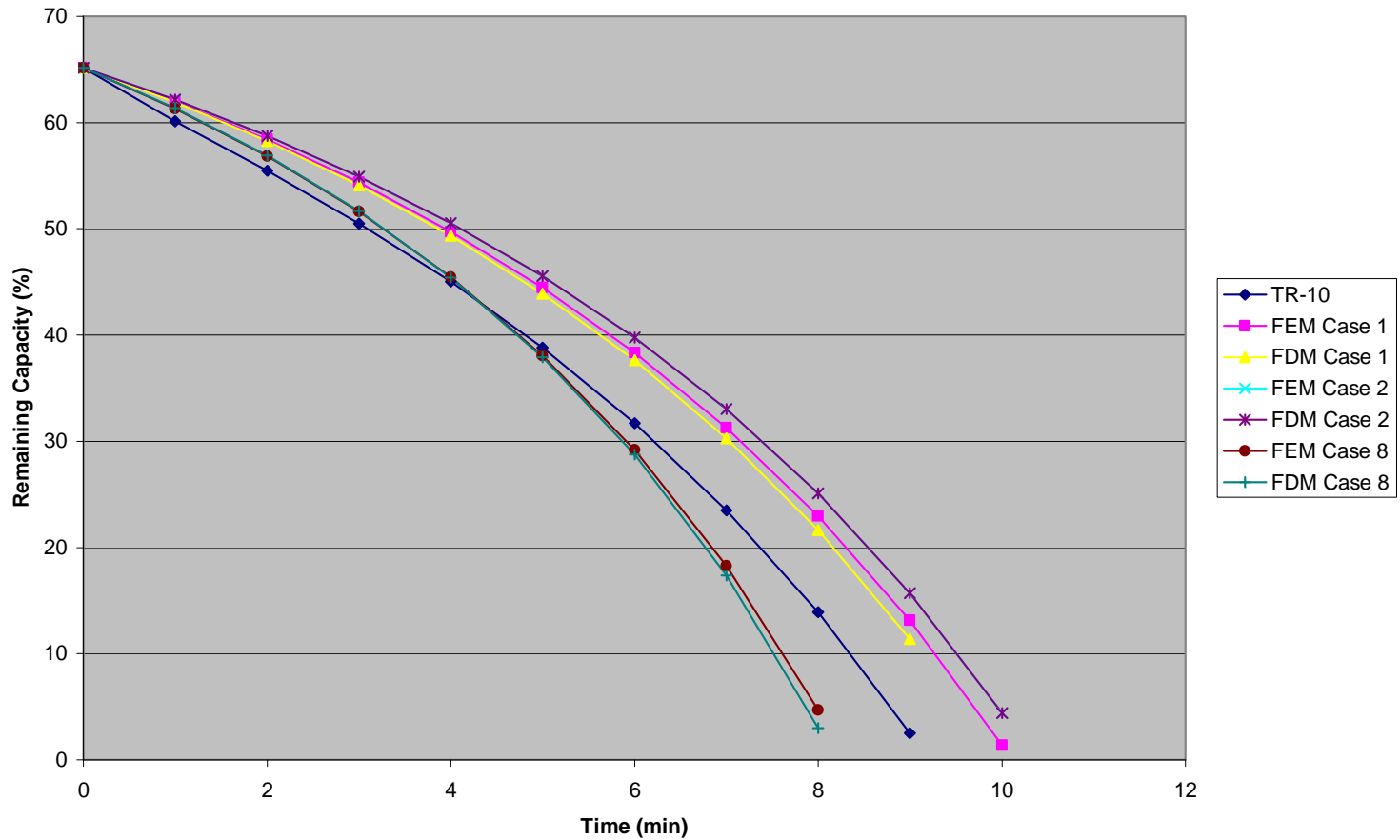
ASTM E-119 vs. LD-MI vs. SD-HI 2x10 Beam Loaded 75% to Design Capacity



Lightweight Beam Loaded 75% - Exposure Comparison

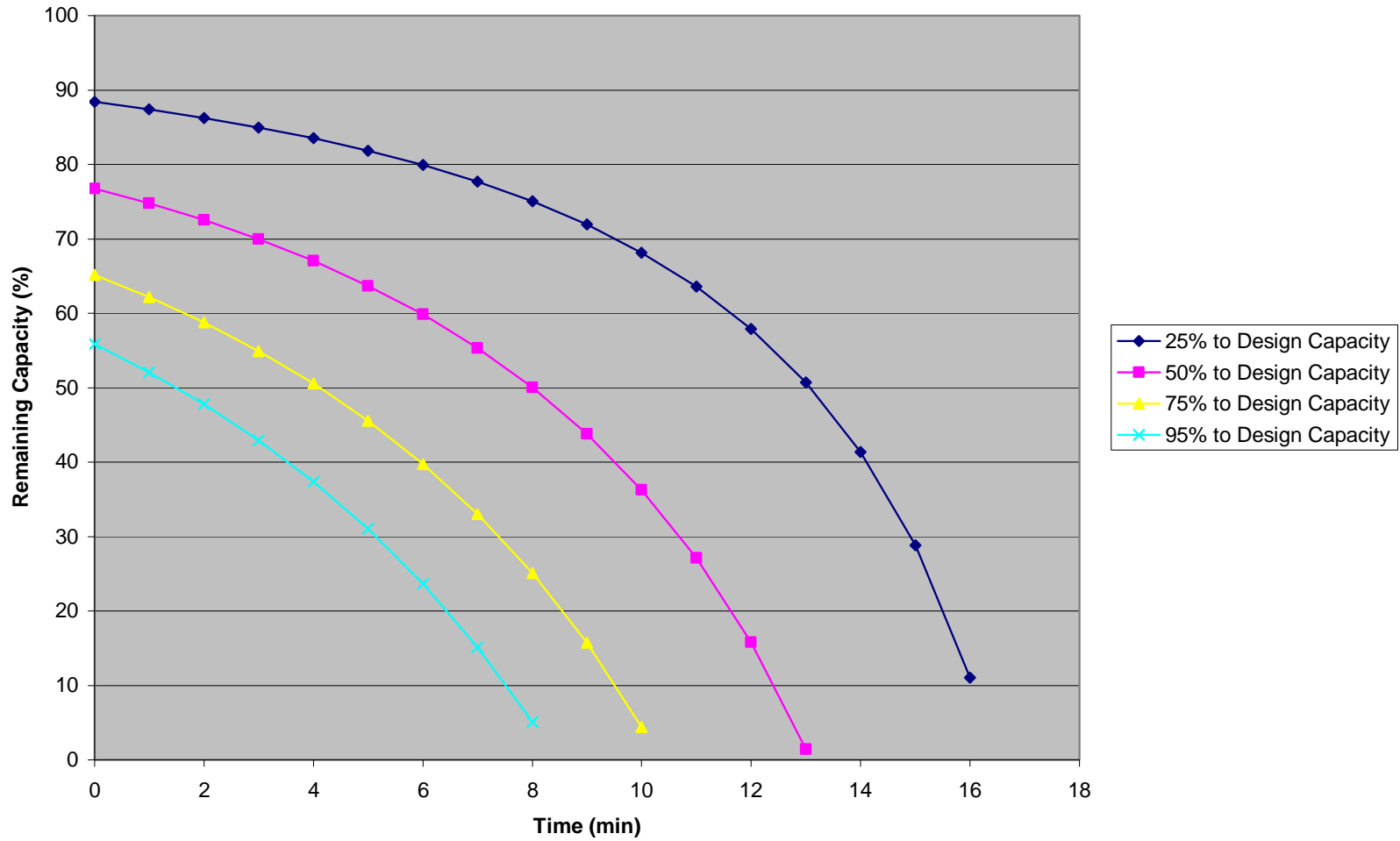
Appendix F – 2x6 Column Time to Failure

2x6 Column Loaded 75% to Design Capacity - Exposed to ASTM E-119



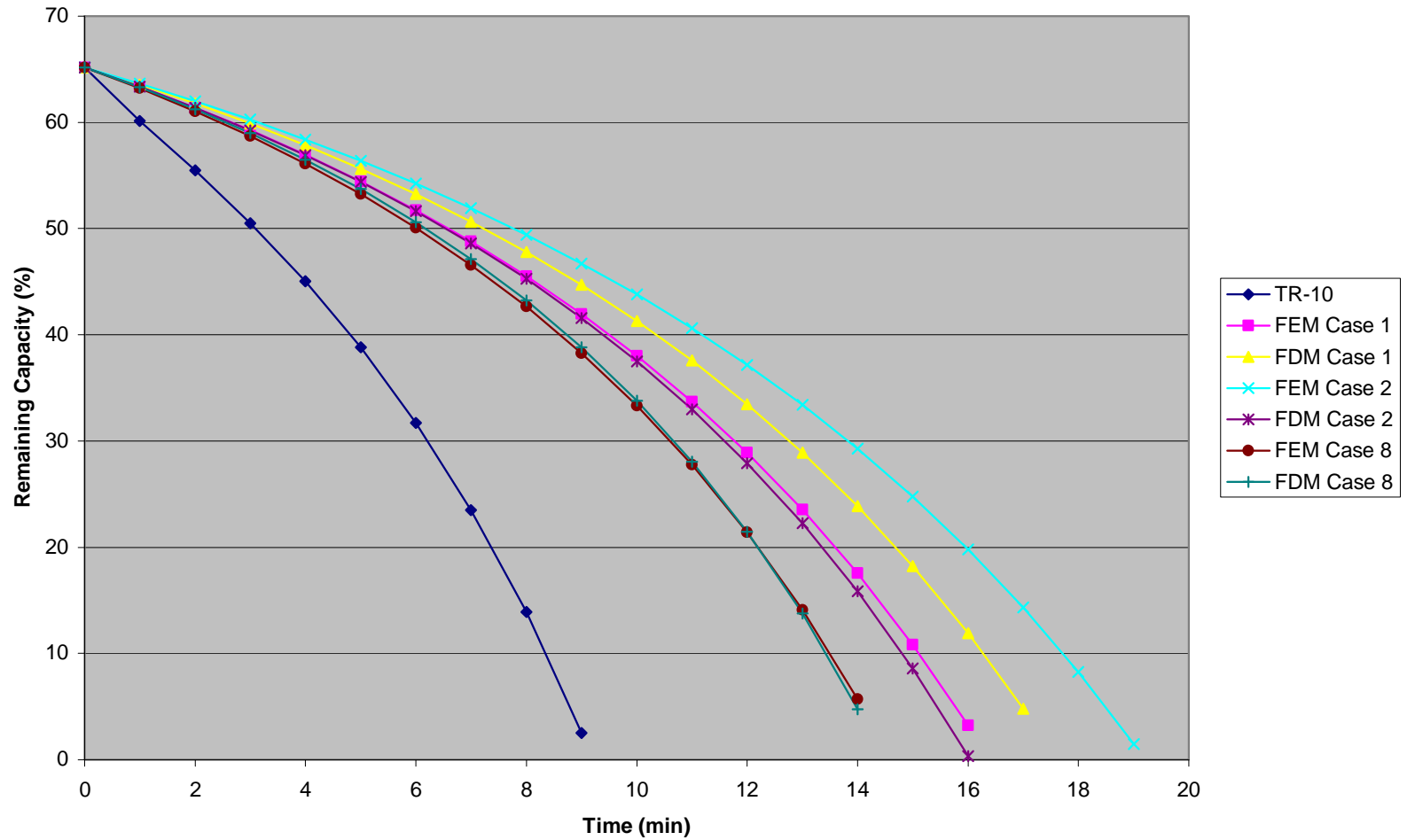
Lightweight Column TR-10 vs. FEM and FDM – ASTM E-119

2x6 Column FDM Case 2 - Exposed to ASTM E-119



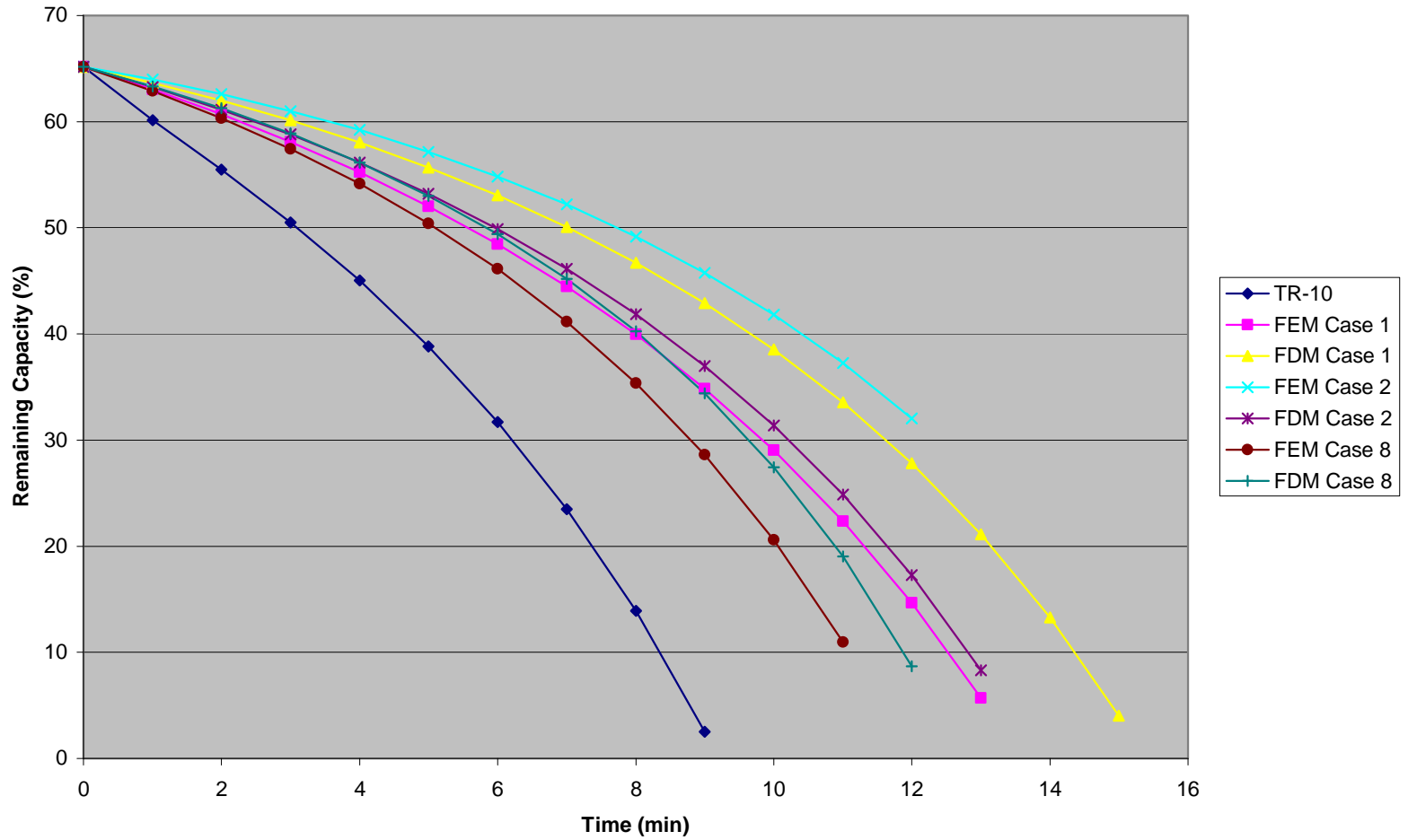
Lightweight Column FDM Case 2 - % to Design Capacity Variation – ASTM E-119

2x6 Column Loaded 75% to Design Capacity - Exposed to LD-MI



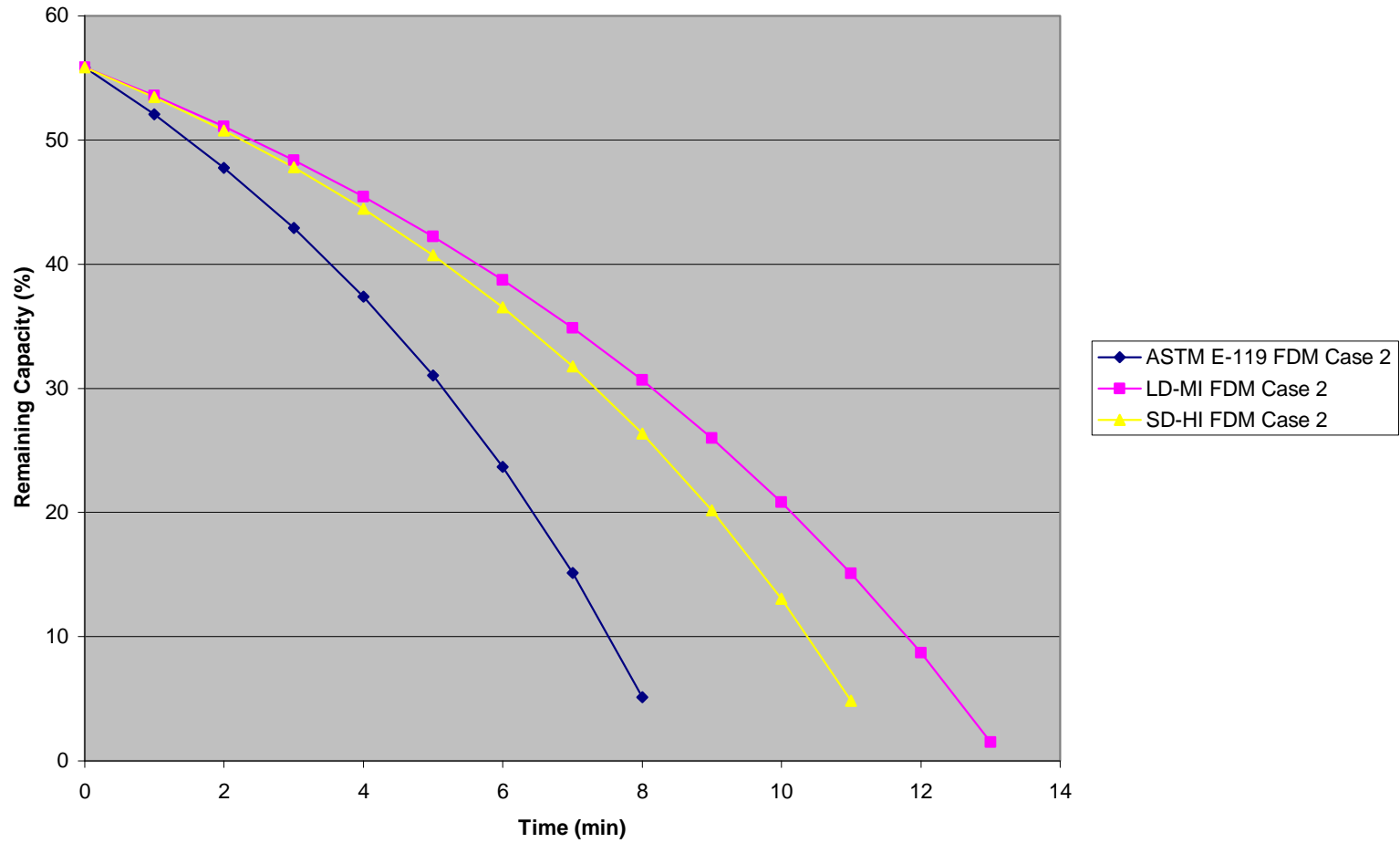
Lightweight Column Loaded to 75% of Design Capacity - LD-MI

2x6 Column Loaded 75% to Design Capacity - Exposed to SD-HI



Lightweight Column Loaded to 75% of Design Capacity - SD-HI

ASTM E-119 vs. LD-MI vs. SD-HI 2x6 Column Loaded 95% of Design Capacity



Lightweight Column Loaded 75% - Exposure Comparison